



HAL
open science

Structure-guided optimization of adenosine mimetics as selective and potent inhibitors of coronavirus nsp14 N7-methyltransferases

Marcel Hausdorff, Adrien Delpal, Sarah Barelier, Laura Nicollet, Bruno Canard, Franck Touret, Agathe Colmant, Bruno Coutard, Jean-Jacques Vasseur, Etienne Decroly, et al.

► To cite this version:

Marcel Hausdorff, Adrien Delpal, Sarah Barelier, Laura Nicollet, Bruno Canard, et al.. Structure-guided optimization of adenosine mimetics as selective and potent inhibitors of coronavirus nsp14 N7-methyltransferases. *European Journal of Medicinal Chemistry*, In press, 10.1016/j.ejmech.2023.115474 . hal-04095336

HAL Id: hal-04095336

<https://hal.science/hal-04095336>

Submitted on 11 May 2023

HAL is a multi-disciplinary open access archive for the deposit and dissemination of scientific research documents, whether they are published or not. The documents may come from teaching and research institutions in France or abroad, or from public or private research centers.

L'archive ouverte pluridisciplinaire **HAL**, est destinée au dépôt et à la diffusion de documents scientifiques de niveau recherche, publiés ou non, émanant des établissements d'enseignement et de recherche français ou étrangers, des laboratoires publics ou privés.

Structure-guided optimization of adenosine mimetics as selective and potent inhibitors of coronavirus nsp14 *N*7-methyltransferases

Marcel Hausdorff^a, Adrien Delpal^b, Sarah Barelier^b, Laura Nicollet^a, Bruno Canard^b, Franck Touret^c, Agathe Colmant^c, Bruno Coutard^c, Jean-Jacques Vasseur^a, Etienne Decroly^{b, **}, Françoise Debart^{a, *}

^a IBMM, CNRS, University of Montpellier, ENSCM, Montpellier, France.

^b AFMB, CNRS, Aix-Marseille University, UMR 7257, 163 Avenue de Luminy, Marseille, France.

^c IHU Méditerranée Infection, Unité Virus Emergents, University of Aix-Marseille, 13005 Marseille, France.

*Corresponding Author. E-mail address: francoise.debart@umontpellier.fr (F. Debart).

**Corresponding Author. E-mail address: etienne.decroly@univ-amu.fr (E. Decroly)

ORCID

S. Barelier : 0000-0002-1084-6312

J.-J. Vasseur : 0000-0002-4379-6139

E. Decroly : 0000-0002-6046-024X

F. Debart : 0000-0003-3422-3926

F. Touret : 0000-0002-4734-2249

A. Colmant : 0000-0002-2004-4073

ABSTRACT

The COVID-19 pandemic reveals the urgent need to develop new therapeutics targeting the SARS-CoV-2 replication machinery. The first antiviral drugs were nucleoside analogues targeting RdRp and protease inhibitors active on nsp5 Mpro. In addition to these common antiviral targets, SARS-CoV-2 codes for the highly conserved protein nsp14 harbouring *N*7-methyltransferase (MTase) activity. Nsp14 is involved in cap *N*7-methylation of viral RNA and its inhibition impairs viral RNA translation and immune evasion, making it an attractive new antiviral target. In this work, we followed a structure-guided drug design approach to design bisubstrates mimicking the *S*-adenosylmethionine methyl donor and RNA cap. We developed adenosine mimetics with an *N*-arylsulfonamide moiety in the 5'-position, recently described as

a guanine mimicking the cap structure in a potent adenosine-derived nsp14 inhibitor. Here, the adenine moiety was replaced by hypoxanthine, *N*⁶-methyladenine, or *C*7-substituted 7-deaza-adenine. 26 novel adenosine mimetics were synthesized, one of which selectively inhibits nsp14 *N*7-MTase activity with a subnanomolar IC₅₀ (and seven with a single-digit nanomolar IC₅₀). In the most potent inhibitors, adenine was replaced by two different 7-deaza-adenines bearing either a phenyl or a 3-quinoline group at the *C*7-position via an ethynyl linker. These more complex compounds are barely active on the cognate human *N*7-MTase and docking experiments reveal that their selectivity of inhibition might result from the positioning of their *C*7 substitution in a SAM entry tunnel present in the nsp14 structure and absent in the h*N*7-MTase. These compounds show moderate antiviral activity against SARS-CoV-2 replication in cell culture, suggesting delivery or stability issue.

Keywords: 7-deaza-adenine; arylsulfonamide; bisubstrate; SARS-CoV-2; RNA cap methyltransferase; structure-guided design

Abbreviations: SARS, severe acute respiratory syndrome; MERS, Middle East respiratory syndrome; CoV, coronavirus; COVID19, coronavirus disease 2019; DV3, dengue virus serotype 3; MTase, methyltransferase; nsp14, non-structural protein 14; RdRp, RNA dependent RNA polymerase; 3CLpro, 3-chymotrypsin like protease; Mpro, main protease; PLpro, papain-like protease; SAM, *S*-adenosylmethionine; SAH, *S*-adenosylhomocysteine; hRNMT, human RNA methyltransferase; FBA, filter binding assay; SAR, structure-activity relationships.

1. Introduction

The emergence of new viruses poses a global threat to human health. The COVID-19 pandemic caused by the SARS-CoV-2 illustrates what the world faces with emerging viruses in the absence of appropriate treatments or prophylactic vaccines. After three years of pandemic, approved antiviral treatments for CoV-diseases are still limited to molecules targeting the RNA dependent RNA polymerase (RdRp) activity or the main protease (Mpro) activity [1-4]. The discovery of potent and selective antiviral inhibitors to fight SARS-CoV-2 infection and likely future CoV outbreaks is an urgent research priority. To this end, significant activity has been observed in drug repurposing [5] and many approved drugs have been reported

to block viral replication. Among them, the most promising nucleoside analogues, remdesivir and molnupiravir targeting viral RdRp, and nirmatrelvir inhibiting viral Mpro have shown relative efficacy in clinical trials depending on the stage of infection [6]. Over the past two years, great efforts have been made in structure-based drug design, an effective alternative for developing new antiviral agents targeting viral enzymes [7]. Among the four structural and 16 non-structural proteins encoded by CoVs [8], the papain-like protease (PLpro) and Mpro that are essential for CoV replication have been extensively targeted with peptidomimetics and small molecule inhibitors [9]. Two methyltransferases (MTases), which are engaged in the capping pathway of viral mRNA, are also essential for viral replication, as reverse genetic studies demonstrated that these enzymes play a key role in mRNA translation and prevent viral restriction mediated by host innate immune system [10-12]. These MTases are responsible for the enzymatic cascade of viral RNA cap methylations: first the *N*7-methylation of the guanosine by guanine *N*7-MTase nsp14 and subsequently the 2'-OH methylation of the ribose of the first RNA adenosine by the 2'-*O*-MTase complex nsp10/nsp16 [8, 13]. *N*7-MTase nsp14 was identified as a critical enzyme for the replication of SARS-CoV, as two mutations in the *N*7-MTase catalytic pocket abrogate virus viability [11]. Prior to the emergence of SARS-CoV-2, besides the unselective MTase inhibitors sinefungin and *S*-adenosyl homocysteine (SAH), few inhibitors of SARS-CoV nsp14 had been described, most of them discovered by high-throughput screening [14]. In this context, our group had developed a rational drug design approach to synthesize competitive bisubstrate inhibitors that occupy both the *S*-adenosylmethionine (SAM) methyl donor binding pocket and the cap-binding pocket of SARS-CoV nsp14 [15]. In this series of adenine dinucleoside SAM analogues, the best inhibitor displayed submicromolar activity, with a selective inhibition of *N*7-MTase nsp14 over the human *N*7-MTase. Then, with the emergence of Covid-19, many libraries were screened on SARS-CoV-2 nsp14 but the inhibition results were rather poor [16-20]. In contrast, rational drug design approaches lead to the identification of much more potent inhibitors active at nanomolar [21-25] or subnanomolar concentration [25]. All these new inhibitors are mimics of SAM/SAH and most of them have been modeled in the crystal structure of SARS-CoV nsp14, solved in the presence of SAM (PDB 5C8T) [26]. Very recently, several crystal structures of full-length nsp14 from SARS-CoV-2 were solved, bound to SAH (PDB 7R2V, 7QGI) or to a cap-analogue (PDB 7QIF) [27, 28]. A high-resolution crystal structure of the SARS-CoV-2 *N*7-MTase domain - expressed in fusion with the TELSAM epitope - was also reported [29]. These new structures provide crucial information for understanding the dynamics of nsp14

methyltransferase activity and pave the way for the structure-based development of new antivirals against CoVs.

Our previous work identified potent bisubstrate inhibitors bearing *N*-ethyl arylsulfonamide moieties linked to the 5'-position of an adenosine mimicking that of SAM as a key component occupying the cap RNA substrate binding site. Indeed, this *N*-ethyl arylsulfonamide motif likely accounts for the compounds' high affinity for SARS-CoV-2 nsp14, which results in a double-digit nanomolar inhibition [23]. When the sulfonamide linker was replaced by an amide or an *N*-acylsulfonamide linker, we showed that the inhibitory activity of the nucleoside analogues was lost [15, 30]. In addition, a recent report confirmed the importance of the sulfonamide linker between the adenosine and the aromatic moiety, a 2-naphthalene in this case, to reach nanomolar inhibition of nsp14 [24].

In the present work, we developed a structure-guided drug design approach to design a new series of inhibitors targeting nsp14 *N*7-MTase activity. We used the *N*-aryl-sulfonamide moiety as a guanine mimic of the cap structure and modified the adenine moiety in order to increase the interaction with the SAM binding pocket. We replaced adenine with its analogue, hypoxanthine (HXN), or a *C*7-substituted-7-deaza-adenine, or we added a methyl group at the *N*⁶ position of adenine (*N*⁶mA) (Fig. 1). Thus, we synthesized 26 final compounds **1-26** that were tested for *N*7-MTase inhibitory activity *in vitro*. In the most potent compounds, the adenine is replaced with 7-deaza-adenine bearing either a phenyl (*C*^{7Ph}) or a 3-quinoline group (*C*^{7Q}) attached to the *C*7-position of the nucleobase *via* an ethynyl linker. One of these compounds displays subnanomolar IC₅₀ against the *N*7-MTase activity of SARS-CoVs nsp14 and is barely active on h*N*7-MTase (hRNMT). Docking predictions support the selective inhibition of the viral nsp14 MTase, as the phenyl or 3-quinoline group on the nucleobase occupies a SAM entry tunnel controlled by a mobile loop forming the substrate entry gate, which is absent in the RNMT human ortholog. Finally, the inhibition of the viral replication for the best nsp14 inhibitors was tested in infected cell cultures, where some of the compounds show inhibitory effect at the micromolar range.

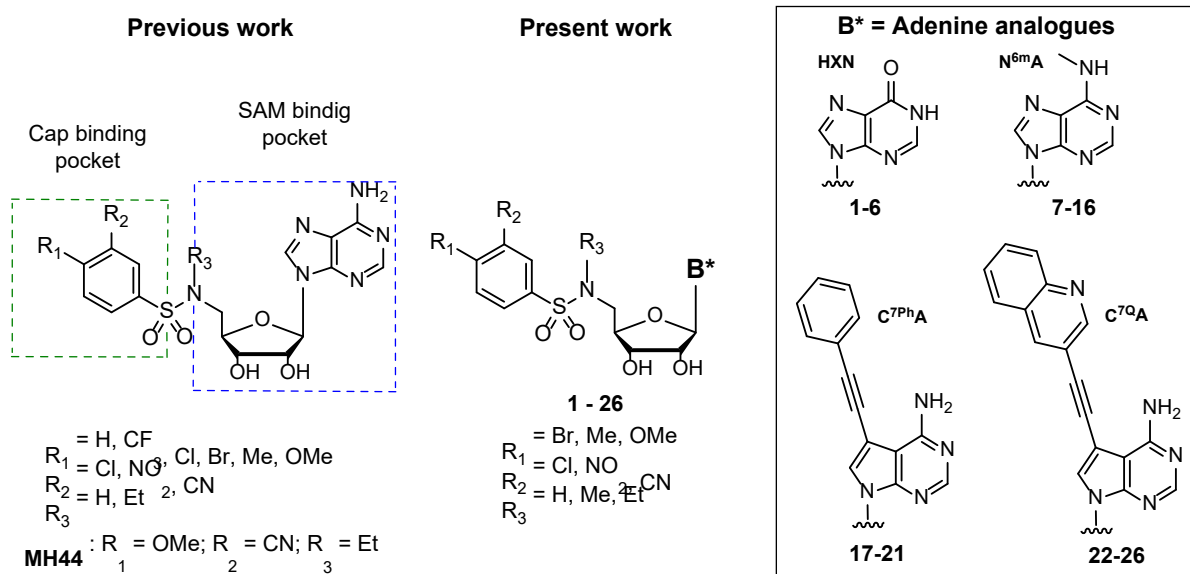


Fig. 1. Design of novel bisubstrate adenosine mimetics **1–26** as potential inhibitors of SARS-CoV-2 nsp14 N7-MTase derived from a previous series of *N*-arylsulfonamide adenosine analogues with **MH44** as the best inhibitor ($IC_{50} = 19 \text{ nM}$) [23].

2. Results and discussion

2.1. Rational design of compounds

We based the design of our new inhibitors on the molecular structure of the previous series of bisubstrate inhibitors containing *N*-ethyl arylsulfonamide moieties, which were shown to be crucial for the affinity and inhibition of the SARS-CoV-2 nsp14 N7-MTase (Fig. 1). Molecular docking studies supported that the arylsulfonamide moiety occupies the cap-guanosine binding pocket of SARS-CoV nsp14 (PDB ID: 5C8T) [23]. The impact of the nature and position of the substituents on the aryl moiety was thus demonstrated, as a *meta* electron-withdrawing substituent (NO_2 , CN , or Cl) and a *para* electron-donating substituent (Me or OMe) were found to be the best combination to yield nsp14 inhibitors with double-digit nanomolar IC_{50} .

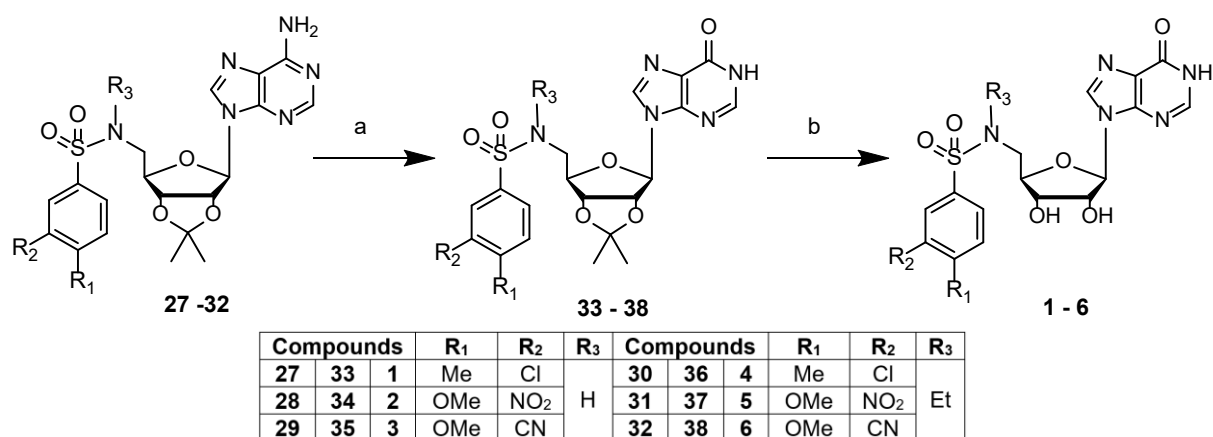
Therefore, in the present work, the 26 synthesized compounds were designed with a phenylsulfonamide moiety bearing one substituent in *meta* (NO_2 , CN , or Cl) and one substituent in *para* (Me , OMe or Br) positions following the same rationale. Moreover, as functionalization of the nitrogen atom of the sulfonamide link with an alkyl group was shown to improve inhibition, an ethyl group was used in compounds **4-6**, **12-16** and a methyl group in nucleoside analogues **17-26**. Here, we focused on improving the interactions between the nucleobase moiety and N7-MTase nsp14, according to docking performed in nsp14 structure. By

mimicking adenine, hypoxanthine with O6 instead of NH₂ at C6 position in the purine ring was chosen to design compounds **1-6**. Furthermore, the addition of a methyl group on the exocyclic NH₂ of adenine in nucleosides **7-16** was intended to increase the lipophilic properties of the inhibitors to favor cellular uptake.

In compounds **17-26**, adenine was replaced by two different 7-deaza-adenines bearing a phenyl or a 3-quinoline group attached to the C7-position of the nucleobase through an ethynyl linker. This modified adenine design was inspired by the work of Nencka et al. where replacement of adenine with various 7-substituted-7-deaza-adenines in SAH nucleoside analogues resulted in nanomolar inhibitors of SARS-CoV-2 nsp14 [22]. These modified nucleobases have been shown to effectively target a side cavity of SARS-CoV nsp14 (PDB 5C8T), which is a substrate entry gate communicating with the SAM binding site [28]. Combined with the *N*-methyl arylsulfonamide scaffold at the 5' position of the adenosine analogue, we anticipated that C7-aryl-substituted 7-deaza-adenine would yield much more potent and selective inhibitors of the SARS-CoV-2 nsp14 N7-MTase (PDB 7R2V). Because of the high similarity between SARS-CoV and SARS-CoV-2 structures (> 95% sequence identity, structural root-mean-square deviation (RMSD) 0.49 Å over 585 backbone atoms) our compounds were tested against both CoVs nsp14 enzymes.

2.2. Chemical synthesis

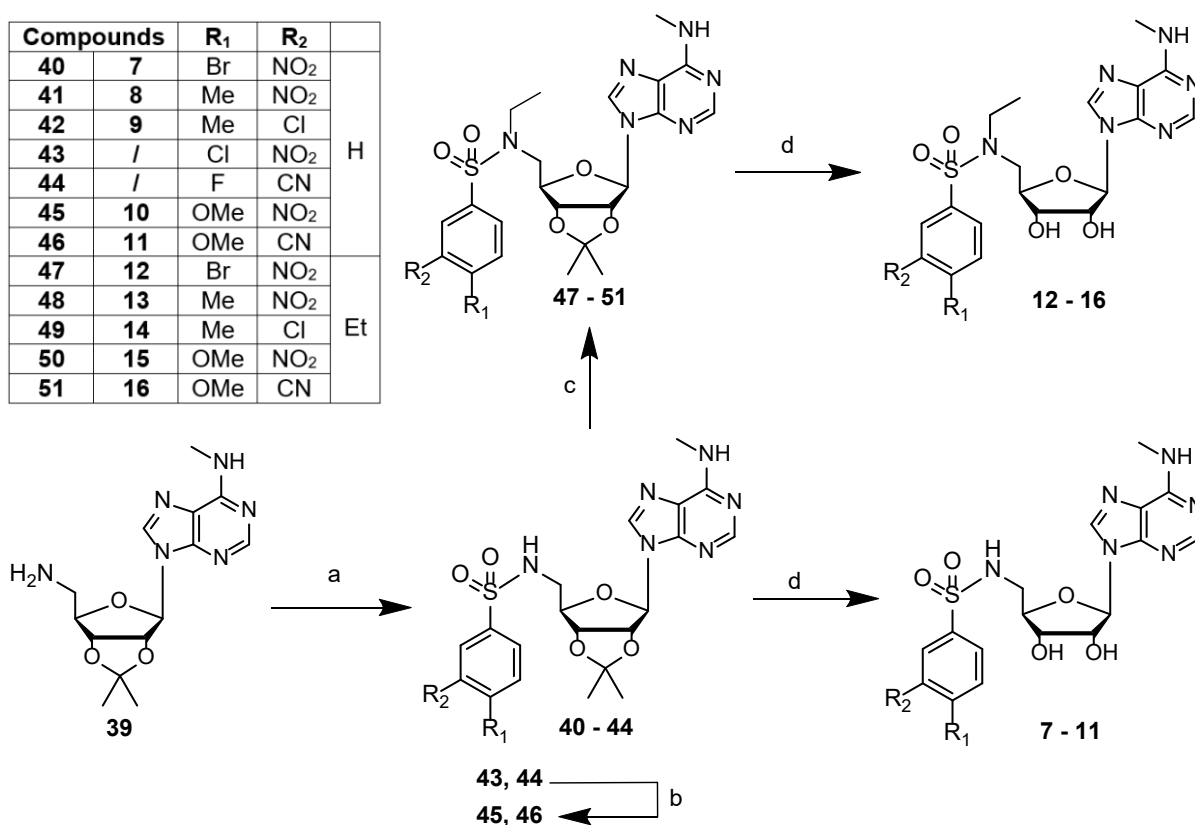
The synthesis of inosine analogues **1-6** began with the preparation of the previously described 5'-*N*-aryl-sulfonamide adenosines **27-32** [23] (Scheme 1). Treatment of **27-32** with NaNO₂ under acidic conditions with a mixture of acetic acid and water (85:15) during 72 h afforded the inosine derivatives **33-38** in satisfactory yields (59-80%) [31]. The addition of a second portion of sodium nitrite after 48 h of reaction is crucial to complete the conversion of adenosine to inosine. Interestingly, no cleavage of the isopropylidene protection was observed, nor was any depurination. The 2', 3'-hydroxyls of intermediates **33-38** were deprotected with a mixture of formic acid and water (1:1) during 24-48 h to obtain the final compounds **1-6** in good yields (63-72%).



Scheme 1. Synthesis of 5'-*N*-arylsulfonamide inosine derivatives **1–6**. (a) NaNO₂, AcOH/H₂O 85:15 v/v, 25 °C, 72 h, 59 – 80%; (b) HCO₂H / H₂O 1:1 v/v, 25 °C, 24–48 h, 63–72%.

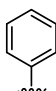
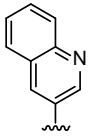
To prepare *N*⁶-methyladenosine compounds **7–16**, we first synthesized 5'-amino-2',3'-*O*-isopropylidene-*N*⁶-methyladenosine **39** following known procedures [32, 33] (Scheme 2). Coupling of **39** with the corresponding commercially available benzenesulfonyl chloride reagents afforded the intermediates **40–44** in 62-91% yields [23]. To obtain compounds **45** and **46** with a *p*-OMe group, aromatic nucleophilic substitution was performed on **43** with a *p*-Cl atom and on **44** with a *p*-F atom using sodium methoxide in methanol at 50 °C. The amino function of compounds **40–42**, **45**, **46** was derivatized with an ethyl group using ethyl *p*-toluenesulfonate, potassium carbonate and potassium iodide to obtain the *N*-ethyl sulfonamide derivatives **47–51** in yields ranging from 48 to 90%. It is noteworthy that a catalytic amount of potassium iodide is required to form ethyl iodide, which is sufficiently reactive to be substituted by the deprotonated sulfonamide while the tosylate reagent is not. In addition, ethyl iodide was used in stoichiometric default to avoid the formation of by-products due to the possible reaction with at least the *N*⁶-amino group. Finally, the isopropylidene groups were removed from **40–42** and **45–51** by treatment with a TFA/water mixture for 30 min to give the desired compounds **7–16**.

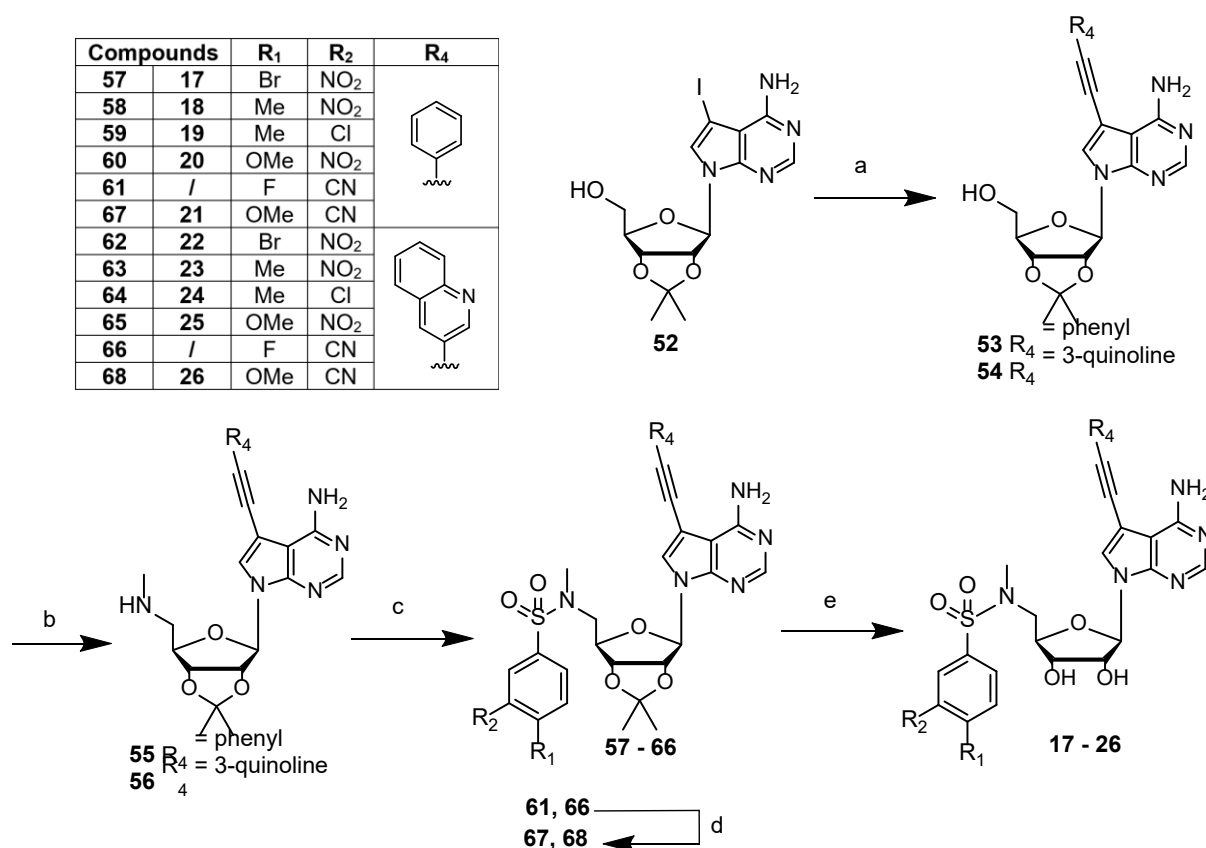
Compounds	R ₁	R ₂	
40	7	Br	NO ₂
41	8	Me	NO ₂
42	9	Me	Cl
43	/	Cl	NO ₂
44	/	F	CN
45	10	OMe	NO ₂
46	11	OMe	CN
47	12	Br	NO ₂
48	13	Me	NO ₂
49	14	Me	Cl
50	15	OMe	NO ₂
51	16	OMe	CN



Scheme 2. Synthesis of 5'-*N*-arylsulfonamide *N*⁶-methyladenosine compounds **7–16**. (a) appropriate substituted benzenesulfonyl chloride, Et₃N, DMF, -10 °C, 1.5–3 h, 62–91%; (b) MeONa 0.5 M/MeOH, 50 °C, 24–48 h, 68–96%; (c) EtOTs, KI, K₂CO₃, DMF, 50 °C, 18 h, 48–90%; (d) TFA/H₂O 8:2 v/v, 25 °C, 30 min, 29–95%.

The 7-ethynylaryl-7-deaza-adenosine nucleosides **17–26** were synthesized from the readily accessible 7-deaza-7-iodo-2',3'-*O*-isopropylideneadenosine **52** [34–36] (Scheme 3). Sonogashira cross-coupling reaction of **52** [22, 37] with commercially available phenylacetylene or prepared 3-ethynylquinoline [38, 39] led to the formation of 7-ethynylphenyl-7-deaza-adenosine **53** and 7-ethynylquinoline-7-deaza-adenosine **54**, respectively, both in high yields (85–95%). The 5'-aminomethyl derivatives **55** and **56** were obtained by reaction of **53** and **54** with mesyl chloride in dichloromethane and then with methylamine. The amino functions of **55** and **56** were functionalized with different benzenesulfonyl chlorides to give **57–66**. From **61** and **66** bearing a fluorine atom in the *para*-position of the phenyl ring, an aromatic nucleophilic substitution with sodium methoxide afforded **67** and **68** with a *p*-OMe group, respectively. Intermediate compounds **57–60**, **62–65**, **67–68** were deprotected in a TFA/H₂O mixture to obtain the final 7-ethynylaryl-7-deaza-adenosine nucleosides **17–26**.

Compounds	17	R ₁	R ₂	R ₄
57	17	Br	NO ₂	
58	18	Me	NO ₂	
59	19	Me	Cl	
60	20	OMe	NO ₂	
61	/	F	CN	
62	21	OMe	CN	
63	22	Br	NO ₂	
64	23	Me	NO ₂	
65	24	Me	Cl	
66	25	OMe	NO ₂	
67	/	F	CN	
68	26	OMe	CN	



Scheme 3. (a) appropriate substituted alkyne reagents, Et₃N, CuI, Pd(PPh₃)₄, THF, 60 °C, 2 h, 85–95%; (b) (i) MsCl, Et₃N, CH₂Cl₂, -10 °C, 30 min, 80–87%, (ii) MeNH₂ 2M/THF, 50 °C, 72 h, 31–55%; (c) appropriate substituted benzenesulfonyl chloride reagents, Et₃N, DMF, -10 °C, 1.5–3 h, 57–95%; (d) MeONa 0.5 M/MeOH, 50 °C, 24–48 h, 73–83%; (e) TFA/H₂O 8:2 v/v, 25 °C, 30 min, 16–66%.

2.3. RNA Methyltransferase Activity Assays

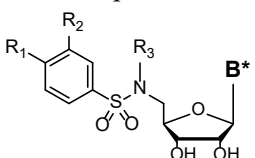
Compounds **1–26** were tested for their ability to inhibit the SARS-CoV and SARS-CoV-2 *N7*-MTases which are involved in viral RNA cap structure methylation. We also assessed the selectivity of the synthesized compounds, by determining the inhibition of the cognate human *N7*-MTase (hRNMT) and of the Dengue virus MTase (NS5). Briefly, the different purified MTases were incubated together with compounds **1–26** at 5 μM and the transfer of [³H]-radiolabeled methyl on synthetic capped RNA (GpppAC₄) was determined by filter binding assay (FBA) [40].

MH44 from our previous series of nsp14 inhibitors is used here as a control (Fig. 1) [23]. The replacement of the exocyclic NH₂ (*N*⁶) with an oxygen atom in inosine is detrimental for the inhibitory activity of the compounds **1–6** at 5 μM against CoV *N7*-MTase nsp14 (Table 1). The addition of a methyl group to the exocyclic NH₂ (*N*⁶) of adenine in **7–11** impairs the inhibition of both CoV MTase activity which is less impacted for compounds **12–16** bearing an ethyl on the sulfonamide bond. The two *C7*-substituted-7-deaza-adenine nucleoside series bearing either

a phenyl (**17-21**) or a 3-quinoline group (**22-26**) exhibit potent inhibitory effect at 5 μ M on SARS-CoV and SARS-CoV-2 *N7*-MTases. In addition, the five series of compounds barely inhibit the dengue virus NS5-MTase or human *N7*-MTase that methylates the mRNA cap structure, suggesting selectivity toward both SARS-CoV *N7*-MTases.

Table 1

Screening for inhibitory activity of compounds **1-26** at 5 μ M on various viral and cellular *N7*-MTases

Compounds					Percentage of MTase activity at 5 μ M (%) ^a								
					N°	B*	R ₁	R ₂	R ₃	SARS-CoV nsp14	SARS-CoV-2 nsp14	DV3 NS5	hRNMT
MH44					A	OMe	CN	Et	4.2 \pm 2.2	0.1 \pm 0.4	n.i	69.5 \pm 16.4	
1		Me	Cl		71.8 \pm 4.8	87.6 \pm 3.3	n.i	n.i					
2	HXN	OMe	NO ₂	H	91.7 \pm 4.8	93.6 \pm 7.9	n.i	n.i					
3		OMe	CN		98.4 \pm 5.0	86.0 \pm 0.2	n.i	n.i					
4		Me	Cl		91.0 \pm 8.6	75.5 \pm 4.5	n.i	n.i					
5	HXN	OMe	NO ₂	Et	69.8 \pm 8.7	56.4 \pm 3.9	86.4 \pm 16.9	n.i					
6		OMe	CN		48.1 \pm 4.8	30.7 \pm 1.6	89.8 \pm 5.9	88.9 \pm 15.9					
7		Br	NO ₂		54.0 \pm 7.3	33.8 \pm 2.0	78.1 \pm 4.4	57.0 \pm 9.8					
8		Me	NO ₂		66.4 \pm 6.9	38.7 \pm 3.6	76.6 \pm 9.5	66.4 \pm 11.3					
9	N ^{6m} A	Me	Cl	H	53.5 \pm 3.3	45.4 \pm 2.8	n.i	92.0 \pm 17.7					
10		OMe	NO ₂		41.9 \pm 2.6	31.5 \pm 1.4	n.i	n.i					
11		OMe	CN		45.1 \pm 0.7	25.4 \pm 2.6	n.i	n.i					
12		Br	NO ₂		29.5 \pm 0.6	15.2 \pm 1.8	98.0 \pm 2.3	n.i					
13		Me	NO ₂		20.1 \pm 1.7	10.9 \pm 0.7	97.1 \pm 5.1	n.i					
14	N ^{6m} A	Me	Cl	Et	10.9 \pm 1.8	8.3 \pm 0.2	n.i	78.0 \pm 1.6					
15		OMe	NO ₂		16.4 \pm 0.1	10.3 \pm 0.3	90.0 \pm 2.8	73.3 \pm 5.1					
16		OMe	CN		4.3 \pm 0.2	4.2 \pm 0.2	80.2 \pm 7.0	55.9 \pm 2.7					
17		Br	NO ₂		3.3 \pm 1.0	5.0 \pm 1.1	96.9 \pm 1.5	95.9 \pm 0.3					
18		Me	NO ₂		1.0 \pm 0.4	1.0 \pm 0.9	93.3 \pm 5.7	n.i					
19	C ^{7Ph} A	Me	Cl	Me	2.4 \pm 0.3	7.0 \pm 4.6	94.8 \pm 3.4	n.i					
20		OMe	NO ₂		0.5 \pm 0.3	0.0 \pm 0.2	91.6 \pm 3.2	n.i					
21		OMe	CN		1.0 \pm 1.0	2.4 \pm 0.3	n.i	n.i					
22	C ^{7Q} A	Br	NO ₂	Me	5.5 \pm 0.9	5.4 \pm 1.1	n.i	52.3 \pm 20.3					
23		Me	NO ₂		1.9 \pm 0.2	4.2 \pm 0.2	96.0 \pm 1.1	86.7 \pm 25.7					

24		Me	Cl		1.5 ± 0.1	3.2 ± 0.3	97.7 ± 2.8	90.7 ± 24.0
25		OMe	NO ₂		0.8 ± 0.4	0.0 ± 0.3	n.i	49.9 ± 18.4
26		OMe	CN		1.4 ± 0.1	0.0 ± 0.3	n.i	53.0 ± 9.6

^aValues are the mean of three independent experiments. The MTase activity was measured using a filter binding assay. Assays were carried out in reaction mixture [40 mM Tris-HCl (pH 8.0), 1 mM DTT, 1 mM MgCl₂, 2 μM SAM and 0.1 μM ³H-SAM] in the presence of 0.7 μM GpppAC₄ synthetic RNA and incubated at 30 °C. SARS-CoV nsp14 (10 nM), SARS-CoV-2 nsp14 N7-MTase (10 nM), Dengue virus NS5-N7 & 2'-O-MTase (0.5 μM), human RNA N7-MTase (hRNMT) (50 nM). The concentration of MTases is adjusted in each assay in order to get similar enzymatic activity in the FBA during the linear phase of the enzymatic reaction. Compounds were previously dissolved in 50% DMSO. ^b**MH44** was the best inhibitor of SARS-CoV-2 N7-MTase in our previous work [23]. n.i: no inhibition detected at 5 μM. **B***: nucleobase with A = adenine; HXN = hypoxanthine; N^{6m}A = N⁶-methyladenine; C^{7Ph}A = C7-phenylethynyl 7-deaza-adenine; C^{7QA} = C7-quinolinethynyl 7-deaza-adenine.

2.4. Dose-response Testing and Docking of Compounds **6-26** against SARS-CoV-2 nsp14

To further decipher the antiviral activity of our compounds, we determined the IC₅₀ values of the best inosine-derived inhibitor **6**, N⁶-methyl adenosine derivatives **7-16** and 7-deaza-adenine nucleosides **17-26**, on SARS-CoV-2 N7-MTase (Table 2). In parallel, we performed docking experiments against the structure of SARS-CoV-2 nsp14, solved in presence of SAH (PDB 7R2V) using Autodock Vina [41] and compared the calculated ΔG values with the IC₅₀ values determined by FBA upon dose response titration (Table 2).

Briefly, SARS-CoV-2 nsp14 was pre-incubated with increasing concentrations of inhibitors and the MTase activity was measured by FBA. After normalization, the IC₅₀ values were deduced by Hill slope ($Y = 100/[1 + ((X/IC_{50})^{Hillslope})]$) curve-fitting. Interestingly, the C7-substituted-7-deaza-adenine nucleosides **17-26** exhibited a potent inhibitory effect with IC₅₀ values in the subnanomolar or nanomolar range. In average, the series of compounds with the 3-quinoline substitution (**22-26**) showed slightly more potent inhibition than the phenyl-substituted compounds **17-21** and the best compound **26** displays an IC₅₀ value of 0.72 nM. The ΔG obtained from the docking on SARS-CoV-2 N7-MTase also suggests that the presence of a 3-quinoline (**22-26**, average score of -11.4 kcal/mol) is slightly more beneficial than a phenyl (**17-21**, average score -10.4 kcal/mol). Regarding the substitution on the N-alkyl arylsulfonamide moiety, the effect on the IC₅₀ values is the same for these two series (3-CN, 4-OMe > 3-NO₂, 4-OMe > 3-NO₂, 4-Me > 3-NO₂, 4-Br > 3-Cl, 4-Me) and is in agreement with our previous results [23]. Furthermore, if we compare the inhibitory activity of **21** and **26** to that of **MH44**, which all harbor the same N-arylsulfonamide moiety (with 3-CN, 4-OMe as phenyl substituents), we notice that replacing adenine with C7-phenyl or C7-quinoline 7-deaza-adenine significantly increases nsp14 inhibition (16-fold for **21** and 26-fold for **26**). On the

other hand, the replacement of adenine by hypoxanthine in **6** and the methyl on the exocyclic NH₂ (N⁶) of adenine in **7-16** result in a lower inhibitory effect on the nsp14 N7-MTase, as evidenced by their overall higher IC₅₀ values in the micromolar or submicromolar range. These compounds also show higher ΔG values in the docking experiments, as expected (average score of -9.1 kcal/mol).

Table 2

Comparison of ΔG values calculated by Autodock Vina with the IC₅₀ values of 21 most active compounds on SARS-CoV-2 N7-MTase activity.

Compounds	SARS-CoV-2 nsp14 Docking ΔG ^a (kcal/mol)	SARS-CoV-2 nsp14 N7-MTase IC ₅₀ ^b (nM)
Sinefungin	-7.9	360 ^c
MH44 ^d	-8.7	19 ± 2
6	-8.3	4000 ± 2800
7	-9.4	3408 ± 1837
8	-9.0	2850 ± 1467
9	-9.8	2180 ± 120
10	-9.0	573 ± 122
11	-9.6	468 ± 150
12	-9.1	383 ± 56
13	-8.7	187 ± 46
14	-9.1	130 ± 89
15	-8.3	274 ± 165
16	-8.9	62 ± 2
17	-10.2	17.3 ± 0.6
18	-10.9	9.5 ± 0.6
19	-10.5	25.6 ± 10
20	-10.1	2.8 ± 1.2
21	-10.1	1.2 ± 0.25
22	-12.0	3.5 ± 1.8
23	-10.9	2.1 ± 1.3
24	-11.1	2.07 ± 0.5
25	-11.3	1.3 ± 1
26	-11.5	0.72 ± 0.4

^aThe docking was performed on the SARS-CoV-2 nsp14 (PDB 7R2V). The ΔG value corresponds to the best pose showing a good fitting between the SAH and the nucleobase of the compounds. ^bConcentration inhibiting MTase activity by 50%; mean value from three independent experiments. ^cvalue from the literature [14]. The MTase activity for IC₅₀ determinations was measured using a filter binding assay. ^d**MH44** was the best inhibitor of SARS-CoV-2 N7-MTase in our previous work [23].

We next determined the selectivity of the best inhibitors of each series on SARS-CoVs and MERS-CoV N7-MTases (Table 3). The IC₅₀ values of compounds **11**, **16**, **21** and **26** on these

MTases show a similar range of *N7*-MTase inhibition demonstrating that these inhibitors might have pan-CoV activity, whereas they are barely active on the cognate hRNMT and not active on NS5 of DV3, confirming their selectivity toward a large range of CoV *N7*-MTases. Remarkably, compounds **21** and **26** inhibit SARS-CoV-2 nsp14 with 47 000- and 230 000-fold much higher selectivity over h*N7*-MTase, respectively, compared to the previous inhibitor **MH44**, which was 2800-fold more selective.

Moreover, a dose-response assay showed no inhibition of SARS-CoV-2 2'-O-MTase (nsp10/nsp16 complex) by compounds **11**, **21** and **26** and a moderate inhibition by *N*⁶-methyl adenine derivative **16** (IC₅₀ 76.9 μM) confirming that these four compounds are highly selective in targeting CoV *N7*-MTases.

Table 3

Comparison of IC₅₀ values of the most active compounds of each series on SARS-CoV, SARS-CoV-2, MERS-CoV, DV3 and human *N7*-MTase activities

Compounds	IC ₅₀ ^a (nM)				
	SARS-CoV-2 nsp14	SARS-CoV nsp14	MERS-CoV nsp14	Human RNMT	DV3 NS5
11	468 ± 150	3994 ± 700	9766 ± 5600	56166 ± 7100	n.i
16	62 ± 2	51.7 ± 32	471.9 ± 147	16100 ± 3860	n.i
21	1.2 ± 0.25	0.8 ± 0.5	1.25 ± 0.25	56500 ± 17930	n.i
26	0.72 ± 0.4	0.141 ± 0.02	2.7 ± 0.8	165300 ± 30700	n.i

^aConcentration inhibiting MTase activity by 50%; mean value from three independent experiments. The MTase activity for IC₅₀ determinations was measured using a filter binding assay as described above. n.i: no inhibition.

2.5. Structural basis for compound selectivity

Molecular modeling experiments of the best inhibitors of each series (compounds **6**, **11**, **16**, **21** and **26**) were further analyzed in order to rationalize their mode of action. Fig. 2 shows that the *C7*-phenyl and *C7*-quinoline 7-deaza-adenine in compounds **21** (panel D) and **26** (panel E) perfectly overlay the adenine nucleobase of SAH present in the structure of SARS-CoV-2 nsp14 (PDB 7R2V). Similar results were obtained in our docking experiments based on the structure of the SARS-CoV nsp14-nsp10 complex solved in the presence of SAM (PDB 5C8T) [23], which shares 95% sequence identity with SARS-CoV-2 nsp14. The amine moiety on the adenine base makes a key interaction with the backbone carbonyl of Tyr368 (Fig. 2D, 2E and 2F), which is lost in the *N*⁶-methyl adenosine derivatives **7-16** (Fig. 2B and 2C) and in the

inosine analogues **1-6** (Fig. 2A). These modifications of N^6 -NH₂ in compounds **1-16** likely impact the orientation of the nucleobase that does not superpose to SAH anymore, and give lower docking scores (Table 2).

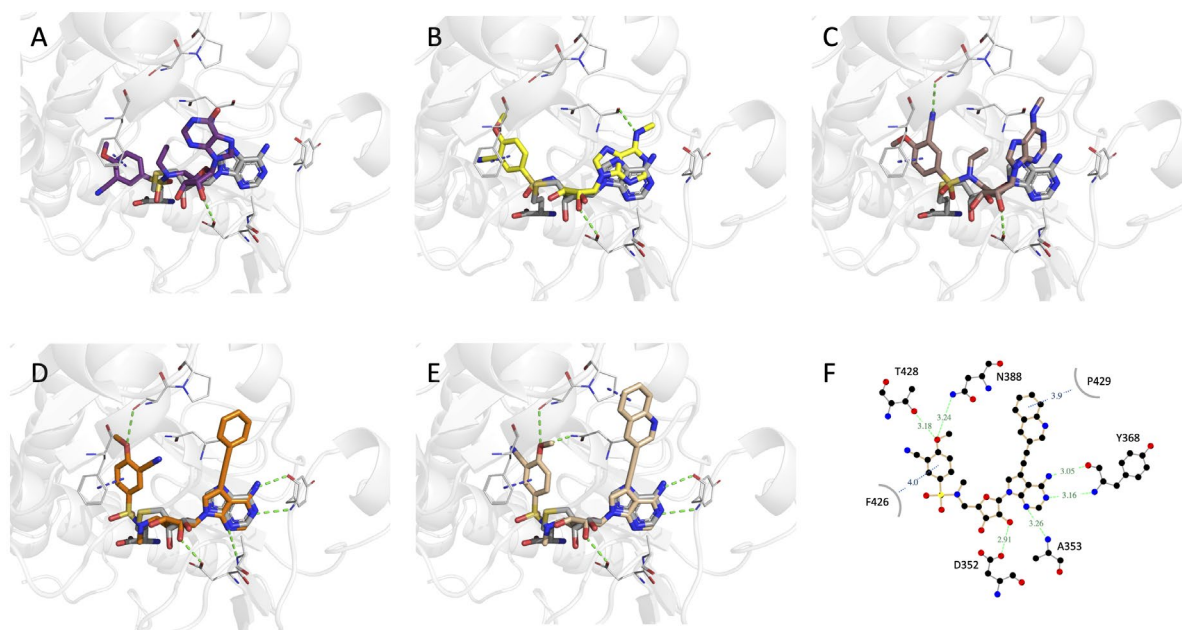


Fig. 2. Overlay of the best inhibitors of each series and the SAH molecule present in the structure of SARS-CoV-2 nsp14. The protein is represented in light grey cartoon, the main residues interacting with the inhibitors are shown in light grey lines. SAH is shown in dark grey sticks. Hydrogen bonds between the inhibitors and the protein are highlighted in green, π -stacking interactions are shown in blue. **A.** Compound **6** (purple sticks). **B.** Compound **11** (yellow sticks). **C.** Compound **16** (light brown sticks). **D.** Compound **21** (orange sticks). **E.** Compound **26** (beige sticks). **F.** 2D representation of the predicted interactions between the best inhibitor **26** and SARS-CoV-2 nsp14.

The *C7*-substituted-7-deaza-adenine nucleosides **17-26** show the best inhibition profile and the docking studies reveal that the phenyl group in **21** and the 3-quinoline substitution in **26** protrude into the SAM entry tunnel present in the SARS-CoV and SARS-CoV-2 structures (Fig. 3A, top and middle panels and Fig. S1). Additionally, the 3-quinoline substitution in **26** makes a pseudo π -stacking interaction with Pro429 (Fig. 2F) which was not observed with the phenyl group in **21**. On the other hand, the SAM entry tunnel is absent in the cognate hRNMT structure, while the presence of an extra helix likely induces a steric clash with the phenyl or 3-quinoline moieties (Fig. 3A, bottom panel). This may participate in the selective inhibition observed on CoV-MTase activities, compared to the weak inhibition of its human ortholog hRNMT. It is worth noting that the apo structure of SARS-CoV-2 nsp14 lacking the SAM/SAH (PDB 7QGI) reveals the presence of a flexible loop (Gln354 – Thr378) closing the SAM entry gate [28], which clashes with compounds **21** and **26**, suggesting that these inhibitors could block the CoV *N7*-MTase in an open conformation (Fig. 3B).

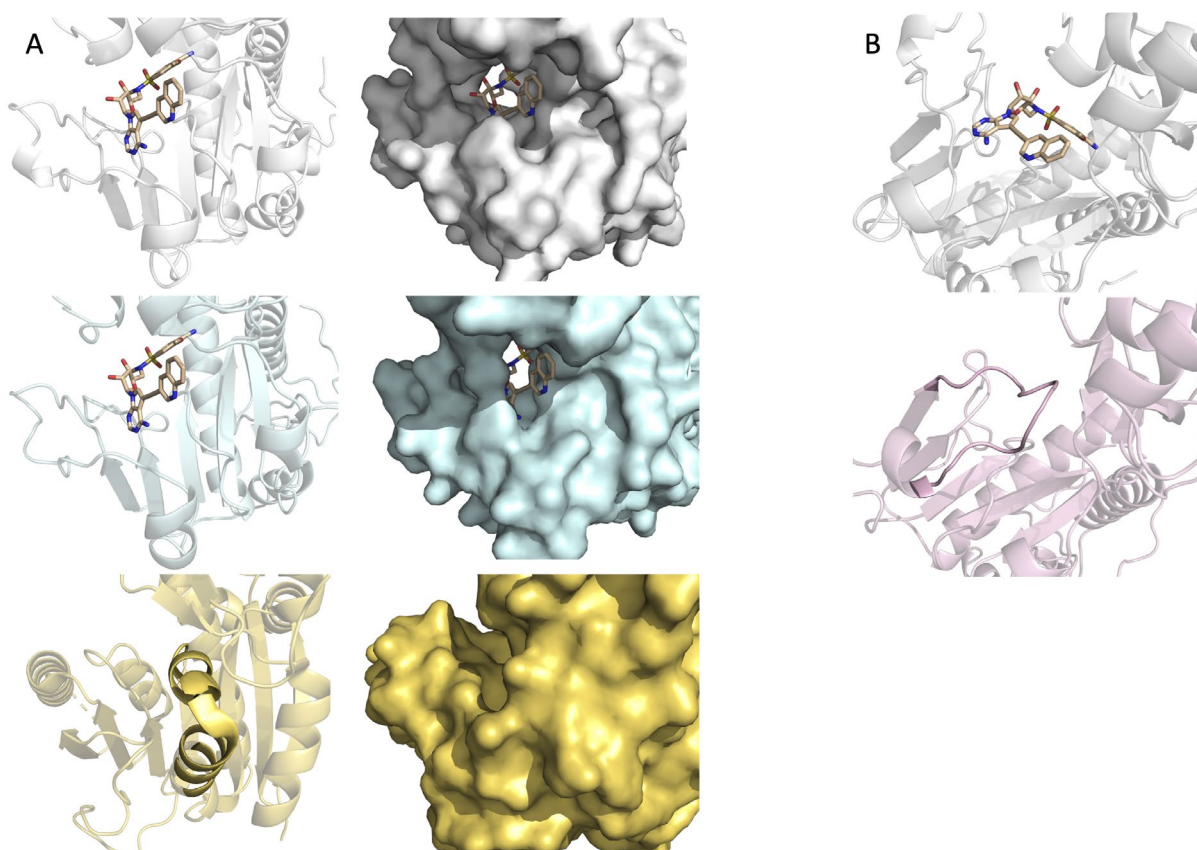


Fig. 3. A. Model of **26** (beige sticks) binding to SARS-CoV-2 nsp14 (PDB 7R2V, grey, top panel) or to SARS-CoV nsp14 (PDB 5C8T, teal, middle panel), showing the 3-quinoline moiety protruding from the SAM entry tunnel, which is absent in the human ortholog enzyme N7-methyltransferase (PDB 3BGV, yellow, bottom panel). **B.** Comparison of the structure of SARS-CoV-2 nsp14 (PDB 7R2V, grey cartoon) bound to **26** (beige sticks) with the apo structure (PDB 7QGI, light pink cartoon), showing the presence of a flexible loop closing the SAM entry gate.

On the 5' side of the nucleoside inhibitors, the phenyl moiety substituted in *meta* (NO₂, CN, or Cl) and *para* (Me, OMe and Br) positions sits in the cap binding pocket and makes a π - π stacking interactions with Phe426 ($d = 3.6 - 4 \text{ \AA}$), as previously reported (Fig. 2, blue dashes) [23]. Additionally, the docking poses of the two best inhibitors **21** and **26** suggest potential interactions of the methoxy substituent with the side-chains of Gln388 and Thr428 (Fig. 2D, 2E and 2F).

2.6. SARS-CoV-2 inhibition assay in Vero E6 TMPRSS2 cells

To assess whether the inhibitory activity observed in SARS-CoV-2 N7-MTase nsp14 inhibition assays translates to viral replication inhibition, the antiviral activity of the best nsp14 inhibitors **17-26** ($0.72 \text{ nM} < IC_{50} < 25.6 \text{ nM}$) was evaluated in cell culture in a viral RNA yield reduction assay using qRT-PCR for viral RNA quantification [42-45]. A dose-response inhibition assay was performed with compounds concentrations from $0.4 \text{ }\mu\text{M}$ to $10 \text{ }\mu\text{M}$ in Vero

E6 TMPRSS2 cells infected with SARS-CoV-2 (BavPat; lineage B.1) (Fig. 4A). The results of this study reveal that most of the compounds exhibited no cytotoxicity for the cells at concentrations up to 10 μ M (Fig. 4B). Compounds **22-26** containing C7-quinolin-ethynyl 7-deaza-adenine moieties showed a moderate activity reaching barely 50% of viral inhibition at 10 μ M concentration in comparison with compounds **17-21** with a phenyl-ethynyl substituent at C7 of adenine that did not display any inhibitory activity (Fig. 4A). The antiviral effect at 10 μ M concentration, albeit weak, suggests that compounds **22-26** were able to enter, at least partly, VeroE6 TMPRSS2 cells to mediate inhibition of SARS-CoV-2 replication.

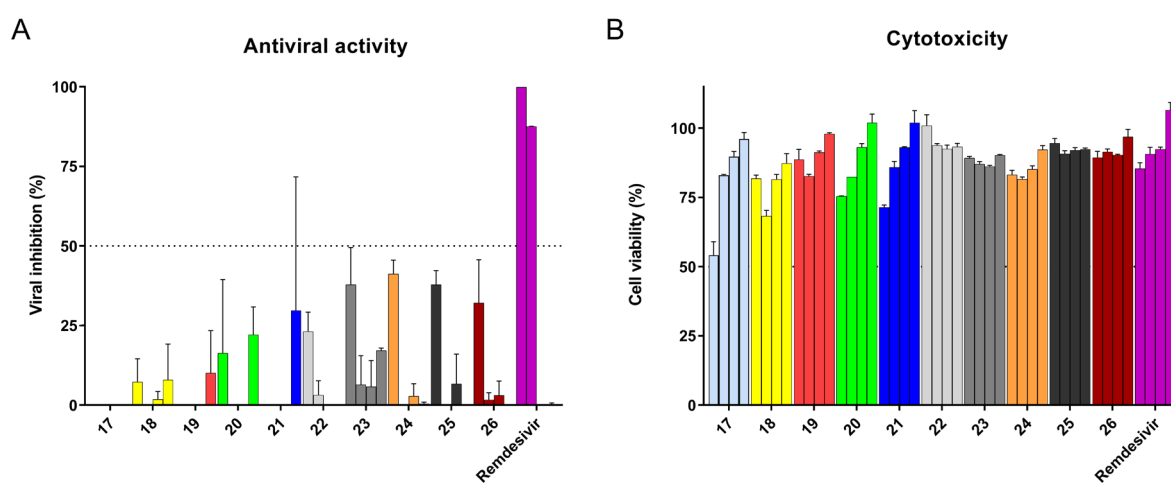


Fig. 4. Dose-response assay on compounds **17-26** on (A) SARS-CoV-2 (B.1) viral inhibition in % of untreated infected control and (B) Vero E6 TMPRSS2 cell viability in % of untreated control. These experiments were performed in duplicate at four concentrations: 10 μ M, 3.3 μ M, 1.1 μ M and 0.4 μ M (from left to right bars). Remdesivir was used as a positive control with the same concentrations.

Our results and the various studies published in the last two years on SARS-CoV-2 nsp14 inhibitors did not reveal any significant antiviral activity, which was unexpected given the potent nanomolar to subnanomolar inhibitions obtained on the purified enzyme [21-25]. Several hypotheses could explain the moderate inhibition observed. The poor activity could result either delivery issue to the viral replication site or from the early metabolism of the compounds in the cells before they reach their target. Nevertheless, a recent study on compounds of similar chemical structure showed that they were stable in plasma and in human liver S9 fraction containing microsomal and cytosolic enzymes [24]. Finally, even several reverse genetic studies have demonstrated that SARS-CoV-2 replication is strongly impaired by mutagenesis of the N7-MTase catalytic site [11], it cannot be ruled out that the antiviral effect of these mutations results from an unidentified nsp14 function and that the nsp14 N7-MTase activity is

not absolutely required for viral replication in our cell system. Further work is now needed to address these different possibilities.

3. Conclusion

Altogether, the SAR presented in this work demonstrates the possibility to optimize the inhibitory activity of adenosine-derived compounds, based on the SAM-bound SARS nsp14 crystal structures. By combining the substitution of the nucleobase at the *C7* position with modifications on the ribose mimicking the GTP moiety, we obtained a series of compounds inhibiting the *N7*-MTase activity of SARS-CoV-2 nsp14 at nanomolar concentrations and one compound with subnanomolar IC_{50} . The nanomolar inhibitions obtained with 7-deaza adenosine analogues as SAH mimetics are consistent with the results of Nencka et al. [22]. It is noteworthy that for the first time, the subnanomolar range could be reached by our scaffold combining the 5'-deoxy 5'-(*N*-methyl *N*-arylsulfonamide) moiety with *C7*-quinolin-ethynyl 7-deaza-adenine. Docking analyses suggest that *C7*-adenine nucleobase superimposes perfectly with the adenine of the SAM in the nsp14 structures, while the 3-quinoline or the phenyl substituent on the nucleobase protrudes into the SAM entry channel. These substituents may thus block the mobile loop that controls the SAM entry gate in its open position and prevent SAM access to the MTase substrate [28].

Because the nsp14 protein from SARS-CoV, SARS-CoV-2 and MERS-CoV share a similar structural organization, we hypothesized that our compounds might have pan-CoV inhibitory activity. This was confirmed by demonstrating that the best compounds inhibit SARS-CoV, SARS CoV-2 and MERS-CoV nsp14 *N7*-MTase activity. In the event of the emergence of a new coronavirus that would lead to a potential pandemic, the development of pan-CoV inhibitors appears to be essential and our original inhibitors fit into this class. Conversely, we did not observe any inhibition of dengue virus NS5 MTase activity and the human *N7*-MTase involved in RNA capping is barely inhibited by our compounds, thus demonstrating their selectivity. The lack of inhibition of human *N7*-MTase is probably related to its different structural organization, as the SAM entry tunnel and the mobile loop recently described for nsp14 are absent in the human ortholog.

This SAR study thus led to a new series of compounds that inhibit *N7*-MTases of coronaviruses with subnanomolar to nanomolar activity, while sparing the cognate human *N7*-MTase. The potent and selective inhibition of these adenosine mimetics on SARS-CoVs and MERS-CoV *N7*-MTases argues for further work to enable their internalization into cells

towards DMV, the stability of compounds upon intracellular penetration and demonstrate cellular antiviral activity against CoVs.

4. Experimental section

4.1. Chemistry

4.1.1. General procedures.

All dry solvents and reagents were purchased from commercial suppliers and were used without further purification. Thin-layer chromatography (TLC) analyses were carried out on silica plate 60 F₂₅₄. Purifications by column chromatography were performed using Biotage Isolera 1 system or Buchi C-815 system with Flash-Pure cartridges (Buchi). NMR experiments were recorded on Bruker 500 or 600 MHz spectrometer at 20 °C. HRMS analyses were obtained with electrospray ionization (ESI) in positive mode on a Q-TOF Micromass spectrometer. Analytical HPLC was performed on a UHPLC ThermoScientific Ultimate 3000 system equipped with a LPG-3400RS pump, a DAD 3000 detector and an WPS-3000TBRS Autosampler, Column Oven TCC-3000SD. Nucleosides **1** – **26** were analyzed by RP-HPLC on a Column Nucleodur C₁₈ ec 100-3, 4.6 x 75 mm (Macherey Nagel) at 30 °C. The following HPLC solvent systems were used: 1% CH₃CN in 50 mM TEAAc (buffer A), 80% CH₃CN in 50 mM TEEAc (buffer B). Flow rate was 1 mL/min. UV detection was performed at 260 nm. Final compounds **1–26** were stored at -20 °C for several months without any degradation.

General method A for the synthesis of compounds 33–38. To a solution of compounds **27–32** [23] in acetic acid/water (85/15 v:v, C = 0.09 M) was added NaNO₂ (15.00 eq). After stirring at 25 °C for 48 h, another NaNO₂ portion (10.00 eq) was added and the mixture was allowed to react at 25 °C for 24 h. After completion of the reaction, the volatiles were removed *in vacuo*, the residue was diluted with AcOEt and washed with water. Aqueous layer was extracted with AcOEt and the combined organic extracts were washed with brine, dried over Na₂SO₄ and concentrated *in vacuo*. The residue was purified by flash column chromatography (dry sample, silica gel, linear gradient 0-5% MeOH in CH₂Cl₂) to give the desired compound as a solid.

5'-deoxy-5'-N-(3-chloro-4-methylbenzenesulfonyl)-2',3'-isopropylideneinosine (33).

Following method A with **27** (163 mg, 0.33 mmol, 1.00 eq), **33** was obtained as an off-white solid (121 mg, 74%). R_f 0.44 (1:9 MeOH/CH₂Cl₂). ¹H-NMR (600 MHz, DMSO-*d*₆) δ 12.43 (s, 1H) ; 8.23 (s, 1H) ; 8.03 (br. s, 1H) ; 8.02 (s, 1H) ; 7.71 (d, J = 1.9 Hz, 1H) ; 7.57 (dd, J = 8.0,

1.9 Hz, 1H) ; 7.49 (d, J = 8.1 Hz, 1H) ; 6.09 (d, J = 2.8 Hz, 1H) ; 5.28 (dd, J = 6.4, 2.8 Hz, 1H) ; 4.88 (dd, J = 6.4, 3.3 Hz, 1H) ; 4.13 (ddd, J = 6.7, 5.5, 3.3 Hz, 1H) ; 3.10 (dd, J = 13.6, 5.6 Hz, 1H) ; 3.03 (dd, J = 13.7, 6.9 Hz, 1H) ; 2.37 (s, 3H) ; 1.50 (s, 3H) ; 1.28 (s, 3H). ¹³C-NMR (150 MHz, DMSO-*d*₆) δ 156.5, 147.4, 145.9, 140.6, 139.5, 139.3, 133.8, 131.8, 126.6, 125.1, 124.8, 113.6, 89.1, 84.5, 83.3, 81.4, 44.4, 26.9, 25.1, 19.7. HRMS (ESI⁺): m/z calcd for C₂₀H₂₃ClN₅O₆S [M+H]⁺: 496.1052, Found 496.1046.

5'-deoxy-5'-N-(3-nitro-4-methoxybenzenesulfonyl)-2',3'-isopropylideneinosine (34).

Following method A with **28** (156 mg, 0.30 mmol, 1.00 eq), **34** was obtained as an off-white solid (123 mg, 79%). R_f 0.54 (1:9 MeOH/CH₂Cl₂). ¹H-NMR (600 MHz, DMSO-*d*₆) δ 12.43 (d, J = 3.9 Hz, 1H) ; 8.25 – 8.18 (m, 2H, H₈) ; 8.10 (t, J = 6.0 Hz, 1H) ; 8.03 (d, J = 3.9 Hz, 1H) ; 7.94 (dd, J = 8.9, 2.3 Hz, 1H) ; 7.46 (d, J = 8.9 Hz, 1H) ; 6.09 (d, J = 2.8 Hz, 1H) ; 5.28 (dd, J = 6.4, 2.9 Hz, 1H) ; 4.88 (dd, J = 6.3, 3.4 Hz, 1H) ; 4.16 – 4.10 (m, 1H) ; 4.00 (s, 3H) ; 3.18 – 3.03 (m, 2H) ; 1.50 (s, 3H) ; 1.28 (s, 3H). ¹³C-NMR (150 MHz, DMSO-*d*₆) δ 156.5, 154.7, 147.4, 146.0, 139.3, 138.4, 132.4, 132.1, 124.8, 123.9, 115.1, 113.7, 89.0, 84.5, 83.3, 81.4, 57.4, 44.4, 26.9, 25.1. HRMS (ESI⁺): m/z calcd for C₂₀H₂₃N₆O₉S [M+H]⁺: 523.1242, Found 523.1223.

5'-deoxy-5'-N-(3-cyano-4-methoxybenzenesulfonyl)-2',3'-isopropylideneinosine (35).

Following method A with **29** (100 mg, 0.20 mmol, 1.00 eq), **35** was obtained as an off-white solid (65 mg, 65%). R_f 0.37 (1:9 MeOH/CH₂Cl₂). ¹H-NMR (500 MHz, DMSO-*d*₆) δ 12.45 (s, 1H) ; 8.22 (s, 1H) ; 8.06 – 7.99 (m, 3H) ; 7.94 (dd, J = 8.7, 2.5 Hz, 1H) ; 7.33 (d, J = 9.0 Hz, 1H) ; 6.08 (d, J = 2.8 Hz, 1H) ; 5.28 (dd, J = 6.5, 2.8 Hz, 1H) ; 4.86 (dd, J = 6.5, 3.3 Hz, 1H) ; 4.12 (td, J = 6.1, 3.5 Hz, 1H) ; 3.98 (s, 3H) ; 3.18 – 3.00 (m, 2H) ; 1.50 (s, 3H) ; 1.28 (s, 3H). ¹³C-NMR (125 MHz, DMSO-*d*₆) δ 163.3, 156.5, 147.5, 146.0, 139.3, 133.4, 132.9, 132.4, 124.8, 115.1, 113.7, 112.9, 100.9, 89.0, 84.5, 83.4, 81.4, 57.1, 44.4, 26.9, 25.2. HRMS (ESI⁺): m/z calcd for C₂₁H₂₃N₆O₇S [M+H]⁺: 503.1343, Found 503.1346.

5'-deoxy-5'-N-(ethyl)-(3-chloro-4-methylbenzenesulfonyl)-2',3'-isopropylideneinosine (36).

Following method A with **30** (135 mg, 0.26 mmol, 1.00 eq), **36** was obtained as an off-white solid (81 mg, 60%). R_f 0.45 (1:9 MeOH/CH₂Cl₂). ¹H-NMR (600 MHz, DMSO-*d*₆) δ 12.45 (s, 1H) ; 8.28 (s, 1H) ; 8.09 (s, 1H) ; 7.70 (d, J = 1.9 Hz, 1H) ; 7.58 (dd, J = 8.0, 1.9 Hz, 1H) ; 7.50 (d, J = 8.2 Hz, 1H) ; 6.17 (d, J = 2.3 Hz, 1H) ; 5.37 (dd, J = 6.4, 2.4 Hz, 1H) ; 5.01 (dd, J = 6.4, 3.3 Hz, 1H) ; 4.28 (ddd, J = 8.4, 5.4, 3.4 Hz, 1H) ; 3.55 (dd, J = 14.7, 5.3 Hz, 1H) ; 3.33 – 3.26 (m, 1H) ; 3.18 – 3.06 (m, 2H) ; 2.37 (s, 3H) ; 1.52 (s, 3H) ; 1.32 (s, 3H) ; 0.87 (t, J = 7.1 Hz,

3H). ¹³C-NMR (150 MHz, DMSO-*d*₆) δ 156.5, 147.5, 146.0, 141.0, 139.5, 138.6, 134.0, 132.0, 126.8, 125.5, 124.8, 113.5, 89.1, 84.9, 83.4, 81.8, 48.9, 43.3, 26.9, 25.2, 19.7, 13.4. HRMS (ESI⁺): m/z calcd for C₂₂H₂₇ClN₅O₆S [M+H]⁺: 524.1365, Found 524.1369.

5'-deoxy-5'-N-(ethyl)-(3-nitro-4-methoxybenzenesulfonyl)-2',3'-isopropylideneinosine (37).

Following method A with **31** (100 mg, 0.18 mmol, 1.00 eq), **37** was obtained as an off-white solid (59 mg, 59%). R_f 0.56 (1:9 MeOH/CH₂Cl₂). ¹H-NMR (600 MHz, DMSO-*d*₆) δ 12.45 (s, 1H); 8.27 (s, 1H); 8.22 (d, J = 2.4 Hz, 1H); 8.08 (s, 1H); 7.96 (dd, J = 9.0, 2.4 Hz, 1H); 7.44 (d, J = 9.1 Hz, 1H); 6.17 (d, J = 2.5 Hz, 1H); 5.36 (dd, J = 6.4, 2.4 Hz, 1H); 5.00 (dd, J = 6.5, 3.5 Hz, 1H); 4.29 (ddd, J = 8.5, 5.3, 3.4 Hz, 1H); 4.00 (s, 3H); 3.57 (dd, J = 14.9, 5.3 Hz, 1H); 3.35 – 3.28 (m, 1H); 3.20 – 3.05 (m, 2H); 1.52 (s, 3H); 1.31 (s, 3H); 0.88 (t, J = 7.1 Hz, 3H). ¹³C-NMR (150 MHz, DMSO-*d*₆) δ 156.5, 154.7, 147.5, 146.1, 139.5, 138.8, 132.7, 131.0, 124.8, 124.0, 115.1, 113.6, 89.0, 84.9, 83.5, 81.8, 57.4, 48.9, 43.4, 26.9, 25.2, 13.4. HRMS (ESI⁺): m/z calcd for C₂₂H₂₇N₆O₉S [M+H]⁺: 551.1541, Found 551.1538.

5'-deoxy-5'-N-(ethyl)-(3-cyano-4-methoxybenzenesulfonyl)-2',3'-isopropylideneinosine (38).

Following method A with **32** (75 mg, 0.14 mmol, 1.00 eq), **38** was obtained as an off-white solid (60 mg, 80%). R_f 0.43 (1:9 MeOH/CH₂Cl₂). ¹H-NMR (500 MHz, DMSO-*d*₆) δ 8.27 (s, 1H); 8.13 (d, J = 2.3 Hz, 1H); 8.08 (s, 1H); 7.96 (dd, J = 9.0, 2.3 Hz, 1H); 7.31 (d, J = 9.0 Hz, 1H); 6.16 (d, J = 2.3 Hz, 1H); 5.36 (dd, J = 6.4, 2.3 Hz, 1H); 4.99 (dd, J = 6.4, 3.4 Hz, 1H); 4.28 (dt, J = 8.4, 4.3 Hz, 1H); 3.99 (s, 3H); 3.56 (dd, J = 14.8, 5.2 Hz, 1H); 3.34 – 3.26 (m, 1H); 3.11 (dp, J = 25.0, 7.3 Hz, 2H); 1.53 (s, 3H); 1.32 (s, 3H); 0.86 (t, J = 7.0 Hz, 3H). ¹³C-NMR (125 MHz, DMSO-*d*₆) δ 163.5, 156.8, 148.6, 146.4, 139.4, 133.8, 132.7, 131.9, 124.8, 115.0, 113.6, 112.9, 101.2, 89.0, 85.1, 83.4, 81.8, 57.2, 48.9, 43.4, 26.9, 25.2, 13.4. HRMS (ESI⁺): m/z calcd for C₂₃H₂₇N₆O₇S [M+H]⁺: 531.1656, Found 531.1667.

2',3'-isopropylidene-7-phenylethynyl-7-deazaadenosine (53).

Et₃N (968 μl, 6.94 mmol, 3.00 eq) and phenylacetylene (508 μl, 4.63 mmol, 2.00 eq) were added to a solution of **52** (1.00 g, 2.31 mmol, 1.00 eq) in THF (C = 0.066 M) under argon. After stirring for 30 min, under an argon flow, CuI (132 mg, 0.69 mmol, 0.30 eq) and Pd(PPh₃)₄ (267 mg, 0.23 mmol, 0.10 eq) were added. After stirring for 2 h at 60°C, silica was added to the mixture and all the volatiles were removed *in vacuo*. The crude was purified by flash column chromatography (dry sample, silica gel, linear gradient 0-5% MeOH in AcOEt) to give **53** as a colorless foam (801 mg, 85%). R_f = 0.63 (1:9 MeOH/AcOEt). ¹H-NMR (600 MHz, DMSO-*d*₆) δ 8.20 (br. s, 1H); 7.91 (s, 1H); 7.63 – 7.55 (m, 2H); 7.47 – 7.38 (m, 3H); 6.24 (d, J = 3.3 Hz,

1H) ; 5.20 – 5.13 (m, 2H) ; 4.93 (dd, J = 6.2, 2.8 Hz, 1H) ; 4.16 (td, J = 4.6, 2.8 Hz, 1H) ; 3.62 – 3.52 (m, 2H) ; 1.55 (s, 3H) ; 1.32 (s, 3H). ¹³C-NMR (150 MHz, DMSO-*d*₆) δ 157.7, 153.0, 149.5, 131.1, 128.7, 128.5, 127.2, 127.2, 122.4, 113.1, 102.1, 95.1, 91.2, 89.0, 85.7, 83.7, 82.7, 81.0, 61.6, 27.1, 25.2. HRMS (ESI+): m/z calcd for C₂₂H₂₃N₄O₄ [M+H]⁺: 407.1714, Found 407.1707.

2',3'-isopropylidene-7-(quinolin-3-ethynyl)-7-deazaadenosine (54).

To a solution of **52** (1.00 g, 2.31 mmol, 1.00 eq) in THF (C = 0.066 M) under argon, were added Et₃N (968 μl, 6.94 mmol, 3.00 eq) and 3-ethynylquinoline (709 mg, 4.63 mmol, 2.00 eq). After stirring for 30 min under an argon flow, CuI (132 mg, 0.69 mmol, 0.30 eq) and Pd(PPh₃)₄ (267 mg, 0.23 mmol, 0.10 eq) were added. After stirring for 2 h at 60°C, silica was added to the mixture and all the volatiles were removed *in vacuo*. The residue was purified by flash column chromatography (dry sample, silica gel, linear gradient 0-5% MeOH in AcOEt) to give **54** as a colorless foam (1.01 g, 95%). R_f = 0.57 (1:9 MeOH/AcOEt). ¹H-NMR (600 MHz, DMSO-*d*₆) δ 9.04 (d, J = 2.2 Hz, 1H) ; 8.65 (d, J = 2.1 Hz, 1H) ; 8.19 (s, 1H) ; 8.05 (dd, J = 8.4, 1.0 Hz, 1H) ; 8.06 - 7.98 (m, 2H) ; 7.80 (ddd, J = 8.5, 6.9, 1.5 Hz, 1H) ; 7.67 (ddd, J = 8.0, 6.8, 1.2 Hz, 1H) ; 6.26 (d, J = 3.2 Hz, 1H) ; 5.23 – 5.16 (m, 2H) ; 4.95 (dd, J = 6.2, 2.9 Hz, 1H) ; 4.18 (td, J = 4.6, 2.8 Hz, 1H) ; 3.64 – 3.53 (m, 2H) ; 1.55 (s, 3H) ; 1.33 (s, 3H). ¹³C-NMR (150 MHz, DMSO-*d*₆) δ 157.6, 153.1, 151.6, 149.6, 146.2, 138.0, 130.3, 128.8, 128.0, 128.0, 127.5, 126.9, 116.8, 113.1, 101.9, 94.7, 89.1, 88.8, 85.9, 85.8, 83.8, 81.1, 61.6, 27.1, 25.2. HRMS (ESI+): m/z calcd for C₂₅H₂₄N₅O₄ [M+H]⁺: 458.1823, Found 458.1826.

5'-deoxy-5'-methylamino-2',3'-isopropylidene-7-phenylethynyl-7-deazaadenosine (55).

Methanesulfonyl chloride (228 μL, 2.95 mmol, 1.20 eq) was added dropwise to a solution of **53** (1.00 g, 2.46 mmol, 1.00 eq) and Et₃N (755 μl, 5.41 mmol, 2.20 eq) in anhydrous CH₂Cl₂ (35.1 mL, C = 0.07 M) at -10 °C under argon. After stirring at -10° C for 30 min, the reaction mixture was diluted with a saturated NH₄Cl solution. The aqueous layer was extracted with CH₂Cl₂ and the combined organic extracts were washed with brine, dried over Na₂SO₄ and concentrated *in vacuo*. The residue was purified by flash column chromatography (liquid sample, silica gel, linear gradient 0-50% acetone in CH₂Cl₂) to give the mesylate compound as a colorless foam (950 mg, 80%). R_f = 0.54 (1:1 acetone/CH₂Cl₂). After drying under reduce pressure, the mesylate compound (870 mg, 1.80 mmol) was treated with a solution of 2M MeNH₂ in THF (18.0 mL, C = 0.1M) in a sealed vessel at 50 °C for 72 h. The mixture was concentrated *in vacuo*, the residue was diluted with AcOEt and brine. Aqueous layer was extracted with AcOEt and the combined organic extracts were washed with brine, dried over

Na₂SO₄ and concentrated *in vacuo*. The residue was purified by flash column chromatography (liquid sample, silica gel, linear gradient 0-12% MeOH in CH₂Cl₂ 1% NEt₃) to give **55** as a foam (416 mg, 55%). $R_f = 0.01$ (1:9 MeOH/CH₂Cl₂). ¹H-NMR (500 MHz, DMSO-*d*₆) δ 8.18 (s, 1H) ; 7.90 (s, 1H) ; 7.62 – 7.56 (m, 2H) ; 7.48 – 7.38 (m, 3H) ; 6.18 (d, J = 3.1 Hz, 1H) ; 5.25 (dd, J = 6.5, 3.2 Hz, 1H) ; 4.91 (dd, J = 6.5, 3.3 Hz, 1H) ; 4.15 (dt, J = 6.2, 3.7 Hz, 1H) ; 2.76 – 2.64 (m, 2H) ; 2.29 (s, 3H) ; 1.53 (s, 3H) ; 1.31 (s, 3H). ¹³C-NMR (125 MHz, DMSO-*d*₆) δ 157.7, 153.1, 149.6, 131.1, 128.7, 128.6, 127.4, 127.2, 122.4, 113.4, 102.1, 95.2, 91.3, 88.6, 84.0, 83.3, 82.7, 81.9, 53.2, 36.1, 27.1, 25.2. HRMS (ESI+): m/z calcd for C₂₃H₂₆N₅O₃ [M+H]⁺: 420.2030, Found 420.2040.

5'-deoxy-5'-methylamino-2',3'-isopropylidene-7-(quinolin-3-ethynyl)-7-deazaadenosine (56)
Methanesulfonyl chloride (205 μL, 2.65 mmol, 1.20 eq) was added dropwise to a solution of **54** (1.01 g, 2.21 mmol, 1.00 eq) and Et₃N (679 μl, 4.87 mmol, 2.20 eq) in anhydrous CH₂Cl₂ (31.6 mL, C = 0.07 M) at -10 °C under argon. After stirring at -10° C for 30 min, the reaction mixture was diluted with a saturated NH₄Cl solution. The aqueous layer was extracted with CH₂Cl₂ and the combined organic extracts were washed with brine, dried over Na₂SO₄ and concentrated *in vacuo*. The residue was purified by flash column chromatography (liquid sample, silica gel, linear gradient 0-50% acetone in CH₂Cl₂) to give the mesylate intermediate as a colorless foam (1.03 g, 87%). $R_f = 0.43$ (1:1 acetone/CH₂Cl₂). After drying, the mesylate compound (1.03 g, 1.92 mmol) was treated with a 2M MeNH₂ solution in THF (19.2 mL, C = 0.1M) in a sealed vessel at 50 °C for 72 h. After completion of the reaction, the mixture was concentrated *in vacuo*, the residue was diluted with AcOEt and brine. Aqueous layer was extracted with AcOEt and the combined organic extracts were washed with brine, dried over Na₂SO₄ and concentrated *in vacuo*. The residue was purified by flash column chromatography (liquid sample, silica gel, linear gradient 0-12% MeOH in CH₂Cl₂ 1% NEt₃) to give **56** as a foam (280 mg, 31%). $R_f = 0.02$ (1:9 MeOH/CH₂Cl₂). ¹H-NMR (600 MHz, DMSO-*d*₆) δ 9.04 (d, J = 2.1 Hz, 1H) ; 8.65 (d, J = 2.3 Hz, 1H) ; 8.20 (s, 1H) ; 8.05 (dd, J = 8.5, 1.0 Hz, 1H, H_{Quin}) ; 8.03 - 7.97 (m, 2H) ; 7.81 (ddd, J = 8.5, 6.9, 1.4 Hz, 1H) ; 7.67 (ddd, J = 8.1, 6.7, 1.2 Hz, 1H) ; 6.20 (d, J = 3.3 Hz, 1H) ; 5.27 (dd, J = 6.4, 3.3 Hz, 1H) ; 4.91 (dd, J = 6.4, 3.3 Hz, 1H) ; 4.16 (td, J = 5.9, 3.3 Hz, 1H) ; 2.75 – 2.63 (m, 2H) ; 2.28 (s, 3H) ; 1.54 (s, 3H) ; 1.32 (s, 3H). ¹³C-NMR (150 MHz, DMSO-*d*₆) δ 157.6, 153.2, 151.7, 149.7, 146.2, 138.0, 130.4, 128.8, 128.2, 128.0, 127.5, 126.9, 116.9, 113.4, 101.9, 94.9, 88.8, 88.7, 85.9, 84.2, 83.3, 82.0, 53.4, 36.3, 27.1, 25.2. HRMS (ESI+): m/z calcd for C₂₆H₂₇N₆O₃ [M+H]⁺: 471.2139, Found 471.2134.

General method B for the synthesis of compounds 40–44, 57–61, 62–66. To a solution of **39** obtained according to described procedures [32, 33], **55** or **56** (1.00 eq) in anhydrous DMF ($C = 0.1$ M) were added Et_3N (2.00 eq) and the corresponding benzenesulfonyl chloride reactant (1.25 eq) in three portions at -10 °C under argon. After stirring at -10 °C for 1.5–3 h, the reaction mixture was diluted with AcOEt and washed with brine. The aqueous layer was extracted with AcOEt and the combined organic extracts were washed with a 2M LiCl solution and brine, dried over Na_2SO_4 and concentrated *in vacuo*. The residue was purified by flash column chromatography to give the desired compound as a solid.

5'-deoxy-5'-N-(3-nitro-4-bromobenzenesulfonyl)-2',3'-isopropylidene-N6-methyladenosine (40).

Following method B with **39** (400 mg, 1.25 mmol, 1.00 eq) and 4-bromo-3-nitrobenzenesulfonyl chloride (469 mg, 1.56 mmol, 1.25 eq), **40** was obtained as a white foam (450 mg, 62%). R_f 0.67 (1:1 acetone/ CH_2Cl_2). $^1\text{H-NMR}$ (500 MHz, $\text{DMSO-}d_6$) δ 8.55 (br. s, 1H); 8.32 (d, $J = 2.1$ Hz, 1H); 8.26 (s, 1H); 8.21 (s, 1H); 8.04 (d, $J = 8.4$ Hz, 1H); 7.87 (br. s, 1H); 7.83 (dd, $J = 8.4, 2.1$ Hz, 1H); 6.12 (d, $J = 2.6$ Hz, 1H); 5.33 (dd, $J = 6.1, 2.6$ Hz, 1H); 4.89 (dd, $J = 6.1, 2.8$ Hz, 1H); 4.16 (td, $J = 6.0, 3.0$ Hz, 1H); 3.24 – 3.15 (m, 2H); 2.95 (s, 3H); 1.50 (s, 3H); 1.27 (s, 3H). $^{13}\text{C-NMR}$ (125 MHz, $\text{DMSO-}d_6$) δ 155.1, 152.7, 149.4, 147.4, 141.2, 139.9, 136.1, 130.9, 123.6, 119.8, 118.0, 113.5, 89.4, 84.4, 83.0, 81.6, 44.5, 27.0, 25.1. HRMS (ESI+): m/z calcd for $\text{C}_{20}\text{H}_{23}\text{BrN}_7\text{O}_7\text{S}$ $[\text{M}+\text{H}]^+$: 584.0558 Found 584.0546.

5'-deoxy-5'-N-(3-nitro-4-methylbenzenesulfonyl)-2',3'-isopropylidene-N6-methyladenosine (41).

Following method B with **39** (400 mg, 1.25 mmol, 1.00 eq) and 4-methyl-3-nitrobenzenesulfonyl chloride (368 mg, 1.56 mmol, 1.25 eq), **41** was obtained as a white foam (522 mg, 80%). R_f 0.53 (1:1 acetone/ CH_2Cl_2). $^1\text{H-NMR}$ (600 MHz, $\text{DMSO-}d_6$) δ 8.38 (br. s, 1H); 8.24 (d, $J = 1.8$ Hz, 1H); 8.23 (s, 1H); 8.19 (s, 1H); 7.86 (dd, $J = 8.1, 1.8$ Hz, 1H); 7.84 (br. s, 1H); 7.58 (d, $J = 8.1, 1\text{H}$); 6.11 (d, $J = 2.8$ Hz, 1H); 5.32 (dd, $J = 6.2, 2.8$ Hz, 1H); 4.90 (dd, $J = 6.2, 2.8$ Hz, 1H); 4.17 (td, $J = 6.1, 3.0$ Hz, 1H); 3.19 (dd, $J = 13.8, 5.2$ Hz, 1H); 3.13 (dd, $J = 13.5, 6.7$ Hz, 1H); 2.96 (s, 3H); 2.55 (s, 3H); 1.50 (s, 3H); 1.28 (s, 3H). $^{13}\text{C-NMR}$ (150 MHz, $\text{DMSO-}d_6$) δ 155.0, 152.6, 148.4, 147.3, 139.9, 139.4, 137.6, 133.9, 130.5, 122.6, 119.8, 113.4, 89.4, 84.4, 83.0, 81.6, 44.5, 26.9, 25.1, 19.7. HRMS (ESI+): m/z calcd for $\text{C}_{21}\text{H}_{26}\text{N}_7\text{O}_7\text{S}$ $[\text{M}+\text{H}]^+$: 520.1609, Found 520.1612.

5'-deoxy-5'-N-(3-chloro-4-methylbenzenesulfonyl)-2',3'-isopropylidene-N6-methyladenosine (42).

Following method B with **39** (400 mg, 1.25 mmol, 1.00 eq) and 3-chloro-4-methylbenzenesulfonyl chloride (351 mg, 1.56 mmol, 1.25 eq), **42** was obtained as a white foam (582 mg, 91%). R_f 0.66 (1:1 acetone/ CH_2Cl_2). $^1\text{H-NMR}$ (600 MHz, $\text{DMSO-}d_6$) δ 8.26 (s, 1H); 8.22 (br. s, 2H); 7.85 (br. s, 1H); 7.68 (d, $J = 1.8$ Hz, 1H); 7.54 (dd, $J = 7.9, 1.7$ Hz, 1H); 7.46 (d, $J = 8.2$ Hz, 1H); 6.12 (d, $J = 2.8$ Hz, 1H); 5.34 (dd, $J = 6.2, 2.8$ Hz, 1H); 4.90 (dd, $J = 6.2, 2.9$ Hz, 1H); 4.16 (td, $J = 5.8, 3.0$ Hz, 1H); 3.15 – 3.04 (m, 2H); 2.96 (s, 3H); 2.35 (s, 3H); 1.51 (s, 3H); 1.28 (s, 3H). $^{13}\text{C-NMR}$ (150 MHz, $\text{DMSO-}d_6$) δ 155.1, 152.6, 147.4, 140.6, 139.9, 139.5, 133.8, 131.9, 126.5, 125.1, 119.9, 113.5, 89.5, 84.3, 82.9, 81.6, 44.5, 26.9, 25.1, 19.6. HRMS (ESI+): m/z calcd for $\text{C}_{21}\text{H}_{26}\text{ClN}_6\text{O}_5\text{S}$ $[\text{M}+\text{H}]^+$: 509.1368, Found 509.1369.

5'-deoxy-5'-N-(3-nitro-4-chlorobenzenesulfonyl)-2',3'-isopropylidene-N6-methyladenosine (43).

Following method B with **39** (500 mg, 1.56 mmol, 1.00 eq) and 4-chloro-3-nitrobenzenesulfonyl chloride (499 mg, 1.95 mmol, 1.25 eq), **43** was obtained as a white foam (524 mg, 62%). R_f 0.65 (1:1 acetone/ CH_2Cl_2). $^1\text{H-NMR}$ (500 MHz, $\text{DMSO-}d_6$) δ 8.55 (br. s, 1H); 8.35 (d, $J = 2.2$ Hz, 1H); 8.25 (s, 1H); 8.21 (s, 1H); 9.94 (dd, $J = 8.5, 2.3$ Hz, 1H); 7.87 (d, $J = 8.3$ Hz, 2H); 6.12 (d, $J = 2.6$ Hz, 1H); 5.33 (dd, $J = 6.2, 2.6$ Hz, 1H); 4.90 (dd, $J = 6.2, 3.0$ Hz, 1H); 4.16 (td, $J = 6.0, 3.1$ Hz, 1H); 3.25 – 3.16 (m, 2H); 2.95 (d, $J = 3.2$ Hz, 3H); 1.50 (s, 3H); 1.27 (s, 3H). $^{13}\text{C-NMR}$ (125 MHz, $\text{DMSO-}d_6$) δ 155.1, 152.7, 147.4, 147.2, 140.6, 139.9, 133.0, 131.2, 129.4, 124.0, 119.8, 113.5, 89.4, 84.4, 83.0, 81.6, 44.5, 27.0, 25.1. HRMS (ESI+): m/z calcd for $\text{C}_{20}\text{H}_{23}\text{ClN}_7\text{O}_7\text{S}$ $[\text{M}+\text{H}]^+$: 540.1063, Found 540.1055.

5'-deoxy-5'-N-(3-cyano-4-fluorobenzenesulfonyl)-2',3'-isopropylidene-N6-methyladenosine (44).

Following method B with **39** (500 mg, 1.56 mmol, 1.00 eq) and 3-cyano-4-fluorobenzenesulfonyl chloride (428 mg, 1.95 mmol, 1.25 eq), **44** was obtained as a white foam (712 mg, 90%). R_f 0.57 (1:1 acetone/ CH_2Cl_2). $^1\text{H-NMR}$ (600 MHz, $\text{DMSO-}d_6$) δ 8.36 (t, $J = 5.6$ Hz, 1H); 8.25 (s, 1H); 8.21 (dd, $J = 5.9, 2.4$ Hz, 2H); 8.02 (ddd, $J = 8.9, 4.9, 2.4$ Hz, 1H); 7.84 (br. s, 1H); 7.59 (t, $J = 8.9$ Hz, 1H); 6.12 (d, $J = 2.7$ Hz, 1H); 5.34 (dd, $J = 6.3, 2.7$ Hz, 1H); 4.91 (dd, $J = 6.2, 2.9$ Hz, 1H); 4.16 (td, $J = 6.5, 3.1$ Hz, 1H); 3.22 – 3.12 (m, 2H); 2.96 (s, 3H); 1.51 (s, 3H); 1.29 (s, 3H). $^{13}\text{C-NMR}$ (150 MHz, $\text{DMSO-}d_6$) δ 165.0, 163.2, 155.0, 152.6, 147.3, 139.9, 137.8, 134.2, 132.0, 119.8, 117.7, 117.6, 113.5, 112.8, 101.4, 101.3, 89.4,

84.4, 82.9, 81.6, 44.5, 26.9, 25.1. HRMS (ESI+): m/z calcd for C₂₁H₂₃FN₇O₅S [M+H]⁺: 504.1460, Found 504.1454.

5'-deoxy-5'-N-(methyl)-(4-bromo-3-nitrobenzenesulfonyl)-2',3'-isopropylidene-7-phenylethynyl-7-deazaadenosine (57).

Following method B with **55** (75 mg, 0.18 mmol, 1.00 eq) and 4-bromo-3-nitrobenzenesulfonyl chloride (67 mg, 0.22 mmol, 1.25 eq), **57** was obtained as an off-white solid (70 mg, 57%). R_f 0.68 (1:9 MeOH/CH₂Cl₂). ¹H-NMR (500 MHz, DMSO-*d*₆) δ 8.33 (d, J = 2.2 Hz, 1H); 8.18 (s, 1H); 8.03 (d, J = 8.3 Hz, 1H); 7.86 (s, 1H); 7.84 (dd, J = 8.4, 2.2 Hz, 1H); 7.61 – 7.56 (m, 2H); 7.47 – 7.37 (m, 3H); 6.20 (d, J = 2.7 Hz, 1H); 5.29 (dd, J = 6.5, 2.7 Hz, 1H); 4.98 (dd, J = 6.5, 3.9 Hz, 1H); 4.26 – 4.20 (m, 1H); 3.50 – 3.44 (m, 1H); 3.31 (dd, J = 14.3, 7.6 Hz, 1H); 2.72 (s, 3H); 1.53 (s, 3H); 1.31 (s, 3H). ¹³C-NMR (125 MHz, DMSO-*d*₆) δ 157.7, 153.2, 149.9, 149.4, 138.0, 136.1, 131.5, 131.2, 128.8, 128.7, 127.8, 124.0, 122.4, 118.4, 113.9, 102.2, 95.4, 91.5, 88.8, 83.6, 83.4, 82.6, 81.6, 51.5, 35.9, 27.0, 25.2. HRMS (ESI+): m/z calcd for C₂₉H₂₈BrN₆O₇S [M+H]⁺: 683.0918, Found 683.0921.

5'-deoxy-5'-N-(methyl)-(4-methyl-3-nitrobenzenesulfonyl)-2',3'-isopropylidene-7-phenylethynyl-7-deazaadenosine (58).

Following method B with **55** (55 mg, 0.12 mmol, 1.00 eq) and 4-methyl-3-nitrobenzenesulfonyl chloride (39 mg, 0.14 mmol, 1.25 eq), **58** was obtained as an off-white solid (77 mg, 95%). R_f 0.74 (1:9 MeOH/CH₂Cl₂). ¹H-NMR (600 MHz, DMSO-*d*₆) δ 8.23 (d, J = 2.1 Hz, 1H); 8.18 (s, 1H); 7.90 (dd, J = 8.0, 2.0 Hz, 1H); 7.87 (s, 1H); 7.65 (d, J = 8.2 Hz, 1H); 7.61 – 7.57 (m, 2H); 7.47 – 7.37 (m, 3H); 6.20 (d, J = 2.7 Hz, 1H); 5.30 (dd, J = 6.6, 2.8 Hz, 1H); 5.00 (dd, J = 6.5, 3.8 Hz, 1H); 4.26 – 4.21 (m, 1H); 3.46 (dd, J = 14.2, 5.4 Hz, 1H); 3.24 (dd, J = 14.2, 7.5 Hz, 1H); 2.70 (s, 3H); 2.55 (s, 1H); 1.53 (s, 3H); 1.32 (s, 3H). ¹³C-NMR (150 MHz, DMSO-*d*₆) δ 157.7, 153.1, 149.3, 148.9, 137.9, 136.1, 134.1, 131.2, 131.0, 128.7, 128.6, 127.8, 123.1, 122.4, 113.8, 102.1, 95.3, 91.3, 88.8, 83.5, 83.4, 82.6, 81.6, 51.4, 35.8, 27.0, 25.2, 19.5. HRMS (ESI+): m/z calcd for C₃₀H₃₁N₆O₇S [M+H]⁺: 619.1970, Found 619.1974.

5'-deoxy-5'-N-(methyl)-(3-chloro-4-methylbenzenesulfonyl)-2',3'-isopropylidene-7-phenylethynyl-7-deazaadenosine (59).

Following method B with **55** (50 mg, 0.12 mmol, 1.00 eq) and 3-chloro-4-methylbenzenesulfonyl chloride (34 mg, 0.15 mmol, 1.25 eq), **59** was obtained as an off-white solid (50 mg, 68%). R_f 0.76 (1:9 MeOH/CH₂Cl₂). ¹H-NMR (600 MHz, DMSO-*d*₆) δ 8.19 (s, 1H); 7.88 (s, 1H); 7.70 (d, J = 1.8 Hz, 1H); 7.61 – 7.55 (m, 3H); 7.53 (d, J = 8.1 Hz, 1H);

7.46 – 7.37 (m, 3H) ; 6.21 (d, J = 2.6 Hz, 1H) ; 5.33 (dd, J = 6.5, 2.7 Hz, 1H) ; 5.02 (dd, J = 6.5, 3.7 Hz, 1H) ; 4.25 – 4.20 (m, 1H) ; 3.42 (dd, J = 14.1, 5.8 Hz, 1H) ; 3.19 – 3.09 (m, 1H) ; 2.66 (s, 3H) ; 2.37 (s, 1H) ; 1.53 (s, 3H) ; 1.32 (s, 3H). ¹³C-NMR (150 MHz, DMSO-*d*₆) δ 157.7, 153.1, 149.4, 141.2, 136.1, 134.1, 132.1, 131.1, 128.7, 128.6, 127.8, 127.0, 125.8, 122.4, 113.6, 102.1, 95.3, 91.3, 88.9, 83.5, 83.4, 82.6, 81.7, 51.4, 35.9, 26.9, 25.2, 19.7. HRMS (ESI+): m/z calcd for C₃₀H₃₁ClN₅O₅S [M+H]⁺: 608.1729, Found 608.1721.

5'-deoxy-5'-N-(methyl)-(4-methoxy-3-nitrobenzenesulfonyl)-2',3'-isopropylidene-7-phenylethynyl-7-deazaadenosine (60).

Following method B with **55** (55 mg, 0.12 mmol, 1.00 eq) and 4-methoxy-3-nitrobenzenesulfonyl chloride (35 mg, 0.14 mmol, 1.25 eq), **60** was obtained as an off-white solid (50 mg, 62%). R_f 0.51 (1:9 MeOH/CH₂Cl₂). ¹H-NMR (600 MHz, DMSO-*d*₆) δ 8.22 (d, J = 2.4 Hz, 1H) ; 8.19 (s, 1H) ; 7.98 – 7.93 (m, 1H) ; 7.88 (s, 1H) ; 7.61 – 7.56 (m, 2H) ; 7.48 (d, J = 9.0 Hz, 1H) ; 7.46 – 7.39 (m, 3H) ; 6.22 (d, J = 2.6 Hz, 1H) ; 5.31 (dd, J = 6.5, 2.7 Hz, 1H) ; 5.00 (dd, J = 6.5, 3.8 Hz, 1H) ; 4.27 – 4.21 (m, 1H) ; 3.99 (s, 1H) ; 3.44 (dd, J = 14.1, 5.6 Hz, 1H) ; 3.20 (dd, J = 14.1, 7.3 Hz, 1H) ; 2.67 (s, 3H) ; 1.53 (s, 3H) ; 1.32 (s, 3H). ¹³C-NMR (150 MHz, DMSO-*d*₆) δ 157.7, 154.9, 153.1, 149.3, 138.9, 133.0, 131.2, 128.7, 128.6, 127.8, 124.3, 122.4, 115.2, 113.7, 102.1, 95.3, 91.3, 88.8, 83.6, 83.4, 82.6, 81.6, 57.4, 51.4, 36.0, 27.0, 25.2. HRMS (ESI+): m/z calcd for C₃₀H₃₁N₆O₈S [M+H]⁺: 635.1919, Found 635.1915.

5'-deoxy-5'-N-(methyl)-(3-cyano-4-fluorobenzenesulfonyl)-2',3'-isopropylidene-7-phenylethynyl-7-deazaadenosine (61).

Following method B with **55** (100 mg, 0.24 mmol, 1.00 eq) and 3-cyano-4-fluorobenzenesulfonyl chloride (65 mg, 0.30 mmol, 1.25 eq), **61** was obtained as an off-white solid (128 mg, 89%). R_f 0.54 (1:9 MeOH/CH₂Cl₂). ¹H-NMR (500 MHz, DMSO-*d*₆) δ 8.36 (dd, J = 5.9, 2.4 Hz, 1H) ; 8.19 (s, 1H) ; 8.08 (ddd, J = 8.9, 4.9, 2.4 Hz, 1H) ; 7.88 (s, 1H) ; 7.66 (t, J = 8.9 Hz, 1H) ; 7.61 – 7.57 (m, 2H) ; 7.47 – 7.37 (m, 3H) ; 6.21 (d, J = 2.7 Hz, 1H) ; 5.31 (dd, J = 6.5, 2.7 Hz, 1H) ; 4.99 (dd, J = 6.5, 3.8 Hz, 1H) ; 4.26 – 4.20 (m, 1H) ; 3.45 (dd, J = 14.3, 5.3 Hz, 1H) ; 3.24 (dd, J = 14.3, 7.5 Hz, 1H) ; 2.69 (s, 3H) ; 1.53 (s, 3H) ; 1.32 (s, 3H). ¹³C-NMR (125 MHz, DMSO-*d*₆) δ 165.7, 163.6, 157.7, 153.2, 149.4, 135.0, 134.8, 134.7, 133.3, 131.2, 128.8, 128.7, 127.8, 122.4, 117.9, 117.8, 113.8, 112.8, 102.1, 101.9, 101.8, 95.4, 91.4, 88.7, 83.5, 82.6, 81.5, 51.4, 36.0, 27.0, 25.2. HRMS (ESI+): m/z calcd for C₃₀H₂₈FN₆O₅S [M+H]⁺: 603.1820, Found 603.1814.

5'-deoxy-5'-N-(methyl)-(3-nitro-4-bromobenzenesulfonyl)-2',3'-isopropylidene-7-(quinolin-3-ethynyl)-7-deazaadenosine (62).

Following method A with **56** (55 mg, 0.12 mmol, 1.00 eq) and 3-nitro-4-bromobenzenesulfonyl chloride (44 mg, 0.15 mmol, 1.25 eq), **62** was obtained as an off-white solid (75 mg, 87%). R_f 0.54 (1:9 MeOH/CH₂Cl₂). ¹H-NMR (600 MHz, DMSO-*d*₆) δ 9.04 (d, *J* = 2.1 Hz, 1H) ; 8.65 (dd, *J* = 2.1, 0.8 Hz, 1H) ; 8.35 (d, *J* = 2.1 Hz, 1H) ; 8.20 (s, 1H) ; 8.06 (s, 1H) ; 8.04 (s, 1H) ; 8.01 (dd, *J* = 8.2, 1.5 Hz, 1H) ; 7.96 (s, 1H) ; 7.85 (dd, *J* = 8.4, 2.2 Hz, 1H) ; 7.81 (ddd, *J* = 8.3, 6.9, 1.4 Hz, 1H) ; 7.68 (ddd, *J* = 8.1, 6.8, 1.2 Hz, 1H) ; 6.24 (d, *J* = 2.6 Hz, 1H) ; 5.32 (dd, *J* = 6.5, 2.7 Hz, 1H) ; 5.00 (dd, *J* = 6.5, 3.9 Hz, 1H) ; 4.25 (ddd, *J* = 7.6, 5.4, 4.0 Hz, 1H) ; 3.53 – 3.46 (m, 2H) ; 2.73 (s, 1H) ; 1.54 (s, 3H) ; 1.33 (s, 3H). ¹³C-NMR (150 MHz, DMSO-*d*₆) δ 157.7, 153.2, 151.6, 149.8, 149.4, 146.2, 138.0, 136.0, 131.4, 130.4, 128.8, 128.5, 128.0, 127.5, 126.9, 125.9, 123.9, 118.4, 116.8, 113.8, 102.0, 95.0, 88.9, 88.8, 85.6, 83.5, 81.5, 51.4, 35.9, 26.9, 25.2. HRMS (ESI⁺): *m/z* calcd for C₃₂H₂₈BrN₇O₇S [M+H]⁺: 734.1027, Found 734.1039.

5'-deoxy-5'-N-(methyl)-(3-nitro-4-methylbenzenesulfonyl)-2',3'-isopropylidene-7-(quinolin-3-ethynyl)-7-deazaadenosine (63).

Following method A with **56** (40 mg, 0.08 mmol, 1.00 eq) and 3-nitro-4-methylbenzenesulfonyl chloride (25 mg, 0.11 mmol, 1.25 eq), **63** was obtained as an off-white solid (40 mg, 70%). R_f 0.51 (1:9 MeOH/CH₂Cl₂). ¹H-NMR (600 MHz, DMSO-*d*₆) δ 9.04 (d, *J* = 2.1 Hz, 1H) ; 8.65 (dd, *J* = 2.2, 0.7 Hz, 1H) ; 8.23 (d, *J* = 2.0 Hz, 1H) ; 8.20 (s, 1H) ; 8.05 (dd, *J* = 8.3, 1.0 Hz, 1H) ; 8.01 (dd, *J* = 8.2, 1.4 Hz, 1H) ; 7.96 (s, 1H) ; 7.91 (dd, *J* = 8.1, 2.0 Hz, 1H) ; 7.81 (ddd, *J* = 8.4, 6.9, 1.4 Hz, 1H) ; 7.71 – 7.63 (m, 2H) ; 6.23 (d, *J* = 2.7 Hz, 1H) ; 5.32 (dd, *J* = 6.5, 2.7 Hz, 1H) ; 5.02 (dd, *J* = 6.5, 3.8 Hz, 1H) ; 4.25 (ddd, *J* = 7.4, 5.3, 3.7 Hz, 1H) ; 3.52 – 3.45 (m, 1H) ; 3.31 – 3.23 (m, 1H) ; 2.72 (s, 1H) ; 2.55 (s, 1H) ; 1.54 (s, 3H) ; 1.33 (s, 3H). ¹³C-NMR (150 MHz, DMSO-*d*₆) δ 157.7, 153.2, 151.6, 149.4, 148.9, 146.2, 138.0, 137.9, 136.2, 134.1, 131.0, 130.4, 128.8, 128.6, 128.0, 127.5, 126.9, 123.0, 116.8, 113.7, 102.0, 94.9, 88.9, 88.8, 85.7, 83.5, 81.6, 51.4, 35.8, 26.9, 25.2, 19.5. HRMS (ESI⁺): *m/z* calcd for C₃₃H₃₂N₇O₇S [M+H]⁺: 670.2078, Found 670.2089.

5'-deoxy-5'-N-(methyl)-3-chloro-4-methylbenzenesulfonyl)-2',3'-isopropylidene-7-(quinolin-3-ethynyl)-7-deazaadenosine (64).

Following method A with **56** (55 mg, 0.12 mmol, 1.00 eq) and 3-chloro-4-methylbenzenesulfonyl chloride (33 mg, 0.15 mmol, 1.25 eq), **64** was obtained as an off-white solid (55 mg, 71%). R_f 0.70 (1:9 MeOH/CH₂Cl₂). ¹H-NMR (600 MHz, DMSO-*d*₆) δ 9.04 (d, *J* = 2.3 Hz, 1H) ; 8.65 (d, *J* = 2.1 Hz, 1H) ; 8.21 (s, 1H) ; 8.05 (d, *J* = 8.5 Hz, 1H) ; 8.01 (dd, *J* =

8.3, 1.3 Hz, 1H) ; 7.97 (s, 1H) ; 7.81 (ddd, J = 8.4, 6.9, 1.5 Hz, 1H) ; 7.71 (d, J = 1.8 Hz, 1H) ; 7.70 – 7.64 (m, 1H) ; 7.58 (dd, J = 8.0, 1.9 Hz, 1H) ; 7.54 (d, J = 8.1 Hz, 1H) ; 6.24 (d, J = 2.6 Hz, 1H) ; 5.35 (dd, J = 6.5, 2.6 Hz, 1H) ; 5.04 (dd, J = 6.5, 3.7 Hz, 1H) ; 4.24 (ddd, J = 7.3, 5.8, 3.7 Hz, 1H) ; 3.44 (dd, J = 14.1, 5.8 Hz, 1H) ; 3.16 (dd, J = 14.1, 7.2 Hz, 1H) ; 2.67 (s, 1H) ; 2.38 (s, 1H) ; 1.54 (s, 3H) ; 1.33 (s, 3H). ¹³C-NMR (150 MHz, DMSO-*d*₆) δ 157.7, 153.1, 151.6, 149.5, 146.2, 141.2, 138.0, 136.2, 134.1, 132.1, 130.4, 128.8, 128.6, 128.0, 127.5, 127.0, 126.9, 125.8, 116.8, 113.7, 102.0, 95.0, 89.0, 88.8, 85.8, 83.6, 83.4, 81.7, 51.4, 35.9, 26.9, 25.2, 19.7. HRMS (ESI+): m/z calcd for C₃₃H₃₂ClN₆O₅S [M+H]⁺: 659.1838, Found 659.1834.

5'-deoxy-5'-N-(methyl)-(3-nitro-4-methoxybenzenesulfonyl)-2',3'-isopropylidene-7-(quinolin-3-ethynyl)-7-deazaadenosine (65).

Following method A with **56** (55 mg, 0.12 mmol, 1.00 eq) and 4-methoxy-3-nitrobenzenesulfonyl chloride (35 mg, 0.14 mmol, 1.25 eq), **65** was obtained as an off-white solid (69 mg, 86%). R_f 0.51 (1:9 MeOH/CH₂Cl₂). ¹H-NMR (600 MHz, DMSO-*d*₆) δ 9.04 (d, J = 2.1 Hz, 1H) ; 8.64 (dd, J = 2.1, 0.8 Hz, 1H) ; 8.22 (d, J = 2.4 Hz, 1H) ; 8.20 (s, 1H) ; 8.05 (dd, J = 8.3, 1.0 Hz, 1H) ; 8.01 (dd, J = 8.2, 1.4 Hz, 1H) ; 7.99 – 7.93 (m, 2H) ; 7.81 (ddd, J = 8.3, 6.9, 1.5 Hz, 1H) ; 7.67 (ddd, J = 8.1, 6.8, 1.2 Hz, 1H) ; 7.48 (d, J = 9.1 Hz, 1H) ; 6.24 (d, J = 2.7 Hz, 1H) ; 5.34 (dd, J = 6.6, 2.7 Hz, 1H) ; 5.02 (dd, J = 6.5, 3.8 Hz, 1H) ; 4.25 (ddd, J = 7.3, 5.5, 3.7 Hz, 1H) ; 3.99 (s, 3H) ; 3.46 (dd, J = 14.1, 5.6 Hz, 1H) ; 3.22 (dd, J = 14.1, 7.3 Hz, 1H) ; 2.68 (s, 1H) ; 1.54 (s, 3H) ; 1.33 (s, 3H). ¹³C-NMR (150 MHz, DMSO-*d*₆) δ 157.4, 154.6, 152.9, 151.4, 149.2, 145.9, 138.6, 137.7, 132.7, 130.1, 128.6, 128.4, 128.3, 127.7, 127.2, 126.6, 124.0, 116.5, 114.9, 113.5, 101.7, 94.7, 88.7, 88.6, 85.5, 83.3, 83.2, 81.4, 57.1, 51.1, 35.7, 26.7, 24.9. HRMS (ESI+): m/z calcd for C₃₃H₃₂N₇O₈S [M+H]⁺: 686.2028, Found 686.2031.

5'-deoxy-5'-N-(methyl)-(3-cyano-4-fluorobenzenesulfonyl)-2',3'-isopropylidene-7-(quinolin-3-ethynyl)-7-deazaadenosine (66).

Following method A with **56** (103 mg, 0.22 mmol, 1.00 eq) and 3-cyano-4-fluorobenzenesulfonyl chloride (60 mg, 0.27 mmol, 1.25 eq), **66** was obtained as an off-white solid (130 mg, 91%). R_f 0.62 (1:9 MeOH/CH₂Cl₂). ¹H-NMR (600 MHz, DMSO-*d*₆) δ 9.04 (d, J = 2.1 Hz, 1H) ; 8.64 (d, J = 2.3 Hz, 1H) ; 8.36 (dd, J = 5.9, 2.4 Hz, 1H) ; 8.21 (s, 1H) ; 8.09 (ddd, J = 9.0, 4.9, 2.4 Hz, 1H) ; 8.05 (d, J = 8.5 Hz, 1H) ; 8.01 (dd, J = 8.3, 1.5 Hz, 1H) ; 7.96 (s, 1H) ; 7.81 (ddd, J = 8.4, 6.9, 1.6 Hz, 1H) ; 7.72 – 7.63 (m, 2H) ; 6.24 (d, J = 2.6 Hz, 1H) ; 5.33 (dd, J = 6.5, 2.7 Hz, 1H) ; 5.00 (dd, J = 6.5, 3.8 Hz, 1H) ; 4.25 (ddd, J = 7.5, 5.3, 3.9 Hz, 1H) ; 3.52 – 3.44 (m, 1H) ; 3.31-3.24 (m, 1H) ; 2.71 (s, 3H) ; 1.55 (s, 3H) ; 1.33 (s, 3H). ¹³C-NMR (150 MHz, DMSO-*d*₆) δ 165.4, 163.7, 157.6, 153.1, 151.6, 149.4, 146.2, 138.0, 134.9,

134.8, 134.7, 133.3, 130.4, 128.8, 128.5, 128.0, 127.5, 126.9, 118.4, 117.9, 117.7, 116.8, 113.8, 112.7, 102.0, 95.0, 88.9, 88.8, 85.7, 83.5, 81.5, 51.4, 35.9, 27.0, 25.2. HRMS (ESI+): m/z calcd for C₃₃H₂₉FN₇O₅S [M+H]⁺: 654.1929, Found 654.1934.

General method C for the synthesis of compounds 45, 46, 67 and 68. A solution of 0.5 M MeONa in MeOH (5.00 eq) was added to a solution of intermediate compounds **43**, **44**, **61**, **66** (1.00 eq) in MeOH (C = 0.2 M) under argon. The reaction mixture was stirred and heated at 50 °C until completion of the reaction. The crude was diluted with AcOEt and neutralized with a saturated NH₄Cl solution. The aqueous layer was extracted with AcOEt and the combined organic extracts were washed with brine, dried over Na₂SO₄ and concentrated *in vacuo*. The residue was purified by flash column chromatography (liquid sample, silica gel, linear gradient 0-5% MeOH in AcOEt) to give the desired compound as a solid.

5'-deoxy-5'-N-(3-nitro-4-methoxybenzenesulfonyl)-2',3'-isopropylidene-N6-methyladenosine (45).

Following method C with **43** (376 mg, 0.69 mmol, 1.00 eq), **45** was obtained as an off-white solid (256 mg, 68%). R_f 0.40 (1:9 MeOH/AcOEt). ¹H-NMR (500 MHz, DMSO-*d*₆) δ 8.29 (br. s, 1H) ; 8.26 (s, 1H) ; 8.21 (s, 1H) ; 8.19 (d, *J* = 2.3 Hz, 1H) ; 7.91 (dd, *J* = 9.0, 2.3 Hz, 1H) ; 7.87 (br. s, 1H) ; 7.44 (d, *J* = 9.0 Hz, 1H) ; 6.12 (d, *J* = 2.8 Hz, 1H) ; 5.34 (dd, *J* = 6.2, 2.8 Hz, 1H) ; 4.91 (dd, *J* = 6.2, 2.9 Hz, 1H) ; 4.17 (td, *J* = 6.1, 2.9 Hz, 1H) ; 3.98 (s, 1H) ; 3.17 – 3.07 (m, 2H) ; 2.95 (s, 3H) ; 1.51 (s, 3H) ; 1.28 (s, 3H). ¹³C-NMR (125 MHz, DMSO-*d*₆) δ 155.1, 154.8, 152.7, 147.4, 139.9, 138.4, 132.5, 132.0, 123.9, 119.8, 115.2, 113.5, 89.4, 84.4, 83.0, 81.6, 57.4, 44.5, 27.0, 25.1. HRMS (ESI+): m/z calcd for C₂₁H₂₆ClN₇O₈S [M+H]⁺: 536.1558, Found 536.1568.

5'-deoxy-5'-N-(3-cyano-4-methoxybenzenesulfonyl)-2',3'-isopropylidene-N6-methyladenosine (46).

Following method C with **44** (600 mg, 1.19 mmol, 1.00 eq), **46** was obtained as an off-white solid (590 mg, 96%). R_f 0.41 (1:9 MeOH/AcOEt). ¹H-NMR (600 MHz, DMSO-*d*₆) δ 8.26 (s, 1H) ; 8.21 (s, 1H) ; 8.18 (t, *J* = 6.1 Hz, 1H) ; 8.01 (d, *J* = 2.3 Hz, 1H) ; 7.92 (dd, *J* = 9.0, 2.4 Hz, 1H) ; 7.84 (br. s, 1H) ; 7.31 (d, *J* = 9.1 Hz, 1H) ; 6.12 (d, *J* = 2.9 Hz, 1H) ; 5.34 (dd, *J* = 6.4, 2.8 Hz, 1H) ; 4.90 (dd, *J* = 6.4, 2.9 Hz, 1H) ; 4.16 (td, *J* = 5.8, 2.9 Hz, 1H) ; 3.97 (s, 3H) ; 3.16 – 3.07 (m, 2H) ; 2.96 (s, 3H) ; 1.51 (s, 3H) ; 1.29 (s, 3H). ¹³C-NMR (150 MHz, DMSO-*d*₆) δ 163.3, 155.0, 152.6, 147.4, 139.9, 133.3, 132.8, 132.2, 119.8, 115.1, 113.4, 112.9, 100.9, 89.4,

84.4, 82.9, 81.6, 57.1, 44.4, 26.9, 25.1. HRMS (ESI⁺): m/z calcd for C₂₂H₂₆N₇O₆S [M+H]⁺: 516.1660, Found 516.1660.

5'-deoxy-5'-N-(methyl)-(3-cyano-4-methoxybenzenesulfonyl)-2',3'-isopropylidene-7-phenylethynyl-7-deazaadenosine (67).

Following method C with **61** (128 mg, 0.21 mmol, 1.00 eq), **67** was obtained as an off-white solid (95 mg, 73%). R_f 0.58 (1:9 MeOH/AcOEt). ¹H-NMR (500 MHz, DMSO-*d*₆) δ 8.19 (s, 1H) ; 8.13 (d, J = 2.4 Hz, 1H) ; 7.96 (dd, J = 8.9, 2.4 Hz, 1H) ; 7.89 (s, 1H) ; 7.62 – 7.56 (m, 2H) ; 7.47 – 7.37 (m, 3H) ; 7.36 (t, J = 9.1 Hz, 1H) ; 6.22 (d, J = 2.7 Hz, 1H) ; 5.32 (dd, J = 6.5, 2.7 Hz, 1H) ; 5.00 (dd, J = 6.5, 3.7 Hz, 1H) ; 4.26 – 4.20 (m, 1H) ; 3.98 (s, 1H) ; 3.41 (dd, J = 14.1, 5.6 Hz, 1H) ; 3.15 (dd, J = 14.5, 7.6 Hz, 1H) ; 2.64 (s, 3H) ; 1.53 (s, 3H) ; 1.32 (s, 3H). ¹³C-NMR (125 MHz, DMSO-*d*₆) δ 163.7, 157.7, 153.2, 149.4, 134.2, 133.0, 131.2, 129.4, 128.8, 128.7, 127.8, 122.4, 115.0, 113.7, 113.1, 102.1, 101.4, 95.4, 91.4, 88.8, 83.6, 83.4, 82.6, 81.6, 57.2, 51.4, 36.0, 27.0, 25.2. HRMS (ESI⁺): m/z calcd for C₃₁H₃₁N₆O₆S [M+H]⁺: 615.2020, Found 615.2015.

5'-deoxy-5'-N-(methyl)-(3-cyano-4-methoxybenzenesulfonyl)-2',3'-isopropylidene-7-(quinolin-3-ethynyl)-7-deazaadenosine (68).

Following method C with **66** (130 mg, 0.20 mmol, 1.00 eq), **68** was obtained as an off-white solid (110 mg, 83%). R_f 0.53 (1:9 MeOH/AcOEt). ¹H-NMR (600 MHz, DMSO-*d*₆) δ 9.04 (d, J = 2.1 Hz, 1H) ; 8.64 (d, J = 2.3 Hz, 1H) ; 8.21 (s, 1H) ; 8.12 (d, J = 2.4 Hz, 1H) ; 8.05 (d, J = 8.5 Hz, 1H) ; 8.01 (dd, J = 8.6, 1.4 Hz, 1H) ; 7.99 – 7.93 (m, 2H) ; 7.81 (ddd, J = 8.3, 6.9, 1.5 Hz, 1H) ; 7.67 (ddd, J = 8.2, 6.8, 1.2 Hz, 1H) ; 7.36 (d, J = 9.1 Hz, 1H) ; 6.25 (d, J = 2.7 Hz, 1H) ; 5.34 (dd, J = 6.5, 2.7 Hz, 1H) ; 5.02 (dd, J = 6.4, 3.8 Hz, 1H) ; 4.24 (ddd, J = 7.3, 5.5, 3.7 Hz, 1H) ; 3.98 (s, 3H) ; 3.44 (dd, J = 14.1, 5.5 Hz, 1H) ; 3.19 (dd, J = 14.1, 7.3 Hz, 1H) ; 2.66 (s, 1H) ; 1.55 (s, 3H) ; 1.34 (s, 3H). ¹³C-NMR (150 MHz, DMSO-*d*₆) δ 163.7, 157.6, 153.1, 151.6, 149.5, 146.2, 138.0, 134.1, 132.9, 130.4, 129.5, 128.8, 128.5, 128.0, 127.5, 126.8, 116.8, 115.0, 113.7, 113.0, 102.0, 101.3, 95.0, 88.9, 88.8, 85.7, 83.6, 83.4, 81.6, 57.1, 51.4, 35.9, 26.9, 25.2. HRMS (ESI⁺): m/z calcd for C₃₄H₃₂N₇O₆S [M+H]⁺: 666.2129, Found 666.2141.

General method D for the synthesis of compounds 47–51. A suspension of compounds **40–42, 45, 46** (1.00 eq), ethyl *p*-toluenesulfonate (1.50 eq), KI (0.10 eq) and K₂CO₃ (3.00 eq) in anhydrous DMF (C = 0.1 M) was stirred under argon at 50 °C for 16 h. After cooling to room temperature, the reaction mixture was diluted with AcOEt and water. The organic layer was washed with 1M NaOH solution, then the aqueous layer was extracted with AcOEt and the

combined organic extracts were washed with a 2M LiCl solution then brine, dried over Na₂SO₄ and concentrated *in vacuo*. The residue was purified by column chromatography (liquid deposit, silica gel, linear gradient 1-3% MeOH in CH₂Cl₂) to give the desired compound as a foam.

5'-deoxy-5'-N-(ethyl)-(3-nitro-4-bromobenzenesulfonyl)-2',3'-isopropylidene-N6-methyladenosine (47).

Following method D with **40** (200 mg, 0.34 mmol, 1.00 eq), **47** was obtained as a white foam (129 mg, 62%). R_f0.71 (1:9 MeOH/CH₂Cl₂). ¹H-NMR (600 MHz, DMSO-*d*₆) δ 8.34 (d, *J* = 2.3, 1H); 8.29 (s, 1H); 8.26 (s, 1H); 8.00 (d, *J* = 8.4, 1H); 7.82 (dd, *J* = 8.4, 2.2 Hz, 1H); 7.81 (br. s, 1H); 6.20 (d, *J* = 2.1 Hz, 1H); 5.45 (dd, *J* = 6.3, 2.1 Hz, 1H); 5.04 (dd, *J* = 6.3, 3.2 Hz, 1H); 4.32 – 4.29 (m, 1H); 3.63 (dd, *J* = 14.8, 5.2 Hz, 1H); 3.40 (dd, *J* = 14.9, 8.4 Hz, 1H); 3.16 – 3.10 (m, 2H); 2.95 (s, 3H); 1.52 (s, 3H); 1.32 (s, 3H); 0.84 (t, *J* = 7.1 Hz, 3H). ¹³C-NMR (150 MHz, DMSO-*d*₆) δ 155.0, 152.7, 149.8.7, 147.5, 140.0, 135.9, 131.1, 123.7, 119.7, 118.0, 113.4, 89.2, 84.9, 83.2, 82.0, 48.9, 43.6, 26.9, 25.1, 13.3. HRMS (ESI⁺): *m/z* calcd for C₂₂H₂₇BrN₇O₇S [M+H]⁺: 612.0871, Found 612.0862.

5'-deoxy-5'-N-(ethyl)-(3-nitro-4-methylbenzenesulfonyl)-2',3'-isopropylidene-N6-methyladenosine (48).

Following method D with **41** (200 mg, 0.38 mmol, 1.00 eq), **48** was obtained as a white foam (101 mg, 48%). R_f0.62 (1:9 MeOH/CH₂Cl₂). ¹H-NMR (600 MHz, DMSO-*d*₆) δ 8.28 (s, 1H); 8.25 (s, 1H); 8.21 (d, *J* = 2.0, 1H); 7.87 (dd, *J* = 8.0, 2.0 Hz, 1H); 7.81 (br. s, 1H); 7.59 (d, *J* = 8.2, 1H); 6.19 (d, *J* = 2.1 Hz, 1H); 5.44 (dd, *J* = 6.2, 2.1 Hz, 1H); 5.05 (dd, *J* = 6.3, 3.2 Hz, 1H); 4.32 – 4.29 (m, 1H); 3.61 (dd, *J* = 14.7, 5.1 Hz, 1H); 3.37 (dd, *J* = 14.7, 8.3 Hz, 1H); 3.16 – 3.09 (m, 2H); 2.95 (s, 3H); 2.54 (s, 3H); 1.52 (s, 3H); 1.32 (s, 3H); 0.84 (t, *J* = 7.1 Hz, 3H). ¹³C-NMR (150 MHz, DMSO-*d*₆) δ 155.0, 154.7, 152.7, 148.7, 147.5, 140.0, 138.4, 137.6, 133.9, 130.7, 122.7, 119.7, 113.4, 89.2, 84.9, 83.2, 82.0, 48.8, 43.3, 26.9, 25.1, 19.4, 13.3. HRMS (ESI⁺): *m/z* calcd for C₂₃H₃₀N₇O₇S [M+H]⁺: 548.1922, Found 548.1918.

5'-deoxy-5'-N-(ethyl)-(3-chloro-4-methylbenzenesulfonyl)-2',3'-isopropylidene-N6-methyladenosine (49).

Following method D with **42** (250 mg, 0.49 mmol, 1.00 eq), **49** was obtained as a white foam (211 mg, 80%). R_f0.63 (1:1 acetone/CH₂Cl₂). ¹H-NMR (500 MHz, DMSO-*d*₆) δ 8.31 (s, 1H); 8.27 (s, 1H); 7.86 (br. s, 1H); 7.68 (d, *J* = 1.8 Hz, 1H); 7.55 (dd, *J* = 7.8, 1.8 Hz, 1H); 7.48 (d, *J* = 7.8 Hz, 1H); 6.20 (d, *J* = 1.9 Hz, 1H); 5.47 (dd, *J* = 6.1, 1.9 Hz, 1H); 5.07 (dd, *J* = 6.1, 2.9 Hz, 1H); 4.29 (ddd, *J* = 8.2, 5.5, 3.3 Hz, 1H); 3.58 (dd, *J* = 14.6, 5.2 Hz, 1H); 3.27 (dd, *J*

= 14.6, 8.2 Hz, 1H) ; 3.10 – 3.05 (m, 2H) ; 2.94, (d, $J = 2.9$ Hz, 3H) ; 2.36 (s, 3H) ; 1.52 (s, 3H) ; 1.32 (s, 3H) ; 0.81 (t, $J = 6.9$ Hz, 3H). $^{13}\text{C-NMR}$ (125 MHz, DMSO- d_6) δ 156.1, 152.8, 147.6, 141.0, 140.2, 138.6, 134.0, 132.0, 126.8, 125.5, 119.8, 113.3, 89.3, 85.1, 83.2, 82.1, 48.8, 43.4, 26.9, 25.2, 19.7, 13.4. HRMS (ESI+): m/z calcd for $\text{C}_{23}\text{H}_{30}\text{ClN}_6\text{O}_5\text{S}$ $[\text{M}+\text{H}]^+$: 537.1681, Found 537.1684.

5'-deoxy-5'-N-(ethyl)-(4-methoxy-3-nitrobenzenesulfonyl)-2',3'-isopropylidene-N6-methyladenosine (50).

Following method D with **45** (180 mg, 0.34 mmol, 1.00 eq), **50** was obtained as a white foam (170 mg, 90%). R_f 0.38 (1:9 MeOH/ CH_2Cl_2). $^1\text{H-NMR}$ (600 MHz, DMSO- d_6) δ 8.30 (s, 1H) ; 8.26 (s, 1H) ; 8.20 (d, $J = 2.4$ Hz, 1H) ; 7.92 (dd, $J = 8.8, 2.3$ Hz, 1H) ; 7.83 (br. s, 2H) ; 7.42 (d, $J = 9.1$ Hz, 1H) ; 6.21 (d, $J = 2.1$ Hz, 1H) ; 5.46 (dd, $J = 6.3, 2.1$ Hz, 1H) ; 5.06 (dd, $J = 6.4, 3.2$ Hz, 1H) ; 4.32 – 4.29 (m, 1H) ; 3.99 (s, 3H) ; 3.59 (dd, $J = 14.8, 5.2$ Hz, 1H) ; 3.34 – 3.30 (m, 1H) ; 3.11 – 3.07 (m, 2H) ; 2.95 (s, 3H) ; 1.53 (s, 3H) ; 1.32 (s, 3H) ; 0.82 (t, $J = 7.0$ Hz, 3H). $^{13}\text{C-NMR}$ (150 MHz, DMSO- d_6) δ 155.0, 154.7, 152.8, 147.5, 140.1, 133.8, 132.7, 131.0, 124.0, 119.8, 115.1, 113.4, 89.2, 85.1, 83.2, 82.0, 57.4, 48.8, 43.4, 26.9, 25.1, 13.3. HRMS (ESI+): m/z calcd for $\text{C}_{23}\text{H}_{30}\text{N}_7\text{O}_6\text{S}$ $[\text{M}+\text{H}]^+$: 564.1871, Found 564.1869.

5'-deoxy-5'-N-(ethyl)-(3-cyano-4-methoxybenzenesulfonyl)-2',3'-isopropylidene-N6-methyladenosine (51).

Following method D with **46** (250 mg, 0.48 mmol, 1.00 eq), **51** was obtained as a white foam (235 mg, 89%). R_f 0.63 (1:9 MeOH/ CH_2Cl_2). $^1\text{H-NMR}$ (500 MHz, DMSO- d_6) δ 8.31 (s, 1H) ; 8.26 (s, 1H) ; 8.10 (d, $J = 2.3$ Hz, 1H) ; 7.93 (dd, $J = 9.0, 2.4$ Hz, 1H) ; 7.86 (br. s, 2H) ; 7.29 (d, $J = 9.0$ Hz, 1H) ; 6.21 (d, $J = 2.1$ Hz, 1H) ; 5.46 (dd, $J = 6.3, 2.1$ Hz, 1H) ; 5.06 (dd, $J = 6.3, 2.9$ Hz, 1H) ; 4.31 – 4.28 (m, 1H) ; 3.98 (s, 3H) ; 3.58 (dd, $J = 14.8, 5.4$ Hz, 1H) ; 3.29 (dd, $J = 14.8, 8.1$ Hz, 1H) ; 3.13 – 3.03 (m, 2H) ; 2.94 (d, $J = 3.2$ Hz, 3H) ; 1.53 (s, 3H) ; 1.32 (s, 3H) ; 0.80 (t, $J = 7.0$ Hz, 3H). $^{13}\text{C-NMR}$ (125 MHz, DMSO- d_6) δ 163.5, 155.0, 152.8, 147.5, 140.3, 133.8, 132.7, 131.9, 119.8, 115.0, 113.4, 112.9, 101.2, 89.3, 85.2, 83.2, 82.0, 57.1, 48.8, 43.4, 26.9, 25.2, 13.4. HRMS (ESI+): m/z calcd for $\text{C}_{24}\text{H}_{30}\text{N}_7\text{O}_6\text{S}$ $[\text{M}+\text{H}]^+$: 544.1973, Found 544.1965.

General method E for the synthesis of final compounds 1–6. Compounds **33–38** were treated with a formic acid/water solution (1/1 v:v, $C = 0.05$ M). After stirring at 25 °C for 24–48 h until completion of the reaction, solvents were removed *in vacuo* and the crude was co-evaporated three times with absolute EtOH. The residues were purified by flash column chromatography

(dry sample, silica gel, linear gradient 0–10% MeOH in CH₂Cl₂). Fractions containing the pure products were concentrated and trituration in Et₂O afforded the desired compounds as solids.

5'-deoxy-5'-N-(3-chloro-4-methylbenzenesulfonyl)inosine (1).

Following method E with **33** (121 mg, 0.24 mmol, 1.00 eq), **1** was obtained as an off-white solid (80 mg, 72%). *R_f* 0.07 (1:9 MeOH/CH₂Cl₂). ¹H-NMR (600 MHz, DMSO-*d*₆) δ 12.40 (s, 1H) ; 8.27 (s, 1H) ; 8.01 (m, 2H) ; 7.76 (d, *J* = 1.9 Hz, 1H) ; 7.64 (dd, *J* = 8.0, 1.9 Hz) ; 7.53 (d, *J* = 8.1 Hz, 1H) ; 5.82 (d, *J* = 6.0 Hz, 1H) ; 5.54 (s, 1H) ; 5.33 (d, *J* = 4.9 Hz, 1H) ; 4.54 (q, *J* = 5.1 Hz, 1H) ; 4.07 (q, *J* = 3.8 Hz, 1H) ; 3.95 – 3.89 (m, 1H) ; 3.18 – 3.09 (m, 1H) ; 3.07 – 3.00 (m, 1H) ; 2.38 (s, 1H). ¹³C-NMR (150 MHz, DMSO-*d*₆) δ 156.5, 148.1, 145.8, 140.5, 139.7, 139.3, 133.8, 131.9, 126.6, 125.2, 124.6, 87.5, 83.3, 73.1, 70.9, 44.8, 19.7. HRMS (ESI⁺): *m/z* calcd for C₁₇H₁₉ClN₅O₇S [M+H]⁺: 456.0739, Found 456.0737.

5'-deoxy-5'-N-(4-methoxy-3-nitrobenzenesulfonyl)inosine (2).

Following method E with **34** (123 mg, 0.24 mmol, 1.00 eq), **2** was obtained as an off-white solid (72 mg, 63%). *R_f* 0.12 (1:9 MeOH/CH₂Cl₂). ¹H-NMR (600 MHz, DMSO-*d*₆) δ 12.40 (s, 1H) ; 8.27 – 8.23 (m, 2H) ; 8.11 (br. s, 1H) ; 8.03 – 7.99 (m, 2H) ; 7.50 (d, *J* = 9.0 Hz, 1H) ; 5.81 (d, *J* = 6.0 Hz, 1H) ; 5.54 (d, *J* = 6.1 Hz, 1H) ; 5.32 (d, *J* = 4.9 Hz, 1H) ; 4.53 (q, *J* = 5.5 Hz, 1H) ; 4.09 – 4.04 (m, 1H) ; 4.00 (s, 3H) ; 3.95 – 3.89 (m, 1H) ; 3.16 (dd, *J* = 13.6, 4.5 Hz, 1H) ; 3.07 (dd, *J* = 13.6, 6.4 Hz, 1H). ¹³C-NMR (150 MHz, DMSO-*d*₆) δ 156.5, 154.7, 148.1, 145.8, 139.2, 138.5, 132.5, 132.2, 124.6, 123.9, 115.2, 87.5, 83.3, 73.1, 70.9, 57.4, 44.8. HRMS (ESI⁺): *m/z* calcd for C₁₇H₁₉N₆O₉S [M+H]⁺: 483.0929, Found 483.0931.

5'-deoxy-5'-N-(3-cyano-4-methoxybenzenesulfonyl)inosine (3).

Following method E with **35** (65 mg, 0.13 mmol, 1.00 eq), **3** was obtained as an off-white solid (40 mg, 67%). *R_f* 0.08 (1:9 MeOH/CH₂Cl₂). ¹H-NMR (500 MHz, DMSO-*d*₆) δ 12.39 (s, 1H) ; 8.24 (s, 1H) ; 8.09 – 7.97 (m, 4H) ; 7.37 (dd, *J* = 9.0, 1.2 Hz, 1H) ; 5.81 (dd, *J* = 6.1, 1.3 Hz, 1H) ; 4.52 (br. s, 1H) ; 4.05 (br. s, 1H) ; 3.99 (s, 3H) ; 3.92 (br. s, 1H) ; 3.18 – 3.02 (m, 2H). ¹³C-NMR (125 MHz, DMSO-*d*₆) δ 163.2, 156.5, 148.1, 145.8, 139.1, 133.4, 133.0, 132.3, 124.6, 115.1, 112.9, 100.8, 87.5, 83.2, 73.1, 70.9, 57.1, 44.7. HRMS (ESI⁺): *m/z* calcd for C₁₈H₁₉N₆O₇S [M+H]⁺: 463.1030, Found 463.1028.

5'-deoxy-5'-N-(ethyl)-(3-chloro-4-methylbenzenesulfonyl)inosine (4).

Following method E with **36** (174 mg, 0.33 mmol, 1.00 eq), **4** was obtained as an off-white solid (112 mg, 70%). *R_f* 0.08 (1:9 MeOH/CH₂Cl₂). ¹H-NMR (600 MHz, DMSO-*d*₆) δ 12.39 (s,

1H) ; 8.33 (s, 1H) ; 8.06 (s, 1H) ; 7.78 (d, J = 1.9 Hz, 1H) ; 7.66 (dd, J = 8.1, 2.0 Hz, 1H) ; 7.53 (d, J = 8.1 Hz, 1H) ; 5.86 (d, J = 5.7 Hz, 1H) ; 5.57 (d, J = 5.9 Hz, 1H) ; 5.39 (d, J = 5.0 Hz, 1H) ; 4.62 (q, J = 4.9 Hz, 1H) ; 4.15 (p, J = 3.2 Hz, 1H) ; 4.05 (dt, J = 8.3, 4.2 Hz, 1H) ; 3.62 (dd, J = 14.8, 4.6 Hz, 1H) ; 3.38 – 3.33 (m, 1H) ; 3.27 - 3.08 (m, 2H) ; 2.38 (s, 1H) ; 0.97 (t, J = 7.0 Hz, 3H). ¹³C-NMR (150 MHz, DMSO-*d*₆) δ 156.6, 148.2, 145.8, 140.9, 139.3, 138.8, 134.0, 132.0, 126.9, 125.6, 124.6, 87.7, 82.9, 72.9, 71.3, 49.7, 43.4, 19.7, 13.7. HRMS (ESI+): m/z calcd for C₁₉H₂₃ClN₅O₇S [M+H]⁺: 484.1052, Found 484.1051.

5'-deoxy-5'-N-(ethyl)-(4-methoxy-3-nitrobenzenesulfonyl)inosine (5).

Following method E with **37** (32 mg, 0.06 mmol, 1.00 eq), **5** was obtained as an off-white solid (21 mg, 71%). R_f 0.10 (1:9 MeOH/CH₂Cl₂). ¹H-NMR (600 MHz, DMSO-*d*₆) δ 12.40 (s, 1H) ; 8.31 (s, 1H) ; 8.27 (d, J = 2.5 Hz, 1H) ; 8.08 – 8.00 (m, 2H) ; 7.47 (d, J = 9.0 Hz, 1H) ; 5.85 (d, J = 5.8 Hz, 1H) ; 5.58 (br. s, 1H) ; 5.39 (br. s, 1H) ; 4.61 (br. s, 1H) ; 4.13 (br. s, 1H) ; 4.05 (dt, J = 8.3, 4.3 Hz, 1H) ; 4.00 (s, 3H) ; 3.62 (dd, J = 14.8, 4.5 Hz, 1H) ; 3.37 (dd, J = 14.9, 8.3 Hz, 1H) ; 3.25 (dq, J = 14.2, 7.1 Hz, 1H) ; 3.14 (dq, J = 14.2, 7.0 Hz, 1H) ; 0.98 (t, J = 7.1 Hz, 3H). ¹³C-NMR (150 MHz, DMSO-*d*₆) δ 156.6, 154.7, 148.2, 145.9, 139.2, 138.8, 132.8, 131.2, 124.6, 124.0, 115.2, 87.6, 82.9, 72.9, 71.3, 57.4, 49.7, 43.5, 13.7. HRMS (ESI+): m/z calcd for C₁₉H₂₃N₆O₉S [M+H]⁺: 511.1242, Found 511.1235.

5'-deoxy-5'-N-(ethyl)-(3-cyano-4-methoxybenzenesulfonyl)inosine (6).

Following method E with **38** (60 mg, 0.11 mmol, 1.00 eq), **6** was obtained as an off-white solid (40 mg, 67%). R_f 0.08 (1:9 MeOH/CH₂Cl₂). ¹H-NMR (500 MHz, DMSO-*d*₆) δ 12.36 (s, 1H) ; 8.30 (s, 1H) ; 8.15 (s, 1H) ; 8.07 – 8.01 (m, 2H) ; 7.34 (dd, J = 9.1, 1.4 Hz, 1H) ; 5.86 (dd, J = 5.7, 1.4 Hz, 1H) ; 5.54 (br. s, 1H) ; 5.34 (br. s, 1H) ; 4.59 (br. s, 1H) ; 4.13 (br. s, 1H) ; 4.08 - 4.02 (m, 1H) ; 3.99 (s, 3H) ; 3.64 – 3.55 (m, 1H) ; 3.40 – 3.32 (m, 1H) ; 3.27 - 3.08 (m, 2H) ; 0.98 (t, J = 7.1 Hz, 3H). ¹³C-NMR (125 MHz, DMSO-*d*₆) δ 163.4, 156.5, 148.2, 145.8, 139.1, 133.8, 132.7, 132.1, 124.5, 115.0, 112.9, 101.1, 87.6, 82.8, 72.9, 71.2, 57.1, 49.6, 43.3, 13.6. HRMS (ESI+): m/z calcd for C₂₀H₂₃N₆O₇S [M+H]⁺: 491.1343, Found 491.1341.

General method F for the synthesis of final compounds 7–26. Compounds **40–42**, **45–51**, **57–60**, **62–65**, **67**, **68** were treated with a mixture of trifluoroacetic acid/water (8/2 v:v, C = 0.08 M). After stirring at 25 °C for 0.5 h, the solvents were removed *in vacuo* and the crudes were co-evaporated three times with water and three times with MeOH. The residues were dissolved in CH₂Cl₂/MeOH, then 0.5 eq of NEt₃ was added before adding silica to prepare the dry sample. Purification by column chromatography (silica gel, linear gradient 0-10% MeOH

in CH₂Cl₂) was performed. Fractions containing the pure products were concentrated and trituration in Et₂O afforded the desired compounds as solids.

5'-deoxy-5'-N-(3-nitro-4-bromobenzenesulfonyl)-N6-methyladenosine (7).

Following method F with **40** (205 mg, 0.35 mmol, 1.00 eq), **7** was obtained as a white powder (55 mg, 29%). R_f 0.41 (1:9 MeOH/CH₂Cl₂). ¹H-NMR (600 MHz, DMSO-*d*₆) δ 8.78 (br. s, 1H) ; 8.36 (d, *J* = 2.1 Hz, 1H) ; 8.26 (s, 1H) ; 8.22 (s, 1H) ; 8.03 (d, *J* = 8.3 Hz, 1H) ; 7.91 (dd, , *J* = 8.5, 2.2 Hz, 1H) ; 7.81 (br. s, 1H) ; 5.82 (d, *J* = 6.3 Hz, 1H) ; 5.51 (d, *J* = 6.2 Hz, 1H) ; 5.32 (d, *J* = 4.7 Hz, 1H) ; 4.64 (q, , *J* = 6.2 Hz, 1H) ; 4.09 – 4.07 (m, 1H) ; 3.99 – 3.97 (m, 1H) ; 3.21 (s, 2H) ; 2.96 (s, 3H). ¹³C-NMR (150 MHz, DMSO-*d*₆) δ 155.2, 152.4, 149.5, 147.9, 141.3, 140.0, 136.2, 131.0, 123.6, 120.0, 117.9, 88.1, 83.4, 72.6, 71.2, 44.9, 27.1. HRMS (ESI⁺): *m/z* calcd for C₁₇H₁₉BrN₇O₇S [M+H]⁺: 544.0245, Found 544.0249.

5'-deoxy-5'-N-(3-nitro-4-methylbenzenesulfonyl)-N6-methyladenosine (8).

Following method F with **41** (100 mg, 0.19 mmol, 1.00 eq), **8** was obtained as a white powder (61 mg, 66%). R_f 0.45 (1:9 MeOH/CH₂Cl₂). ¹H-NMR (600 MHz, DMSO-*d*₆) δ 8.61 (br. s, 1H) ; 8.30 (d, *J* = 1.9 Hz, 1H) ; 8.25 (s, 1H) ; 8.21 (s, 1H) ; 7.96 (dd, , *J* = 7.9, 1.9 Hz, 1H) ; 7.82 (br. s, 1H) ; 7.64 (d, *J* = 8.1 Hz, 1H) ; 5.82 (d, *J* = 6.2 Hz, 1H) ; 5.47 (d, *J* = 6.2 Hz, 1H) ; 5.29 (d, *J* = 4.8 Hz, 1H) ; 4.65 (q, , *J* = 6.1 Hz, 1H) ; 4.10 – 4.08 (m, 1H) ; 3.99 – 3.96 (m, 1H) ; 3.20 – 3.14 (m, 2H) ; 2.96 (s, 3H) ; 2.55 (s, 3H). ¹³C-NMR (150 MHz, DMSO-*d*₆) δ 155.1, 152.4, 148.5, 147.8, 140.0, 139.5, 137.5, 134.0, 130.5, 122.6, 120.0, 88.0, 83.3, 72.5, 71.1, 44.9, 26.9, 19.6. HRMS (ESI⁺): *m/z* calcd for C₁₈H₂₂N₇O₇S [M+H]⁺: 480.1296, Found 480.1292.

5'-deoxy-5'-N-(3-chloro-4-methylbenzenesulfonyl)-N6-methyladenosine (9).

Following method F with **42** (100 mg, 0.20 mmol, 1.00 eq), **9** was obtained as a white powder (88 mg, 95%). R_f 0.36 (1:9 MeOH/CH₂Cl₂). ¹H-NMR (600 MHz, DMSO-*d*₆) δ 8.45 (t, *J* = 5.3 Hz, 1H) ; 8.28 (s, 1H) ; 8.22 (s, 1H) ; 7.84 (br. s, 1H) ; 7.75 (d, *J* = 1.8 Hz, 1H) ; 7.63 (dd, *J* = 8.0, 1.9 Hz, 1H) ; 7.53 (d, *J* = 7.9 Hz, 1H) ; 5.83 (d, *J* = 6.4 Hz, 1H) ; 5.48 (d, *J* = 6.2 Hz, 1H) ; 5.31 (d, *J* = 4.7 Hz, 1H) ; 4.67 (q, *J* = 5.6 Hz, 1H) ; 4.09 (q, *J* = 4.7, 1H) ; 3.97 (q, *J* = 4.7, 1H) ; 3.14 – 3.06 (m, 2H) ; 2.96 (s, 3H) ; 2.38 (s, 3H). ¹³C-NMR (125 MHz, DMSO-*d*₆) δ 155.1, 152.4, 147.9, 140.6, 140.1, 139.6, 133.9, 132.1, 126.6, 125.2, 120.0, 88.0, 83.4, 72.5, 71.1, 44.9, 27.0, 19.7. HRMS (ESI⁺): *m/z* calcd for C₁₈H₂₂ClN₆O₅S [M+H]⁺: 469.1055, Found 469.1056.

5'-deoxy-5'-N-(3-nitro-4-methoxybenzenesulfonyl)-N6-methyladenosine (10).

Following method F with **45** (410 mg, 0.76 mmol, 1.00 eq), **10** was obtained as a white foam (before trituration) (345 mg, 91%). R_f 0.47 (1:9 MeOH/CH₂Cl₂). ¹H-NMR (600 MHz, DMSO-*d*₆) δ 8.52 (br. s, 1H) ; 8.27 (s, 1H) ; 8.25 (d, *J* = 2.4 Hz, 1H) ; 8.23 (br. s, 1H) ; 8.00 (dd, *J* = 8.9, 2.3 Hz, 1H) ; 7.82 (br. s, 1H) ; 7.50 (d, *J* = 9.0 Hz, 1H) ; 5.83 (d, *J* = 6.2 Hz, 1H) ; 5.48 (d, *J* = 6.1 Hz, 1H) ; 5.30 (d, *J* = 4.7 Hz, 1H) ; 4.66 (q, *J* = 5.9 Hz, 1H) ; 4.09 (td, *J* = 4.7, 3.1 Hz, 1H) ; 4.01 – 3.96 (m, 4H) ; 3.17 – 3.11 (m, 2H) ; 2.96 (br. s, 3H). ¹³C-NMR (150 MHz, DMSO-*d*₆) δ 155.1, 154.7, 152.4, 147.9, 140.0, 138.5, 132.4, 132.1, 123.8, 120.0, 115.3, 88.1, 83.3, 72.5, 71.1, 57.3, 44.8, 27.0. HRMS (ESI+): *m/z* calcd for C₁₈H₂₂N₇O₈S [M+H]⁺: 496.1245, Found 496.1246.

5'-deoxy-5'-N-(3-cyano-4-methoxybenzenesulfonyl)-N6-methyladenosine (11).

Following method F with **46** (100 mg, 0.19 mmol, 1.00 eq), **11** was obtained as a white powder (65 mg, 70%). R_f 0.20 (1:9 MeOH/CH₂Cl₂). ¹H-NMR (600 MHz, DMSO-*d*₆) δ 8.44 (t, *J* = 5.4 Hz, 1H) ; 8.27 (s, 1H) ; 8.23 (s, 1H) ; 8.08 (t, *J* = 2.4 Hz, 1H) ; 8.01 (dd, *J* = 9.0, 2.4 Hz, 1H) ; 7.84 (br. s, 1H) ; 7.37 (d, *J* = 9.0 Hz, 1H) ; 5.83 (d, *J* = 6.4 Hz, 1H) ; 5.48 (d, *J* = 6.3 Hz, 1H) ; 5.30 (d, *J* = 4.7 Hz, 1H) ; 4.65 (q, *J* = 6.1 Hz, 1H) ; 4.08 – 4.06 (m, 1H) ; 3.99 – 3.96 (m, 1H) ; 3.99 (s, 1H) ; 3.13 – 3.11 (m, 2H) ; 2.96 (s, 3H). ¹³C-NMR (150 MHz, DMSO-*d*₆) δ 163.3, 155.1, 152.4, 147.9, 140.1, 133.4, 132.9, 132.2, 120.0, 115.1, 113.1, 100.9, 88.0, 83.4, 72.5, 71.1, 57.1, 44.8, 27.0. HRMS (ESI+): *m/z* calcd for C₁₉H₂₂N₇O₆S [M+H]⁺: 476.1360, Found 476.1356.

5'-deoxy-5'-N-(ethyl)-(3-nitro-4-bromobenzenesulfonyl)-N6-methyladenosine (12).

Following method F with **47** (123 mg, 0.20 mmol, 1.00 eq), **12** was obtained as a yellow oil (104 mg, 84%). R_f 0.42 (1:9 MeOH/CH₂Cl₂). ¹H-NMR (600 MHz, DMSO-*d*₆) δ 8.41 (d, *J* = 2.2 Hz, 1H) ; 8.33 (s, 1H) ; 8.23 (br. s, 1H) ; 8.03 (d, *J* = 8.5 Hz, 1H) ; 7.93 (dd, *J* = 8.4, 2.3 Hz, 1H) ; 7.77 (br. s, 1H) ; 5.88 (d, *J* = 5.8 Hz, 1H) ; 5.53 (d, *J* = 6.1 Hz, 1H) ; 5.36 (d, *J* = 5.1 Hz, 1H) ; 4.76 (q, *J* = 5.7 Hz, 1H) ; 4.19 (q, *J* = 4.9 Hz, 1H) ; 4.06 (dt, *J* = 8.2, 4.1 Hz, 1H) ; 3.69 (dd, *J* = 15.0, 4.5 Hz, 1H) ; 3.45 (dd, *J* = 14.8, 8.4 Hz, 1H) ; 3.28 (dq, *J* = 14.2, 7.0 Hz, 1H) ; 3.17 (dq, *J* = 14.1, 7.0 Hz, 1H) ; 2.95 (s, 3H) ; 0.98 (t, *J* = 7.0 Hz, 3H). ¹³C-NMR (150 MHz, DMSO-*d*₆) δ 155.0, 152.6, 149.8, 148.3, 140.3, 139.9, 136.0, 131.2, 123.7, 119.8, 118.0, 87.9, 82.8, 72.3, 71.4, 49.8, 43.6, 27.0, 13.8. HRMS (ESI+): *m/z* calcd for C₁₉H₂₃BrN₇O₇S [M+H]⁺: 572.0558, Found 572.0555.

5'-deoxy-5'-N-(ethyl)-(3-nitro-4-methylbenzenesulfonyl)-N6-methyladenosine (13).

Following method F with **48** (101 mg, 0.18 mmol, 1.00 eq), **13** was obtained as a white solid foam (80 mg, 86%). R_f 0.27 (1:9 MeOH/CH₂Cl₂). ¹H-NMR (600 MHz, DMSO-*d*₆) δ 8.31 (s, 1H) ; 8.29 (d, *J* = 2.0 Hz, 1H) ; 8.22 (br. s, 1H) ; 7.98 (dd, *J* = 8.1, 2.0 Hz, 1H) ; 7.76 (br. s, 1H) ; 7.63 (d, *J* = 8.2 Hz, 1H) ; 5.86 (d, *J* = 5.8 Hz, 1H) ; 5.51 (d, *J* = 6.1 Hz, 1H) ; 5.36 (d, *J* = 5.0 Hz, 1H) ; 4.76 (q, *J* = 5.6 Hz, 1H) ; 4.20 (q, *J* = 4.8 Hz, 1H) ; 4.06 (dt, *J* = 8.3, 4.2 Hz, 1H) ; 3.70 (dd, *J* = 14.8, 4.5 Hz, 1H) ; 3.40 (dd, *J* = 14.8, 8.4 Hz, 1H) ; 3.27 (dq, *J* = 14.1, 7.2 Hz, 1H) ; 3.16 (dq, *J* = 14.1, 7.0 Hz, 1H) ; 2.95 (s, 3H) ; 2.55 (s, 3H) ; 0.98 (t, *J* = 7.1 Hz, 3H). ¹³C-NMR (150 MHz, DMSO-*d*₆) δ 155.0, 152.6, 148.8, 148.2, 140.0, 138.6, 137.7, 134.0, 130.8, 122.8, 119.9, 87.9, 82.7, 72.3, 71.3, 49.6, 43.4, 27.0, 19.5, 13.7. HRMS (ESI⁺): *m/z* calcd for C₂₀H₂₆N₇O₇S [M+H]⁺: 508.1609, Found 508.1608.

5'-deoxy-5'-N-(ethyl)-(3-chloro-4-methylbenzenesulfonyl)-N6-methyladenosine (14).

Following method F with **49** (100 mg, 0.19 mmol, 1.00 eq), **14** was obtained as a white powder (86 mg, 95%). R_f 0.45 (1:9 MeOH/CH₂Cl₂). ¹H-NMR (500 MHz, DMSO-*d*₆) δ 8.35 (s, 1H) ; 8.24 (s, 1H) ; 7.80 (br. s, 1H) ; 7.78 (d, *J* = 1.9 Hz, 1H) ; 7.66 (dd, *J* = 8.0, 1.9 Hz, 1H) ; 7.53 (d, *J* = 8.0 Hz, 1H) ; 5.88 (d, *J* = 5.9 Hz, 1H) ; 5.47 (dd, *J* = 6.1, 1.9 Hz, 1H) ; 5.53 (d, *J* = 6.2 Hz, 1H) ; 5.31 (d, *J* = 4.9 Hz, 1H) ; 4.83 – 4.79 (m, 1H) ; 4.23 – 2.20 (m, 1H) ; 4.05 (q, 1H, *J* = 3.4 Hz) ; 3.71 (dd, *J* = 14.9, 5.0 Hz, 1H) ; 3.32 (dd, *J* = 14.9, 5.0 Hz, 1H) ; 3.22 (q, *J* = 7.1 Hz, 1H) ; 3.11 (q, *J* = 7.1 Hz, 1H) ; 2.95 (s, 3H) ; 2.95 (s, 3H) ; 0.95 (t, *J* = 7.1 Hz, 3H). ¹³C-NMR (125 MHz, DMSO-*d*₆) δ 155.0, 152.6, 148.3, 141.0, 140.1, 138.8, 134.0, 132.1, 126.9, 125.6, 120.0, 87.9, 83.0, 72.2, 71.4, 55.0, 43.5, 27.0, 19.7, 13.8. HRMS (ESI⁺): *m/z* calcd for C₂₀H₂₆ClN₆O₅S [M+H]⁺: 497.1382, Found 497.1378.

5'-deoxy-5'-N-(ethyl)-(3-nitro-4-methoxybenzenesulfonyl)-N6-methyladenosine (15).

Following method F with **50** (100 mg, 0.18 mmol, 1.00 eq), **15** was obtained as an oil (80 mg, 86%). R_f 0.35 (1:9 MeOH/CH₂Cl₂). ¹H-NMR (500 MHz, DMSO-*d*₆) δ 8.33 (s, 1H) ; 8.27 (d, *J* = 2.4 Hz, 1H) ; 8.23 (br. s, 1H) ; 8.02 (dd, *J* = 8.9, 2.4 Hz, 1H) ; 7.78 (br. s, 1H) ; 7.46 (d, *J* = 9.0 Hz, 1H) ; 5.88 (d, *J* = 5.9 Hz, 1H) ; 5.51 (d, *J* = 6.1 Hz, 1H) ; 5.36 (d, *J* = 5.0 Hz, 1H) ; 4.78 (q, *J* = 5.8 Hz, 1H) ; 4.23 – 4.17 (m, 1H) ; 4.06 (ddd, *J* = 8.3, 4.5, 3.6 Hz, 1H) ; 4.00 (s, 3H) ; 3.69 (dd, *J* = 15.0, 4.7 Hz, 1H) ; 3.37 (dd, *J* = 14.8, 8.3 Hz, 1H) ; 3.25 (dq, *J* = 14.1, 7.0 Hz, 1H) ; 3.13 (dq, *J* = 14.2, 7.0 Hz, 1H) ; 2.95 (s, 3H) ; 0.97 (t, *J* = 7.1 Hz, 3H). ¹³C-NMR (125 MHz, DMSO-*d*₆) δ 155.0, 154.7, 152.6, 148.3, 140.0, 138.8, 132.7, 131.3, 124.0, 119.9, 115.2, 87.9, 82.9, 72.2, 71.4, 57.4, 50.0, 43.5, 27.0, 13.8. HRMS (ESI⁺): *m/z* calcd for C₂₀H₂₆N₇O₈S [M+H]⁺: 524.1558, Found 524.1556.

5'-deoxy-5'-N-(ethyl)-(3-cyano-4-methoxybenzenesulfonyl)-N6-methyladenosine (16).

Following method F with **51** (100 mg, 0.18 mmol, 1.00 eq), **16** was obtained as a white powder (47 mg, 50%). R_f 0.38 (1:9 MeOH/CH₂Cl₂). ¹H-NMR (500 MHz, DMSO-*d*₆) δ 8.35 (s, 1H) ; 8.24 (s, 1H) ; 8.18 (d, *J* = 2.3 Hz, 1H) ; 8.03 (dd, *J* = 9.0, 2.3 Hz, 1H) ; 7.80 (br. s, 1H) ; 7.34 (d, *J* = 9.0 Hz, 1H) ; 5.88 (d, *J* = 6.0 Hz, 1H) ; 5.53 (d, *J* = 6.1 Hz, 1H) ; 5.38 (d, *J* = 4.9 Hz, 1H) ; 4.80 – 4.77 (m, 1H) ; 4.21 – 4.18 (m, 1H) ; 4.07 – 4.03 (m, 1H) ; 3.99 (s, 3H) ; 3.67 (dd, *J* = 14.5, 4.7 Hz, 1H) ; 3.35 – 3.31 (m, 1H) ; 3.27 – 3.07 (m, 2H) ; 2.95 (s, 3H) ; 0.95 (t, *J* = 7.0 Hz, 3H). ¹³C-NMR (125 MHz, DMSO-*d*₆) δ 163.5, 155.0, 152.7, 148.3, 140.1, 133.9, 132.7, 132.0, 119.9, 115.1, 113.0, 101.2, 87.8, 83.0, 72.2, 71.4, 57.2, 49.7, 43.5, 27.0, 13.8. HRMS (ESI+): *m/z* calcd for C₂₁H₂₆N₇O₆S [M+H]⁺: 504.1646, Found 504.1652.

5'-deoxy-5'-N-(methyl)-(4-bromo-3-nitrobenzenesulfonyl)-7-phenylethynyl-7-deazaadenosine (17).

Following method F with **57** (54 mg, 0.08 mmol, 1.00 eq), **17** was obtained as an off-white solid (26 mg, 51%). R_f 0.44 (1:9 MeOH/CH₂Cl₂). ¹H-NMR (600 MHz, DMSO-*d*₆) δ 8.41 (d, *J* = 2.1 Hz, 1H) ; 8.16 (s, 1H) ; 8.09 (d, *J* = 8.4 Hz, 1H) ; 7.94 (dd, *J* = 8.4, 2.2 Hz, 1H) ; 7.89 (s, 1H) ; 7.61 – 7.56 (m, 2H) ; 7.48 – 7.37 (m, 3H) ; 6.07 (d, *J* = 5.9 Hz, 1H) ; 5.47 (d, *J* = 6.2 Hz, 1H) ; 5.32 (d, *J* = 5.2 Hz, 1H) ; 4.47 (q, *J* = 5.8 Hz, 1H) ; 4.09 (td, *J* = 5.2, 3.8 Hz, 1H) ; 4.03 (dt, *J* = 8.3, 4.3 Hz, 1H) ; 3.52 (dd, *J* = 14.3, 4.7 Hz, 1H) ; 3.39 – 3.26 (m, 1H) ; 2.78 (s, 3H). ¹³C-NMR (150 MHz, DMSO-*d*₆) δ 157.6, 153.0, 150.1, 149.9, 138.0, 136.1, 131.6, 131.1, 128.7, 128.5, 127.1, 124.0, 122.5, 118.3, 102.1, 95.1, 91.2, 87.0, 82.9, 81.9, 72.9, 71.3, 52.0, 36.0. HRMS (ESI+): *m/z* calcd for C₂₆H₂₄BrN₆O₇S [M+H]⁺: 643.0605, Found 643.0597.

5'-deoxy-5'-N-(methyl)-(3-nitro-4-methylbenzenesulfonyl)-7-phenylethynyl-7-deazaadenosine (18).

Following method F with **58** (77 mg, 0.12 mmol, 1.00 eq), **18** was obtained as an off-white solid (25 mg, 35%). R_f 0.56 (1:9 MeOH/CH₂Cl₂). ¹H-NMR (600 MHz, DMSO-*d*₆) δ 8.29 (d, *J* = 2.0 Hz, 1H) ; 8.16 (s, 1H) ; 8.00 (dd, *J* = 8.1, 1.9 Hz, 1H) ; 7.90 (s, 1H) ; 7.70 (dd, *J* = 8.2, 0.9 Hz, 1H) ; 7.61 – 7.55 (m, 2H) ; 7.47 – 7.36 (m, 3H) ; 6.06 (d, *J* = 5.8 Hz, 1H) ; 5.47 (d, *J* = 6.2 Hz, 1H) ; 5.34 (d, *J* = 5.1 Hz, 1H) ; 4.47 (q, *J* = 5.8 Hz, 1H) ; 4.10 (td, *J* = 5.1, 3.9 Hz, 1H) ; 4.02 (dt, *J* = 8.4, 4.4 Hz, 1H) ; 3.52 (dd, *J* = 14.3, 4.7 Hz, 1H) ; 3.25 (dd, *J* = 14.2, 7.7 Hz, 1H) ; 2.76 (s, 3H) ; 2.57 (s, 3H). ¹³C-NMR (150 MHz, DMSO-*d*₆) δ 157.6, 153.0, 150.1, 148.9, 137.9, 136.2, 134.1, 131.1, 128.7, 128.6, 127.2, 123.1, 122.5, 102.1, 95.1, 91.2, 87.1, 83.0, 82.0, 72.9, 71.2, 52.0, 36.0, 19.5. HRMS (ESI+): *m/z* calcd for C₂₇H₂₇N₆O₇S [M+H]⁺: 579.1656, Found 579.1652.

5'-deoxy-5'-N-(methyl)-(3-chloro-4-methylbenzenesulfonyl)-7-phenylethynyl-7-deazaadenosine (19).

Following method F with **59** (67 mg, 0.11 mmol, 1.00 eq), **19** was obtained as an off-white solid (10 mg, 16%). R_f 0.50 (1:9 MeOH/CH₂Cl₂). ¹H-NMR (600 MHz, DMSO-*d*₆) δ 8.16 (s, 1H); 7.92 (s, 1H); 7.79 (d, *J* = 2.0 Hz, 1H); 7.67 (dd, *J* = 8.0, 1.9 Hz, 1H); 7.61 – 7.56 (m, 3H); 7.46 – 7.38 (m, 3H); 6.07 (d, *J* = 6.1 Hz, 1H); 5.46 (d, *J* = 6.2 Hz, 1H); 5.33 (d, *J* = 5.0 Hz, 1H); 4.49 (q, *J* = 5.9 Hz, 1H); 4.11 (td, *J* = 5.2, 3.8 Hz, 1H); 4.04-3.99 (m, 1H); 3.50 (dd, *J* = 14.1, 4.9 Hz, 1H); 3.17 (dd, *J* = 14.2, 7.5 Hz, 1H); 2.72 (s, 3H); 2.40 (s, 1H). ¹³C-NMR (150 MHz, DMSO-*d*₆) δ 157.6, 153.0, 150.1, 141.2, 136.3, 134.1, 132.1, 131.1, 128.7, 128.5, 127.2, 125.9, 122.5, 102.1, 95.1, 91.2, 87.1, 83.0, 82.1, 72.9, 71.3, 52.1, 36.1, 19.7. HRMS (ESI⁺): *m/z* calcd for C₂₇H₂₇ClN₅O₅S [M+H]⁺: 568.1416, Found 568.1411.

5'-deoxy-5'-N-(methyl)-(3-nitro-4-methoxybenzenesulfonyl)-7-phenylethynyl-7-deazaadenosine (20).

Following method F with **60** (59 mg, 0.09 mmol, 1.00 eq), **20** was obtained as an off-white solid (11 mg, 20%). R_f 0.52 (1:9 MeOH/CH₂Cl₂). ¹H-NMR (600 MHz, DMSO-*d*₆) δ 8.28 (d, *J* = 2.3 Hz, 1H); 8.16 (s, 1H); 8.05 (dd, *J* = 8.9, 2.4 Hz, 1H); 7.91 (s, 1H); 7.61 – 7.56 (m, 2H); 7.53 (d, *J* = 8.9 Hz, 1H); 7.47 – 7.38 (m, 3H); 6.07 (d, *J* = 5.9 Hz, 1H); 5.47 (d, *J* = 6.3 Hz, 1H); 5.33 (d, *J* = 5.1 Hz, 1H); 4.48 (q, *J* = 5.9 Hz, 1H); 4.10 (td, *J* = 5.1, 3.7 Hz, 1H); 4.04-3.99 (m, 4H); 3.50 (dd, *J* = 14.1, 4.9 Hz, 1H); 3.20 (dd, *J* = 14.2, 7.5 Hz, 1H); 2.73 (s, 3H). ¹³C-NMR (150 MHz, DMSO-*d*₆) δ 157.6, 154.9, 153.0, 150.1, 138.9, 133.1, 131.1, 128.7, 128.5, 127.2, 124.3, 122.5, 115.3, 102.1, 95.1, 91.2, 87.0, 83.0, 82.1, 72.9, 71.3, 57.4, 52.0, 36.1. HRMS (ESI⁺): *m/z* calcd for C₂₇H₂₇N₆O₈S [M+H]⁺: 595.1606, Found 595.1611.

5'-deoxy-5'-N-(methyl)-(3-cyano-4-methoxybenzenesulfonyl)-7-phenylethynyl-7-deazaadenosine (21).

Following method F with **67** (95 mg, 0.15 mmol, 1.00 eq), **21** was obtained as an off-white solid (42 mg, 47%). R_f 0.51 (1:9 MeOH/CH₂Cl₂). ¹H-NMR (600 MHz, DMSO-*d*₆) δ 8.19 (d, *J* = 2.3 Hz, 1H); 8.16 (s, 1H); 8.05 (dd, *J* = 9.0, 2.4 Hz, 1H); 7.91 (s, 1H); 7.61 – 7.55 (m, 2H); 7.46 – 7.38 (m, 4H); 6.08 (d, *J* = 6.1 Hz, 1H); 5.46 (s, 1H); 5.33 (s, 1H); 4.48 (t, *J* = 5.6 Hz, 1H); 4.13 – 4.08 (m, 1H); 4.05 – 3.98 (m, 4H); 3.49 (dd, *J* = 14.3, 5.0 Hz, 1H); 3.17 (dd, *J* = 14.3, 7.4 Hz, 1H); 2.72 (s, 3H). ¹³C-NMR (150 MHz, DMSO-*d*₆) δ 163.7, 157.6, 152.9, 150.1, 134.2, 133.0, 131.1, 129.5, 128.7, 128.5, 127.1, 122.5, 115.0, 113.1, 102.1, 101.3, 95.1, 91.2, 87.0, 83.0, 82.1, 72.9, 71.3, 57.1, 52.1, 36.1. HRMS (ESI⁺): *m/z* calcd for C₂₈H₂₇N₆O₆S [M+H]⁺: 575.1707, Found 575.1702.

5'-deoxy-5'-N-(methyl)-(4-bromo-3-nitrobenzenesulfonyl)-7-(quinolin-3-ethynyl)-7-deazaadenosine (22).

Following method F with **62** (72 mg, 0.10 mmol, 1.00 eq), **22** was obtained as an off-white solid (45 mg, 66%). R_f 0.36 (1:9 MeOH/CH₂Cl₂). ¹H-NMR (600 MHz, DMSO-*d*₆) δ 9.04 (d, J = 2.1 Hz, 1H) ; 8.66 – 8.62 (m, 1H) ; 8.42 (d, J = 2.2 Hz, 1H) ; 8.18 (s, 1H) ; 8.09 (d, J = 8.3 Hz, 1H) ; 8.05 (dd, J = 8.3, 1.0 Hz, 1H) ; 8.01 (dd, J = 8.3, 1.5 Hz, 1H) ; 7.98 (s, 1H) ; 7.95 (dd, J = 8.4, 2.2 Hz, 1H) ; 7.81 (ddd, J = 8.3, 6.9, 1.5 Hz, 1H) ; 7.68 (ddd, J = 8.2, 6.9, 1.2 Hz, 1H) ; 6.09 (d, J = 5.9 Hz, 1H) ; 5.49 (d, J = 6.2 Hz, 1H) ; 5.34 (d, J = 5.1 Hz, 1H) ; 4.49 (q, J = 5.9 Hz, 1H) ; 4.11 (td, J = 5.2, 4.1 Hz, 1H) ; 4.04 (dt, J = 8.4, 4.3 Hz, 1H) ; 3.53 (dq, J = 11.8, 7.2, 6.6 Hz, 1H) ; 3.32-3.28 (m, 1H) ; 2.79 (s, 1H). ¹³C-NMR (150 MHz, DMSO-*d*₆) δ 157.6, 153.0, 151.6, 150.1, 149.9, 146.2, 138.0, 136.0, 131.6, 130.3, 128.8, 128.0, 127.9, 127.5, 126.9, 125.9, 124.0, 118.3, 116.9, 102.0, 94.8, 88.7, 87.1, 83.0, 82.0, 73.0, 71.2, 52.0, 36.1. HRMS (ESI+): m/z calcd for C₂₉H₂₅BrN₇O₇S [M+H]⁺: 694.0714, Found 694.0720.

5'-deoxy-5'-N-(methyl)-(4-methyl-3-nitrobenzenesulfonyl)-7-(quinolin-3-ethynyl)-7-deazaadenosine (23).

Following method F with **63** (115 mg, 0.17 mmol, 1.00 eq), **23** was obtained as an off-white solid (68 mg, 63%). R_f 0.33 (1:9 MeOH/CH₂Cl₂). ¹H-NMR (500 MHz, DMSO-*d*₆) δ 9.04 (d, J = 2.1 Hz, 1H) ; 8.65 (d, J = 2.0 Hz, 1H) ; 8.30 (d, J = 1.8 Hz, 1H) ; 8.18 (s, 1H) ; 8.08 – 7.98 (m, 4H) ; 7.84 – 7.78 (m, 1H) ; 7.73 – 7.64 (m, 2H) ; 6.08 (d, J = 5.9 Hz, 1H) ; 5.52 (d, J = 6.2 Hz, 1H) ; 5.38 (d, J = 5.1 Hz, 1H) ; 4.50 (q, J = 5.8 Hz, 1H) ; 4.12 (q, J = 4.7 Hz, 1H) ; 4.04 (dt, J = 8.2, 4.3 Hz, 1H) ; 3.53 (dd, J = 14.3, 4.7 Hz, 1H) ; 3.25 (dd, J = 14.3, 7.7 Hz, 1H) ; 2.77 (s, 3H) ; 2.57 (s, 3H). ¹³C-NMR (125 MHz, DMSO-*d*₆) δ 157.6, 153.1, 151.7, 150.3, 149.0, 146.2, 138.0, 137.9, 136.2, 134.2, 131.2, 130.4, 128.9, 128.0, 127.6, 126.9, 123.2, 117.0, 102.0, 94.8, 88.8, 87.1, 86.2, 82.0, 73.0, 71.3, 52.1, 36.1, 19.6. HRMS (ESI+): m/z calcd for C₃₀H₂₈N₇O₇S [M+H]⁺: 630.1765, Found 630.1762.

5'-deoxy-5'-N-(methyl)-(3-chloro-4-methylbenzenesulfonyl)-7-(quinolin-3-ethynyl)-7-deazaadenosine (24).

Following method F with **64** (30 mg, 0.05 mmol, 1.00 eq), **24** was obtained as an off-white solid (10 mg, 35%). R_f 0.50 (1:9 MeOH/CH₂Cl₂). ¹H-NMR (600 MHz, DMSO-*d*₆) δ 9.04 (d, J = 2.1 Hz, 1H) ; 8.64 (d, J = 2.2 Hz, 1H) ; 8.18 (s, 1H) ; 8.07 – 7.98 (m, 3H) ; 7.84 – 7.78 (m, 2H) ; 7.70 – 7.64 (m, 2H) ; 7.59 (d, J = 8.0 Hz, 1H) ; 6.09 (d, J = 5.9 Hz, 1H) ; 5.49 (d, J = 6.2 Hz, 1H) ; 5.35 (d, J = 5.0 Hz, 1H) ; 4.51 (q, J = 5.8 Hz, 1H) ; 4.13 (q, J = 4.8 Hz, 1H) ; 4.03 (dt, J = 7.7, 4.5 Hz, 1H) ; 3.51 (dd, J = 14.1, 5.0 Hz, 1H) ; 3.19 (dd, J = 14.2, 7.5 Hz, 1H) ; 2.73 (s,

3H) ; 2.40 (s, 3H). ¹³C-NMR (150 MHz, DMSO-*d*₆) δ 157.6, 153.0, 151.7, 150.2, 146.1, 141.2, 137.9, 136.3, 134.1, 132.1, 130.4, 128.8, 128.0, 127.5, 127.1, 126.9, 125.9, 116.9, 102.0, 94.8, 88.7, 87.1, 86.2, 82.2, 72.9, 71.3, 52.1, 36.1, 19.7. HRMS (ESI⁺): m/z calcd for C₃₀H₂₈ClN₆O₅S [M+H]⁺: 619.1525, Found 619.1529.

5'-deoxy-5'-N-(methyl)-(4-methoxy-3-nitrobenzenesulfonyl)-7-(quinolin-3-ethynyl)-7-deazaadenosine (25).

Following method F with **65** (68 mg, 0.10 mmol, 1.00 eq), **25** was obtained as an off-white solid (40 mg, 62%). R_f 0.33 (1:9 MeOH/CH₂Cl₂). ¹H-NMR (600 MHz, DMSO-*d*₆) δ 9.04 (d, J = 2.1 Hz, 1H) ; 8.66 – 8.62 (m, 1H) ; 8.29 (d, J = 2.3 Hz, 1H) ; 8.18 (s, 1H) ; 8.08-8.03 (m, 2H) ; 8.03-7.99 (m, 2H) ; 7.81 (ddd, J = 8.4, 6.8, 1.5 Hz, 1H) ; 7.68 (ddd, J = 8.2, 6.8, 1.2 Hz, 1H) ; 7.53 (d, J = 9.0 Hz, 1H) ; 6.10 (d, J = 5.9 Hz, 1H) ; 5.48 (d, J = 6.2 Hz, 1H) ; 5.34 (d, J = 5.1 Hz, 1H) ; 4.51 (q, J = 5.8 Hz, 1H) ; 4.12 (td, J = 5.1, 3.9 Hz, 1H) ; 4.04 (dt, J = 7.4, 4.5 Hz, 1H) ; 4.01 (s, 3H) ; 3.51 (dd, J = 14.2, 4.8 Hz, 1H) ; 3.23 (dd, J = 14.2, 7.5 Hz, 1H) ; 2.75 (s, 1H). ¹³C-NMR (150 MHz, DMSO-*d*₆) δ 157.6, 154.9, 153.0, 151.6, 150.2, 146.1, 138.9, 137.9, 133.1, 130.3, 128.8, 128.0, 127.5, 126.9, 124.3, 116.9, 115.3, 102.0, 94.8, 88.7, 87.1, 86.1, 82.1, 72.9, 71.3, 57.4, 52.0, 36.1. HRMS (ESI⁺): m/z calcd for C₃₀H₂₈N₇O₈S [M+H]⁺: 646.1715, Found 646.1721.

5'-deoxy-5'-N-(methyl)-(3-cyano-4-methoxybenzenesulfonyl)-7-(quinolin-3-ethynyl)-7-deazaadenosine (26).

Following method F with **68** (100 mg, 0.15 mmol, 1.00 eq), **26** was obtained as an off-white solid (50 mg, 53%). R_f 0.33 (1:9 MeOH/CH₂Cl₂). ¹H-NMR (600 MHz, DMSO-*d*₆) δ 9.04 (d, J = 2.1 Hz, 1H) ; 8.64 (d, J = 2.3 Hz, 1H) ; 8.21 (d, J = 2.4 Hz, 1H) ; 8.18 (s, 1H) ; 8.08-8.03 (m, 2H) ; 8.03-7.99 (m, 2H) ; 7.81 (ddd, J = 8.5, 6.8, 1.5 Hz, 1H) ; 7.68 (ddd, J = 8.1, 6.8, 1.2 Hz, 1H) ; 7.41 (d, J = 9.0 Hz, 1H) ; 6.10 (d, J = 6.0 Hz, 1H) ; 5.49 (d, J = 6.3 Hz, 1H) ; 5.35 (d, J = 5.0 Hz, 1H) ; 4.51 (q, J = 5.9 Hz, 1H) ; 4.12 (td, J = 5.0, 3.6 Hz, 1H) ; 4.03 (ddd, J = 7.4, 4.9, 3.6 Hz, 1H) ; 4.00 (s, 3H) ; 3.50 (dd, J = 14.1, 5.0 Hz, 1H) ; 3.19 (dd, J = 14.2, 7.5 Hz, 1H) ; 2.72 (s, 1H). ¹³C-NMR (150 MHz, DMSO-*d*₆) δ 163.7, 157.6, 153.0, 151.7, 150.3, 146.2, 138.0, 134.2, 133.1, 130.4, 129.5, 128.8, 128.0, 127.5, 126.9, 116.9, 115.1, 113.1, 102.0, 101.3, 94.8, 88.7, 87.0, 86.2, 82.2, 72.9, 71.3, 57.2, 52.1, 36.1. HRMS (ESI⁺): m/z calcd for C₃₁H₂₈N₇O₆S [M+H]⁺: 626.1816, Found 626.1825.

4.2. Expression and purification of recombinant proteins

SARS-CoV and SARS-CoV-2 nsp14 (*N7*-MTase), SARS-CoV-2 nsp10 and nsp16 (*2'*O-MTase), the human RNA *N7*-methyltransferase (hRNMT) and the Dengue virus serotype 3 methyltransferase (NS5 MTase) coding sequences were cloned in fusion with a N-terminus hexa-histidine tag in pET28 plasmids [23] and in Gateway-compatible plasmids as described in [40, 46]. The MERS-CoV nsp14 was produced and purified as previously described [47]. The other proteins were expressed in *E. coli* C2566 and purified in a two-step IMAC using cobalt beads. Briefly, cells were lysed by sonication in a buffer containing 50 mM Tris pH 6.8, 300 mM NaCl, 10 mM imidazole, 5 mM MgCl₂, and 1 mM BME, supplemented with 0.25 mg/mL lysozyme, 10 µg/mL DNase, and 1 mM PMSF. The proteins were next purified through affinity chromatography with HisPur Cobalt resin 480 (Thermo Scientific), washing with an increased concentration of salt (1 M NaCl) and imidazole (20 mM), prior to elution in buffer supplemented with 250 mM imidazole. The second step of purification was performed by size exclusion chromatography (GE Superdex S200) in a final buffer of 50 mM Tris pH 6.8, 300 mM NaCl, 5 mM MgCl₂, and 1 mM BME and the proteins were subsequently concentrated up to 12.5 µM and conserved at -20 °C in a buffer containing 50% of glycerol.

4.3. Determination of the MTase activity by filter binding assay (FBA)

The hRNMT, DV3 NS5, SARS-CoV, SARS-CoV-2 and MERS-CoV nsp14 MTase assays were carried out in reaction mixture [40 mM Tris-HCl (pH 8.0), 1 mM DTT, 1 mM MgCl₂, 2 µM SAM, and 0.1 µM ³H-SAM (Perkin Elmer)] in the presence of 0.7 µM GpppAC₄ synthetic RNA [23] and the corresponding MTases. The SARS-CoV-2 *2'*O-MTase assay was performed in the same experimental conditions except that ⁷mGpppAC₄ synthetic RNA was used in the presence of 1mM MgCl₂. The concentration of MTases was adjusted in each assay in order to get similar enzymatic activity in the FBA during the linear phase of the enzymatic reaction. Briefly, the enzymes were first mixed with the compound suspended in 50% DMSO (2.5% final DMSO) before the addition of RNA substrate and SAM and then incubated at 30 °C. Reactions mixtures were stopped after 30 min by their 10-fold dilution in ice-cold water. Samples were transferred to diethylaminoethyl (DEAE) filtermat (Perkin Elmer) using a Filtermat Harvester (Packard Instruments). The RNA-retaining mats were washed twice with 10 mM ammonium formate pH 8.0, twice with water and once with ethanol. They were soaked with scintillation fluid (Perkin Elmer), and ³H-methyl transfer to the RNA substrates was determined using a Wallac MicroBeta TriLux liquid scintillation counter (Perkin Elmer). For IC₅₀ measurements, values were normalized and fitted with Prism (GraphPad software) using the following

equation: $Y = 100/[1 + ((X/IC_{50})^{\text{Hillslope}})]$. IC_{50} is defined as the inhibitory compound concentration that causes 50% reduction in enzyme activity.

4.4. Molecular docking

All molecular docking experiments were performed using Autodock Vina [41]. The X-ray crystal structure of SARS-CoV-2 nsp14 (PDB 7R2V) was used as the receptor and prepared in Chimera [48]. The ligand structures were drawn and minimized using MarvinSketch (ChemAxon). The receptor and ligand structures were converted to PDBQT format using MGL Tools [49]. The exhaustiveness was set to 10 and default parameters were used, unless otherwise stated. The ligand was treated as flexible and the protein was kept rigid. The grid size was set to 14 x 16 x 20 (Å) and the grid box's center points were set to target the active site of the protein, with the center at X = 14.2, Y = -12.3, Z = -20.1. The docking poses were further filtered for superposition of the adenine nucleobase present in our compounds with the SAH molecule observed in the crystal structure. 3D and 2D representations of protein-ligand complexes were visualized using PyMOL (The PyMOL Molecular Graphics System, Schrödinger, LLC) and Ligplot+, respectively [50].

4.5. SARS-CoV-2 inhibition assay in Vero E6 TMPRSS2 cells

The experimental procedures for the antiviral activity assay against SARS-CoV-2 in cell culture were as previously described [45, 51]. Vero E6 TMPRSS2 cells (ID 100978) were obtained from CFAR and were grown in minimal essential medium (Life Technologies) with 10% heat-inactivated fetal calf serum (FCS; Life Technologies), at 37°C with 5% CO₂ with 1% penicillin/streptomycin (5000 U/mL and 5000 µg/mL respectively; Life Technologies) and supplemented with 1% non-essential amino acids (Life Technologies) and G-418 (Life Technologies). SARS-CoV-2 strain BavPat (lineage B.1) was obtained from Pr. C. Drosten through EVA GLOBAL (<https://www.european-virus-archive.com/>). All experiments with infectious virus were conducted in a biosafety level 3 laboratory. One day prior to infection, 5×10^4 Vero E6 TMPRSS2 cells were seeded per well in 100 µL medium in 96 well culture plates. The next day, four 3-fold dilutions of compounds (from 0.37 µM to 10 µM in duplicate were added to the cells using a Tecan d300e (Tecan) and were supplemented with 25 µL/well of assay medium). Virus control wells were supplemented with 25 µL of assay medium, and 25 µL of a virus mix diluted in medium was added to the wells. The amount of virus working stock used was calibrated prior to the assay, based on a replication kinetics, so that the viral replication was still in the exponential growth phase for the readout as previously described. On each

culture plate, a control compound (Remdesivir, BLDpharm) was tested similarly. Plates were incubated for 2 days at 37°C prior to quantification of the viral genome by real-time RT-PCR. To do so, 100 µL of viral supernatant was collected in S-Block (Qiagen) previously loaded with VXL lysis buffer containing proteinase K and RNA carrier. Cell viability was also determined in order to determine if the absence of viral replication was due to genuine inhibition by the molecules or as an artifact of molecule cytotoxicity, and as another method to observe viral replication inhibition. This was achieved by removing all remaining cell culture supernatant and using CellTiter Blue® (Promega) following manufacturer's instructions. RNA extraction was performed on the collected supernatant using the Qiacube HT automat and the QIAamp 96 DNA kit HT following manufacturer instructions. Viral RNA was quantified by real-time RT-qPCR (GoTaq 1-step qRt-PCR, Promega) using 3.8 µL of extracted RNA and 6.2 µL of RT-qPCR mix and standard fast cycling parameters, i.e., 10 min at 50°C, 2 min at 95°C, and 40 amplification cycles (95°C for 3 s followed by 30 s at 60°C). Quantification was provided by four 2 log serial dilutions of an appropriate T7-generated synthetic RNA standard of known quantities (10² to 10⁸ copies/reaction). RT-qPCR reactions were performed on QuantStudio 12K Flex Real-Time PCR System (Applied Biosystems) and analyzed using QuantStudio 12K Flex Applied Biosystems software v1.2.3. Primers and probe sequences, which target SARS-CoV-2 N gene, were: Fw: GGCCGCAAATTGCACAAT; Rev: CCAATGCGCGACATTCC; Probe: FAM-CCCCCAGCGCTTCAGCGTTCT-BHQ1. For the evaluation of compounds cytotoxicity, the same culture conditions without addition of the virus, and cell viability was measured using CellTiter Blue® (Promega) following manufacturer's instructions. All data obtained were analyzed using GraphPad Prism 9 software (Graphpad software).

Author contributions

All authors have contributed to the manuscript and given approval to the final version of the manuscript. M.H., L.N., J.-J.V. and F.D., design and synthesis of the final compounds; S.B., molecular modeling studies; A.D. and E.D., biochemical assays; F.T., A.C. and B. C., antiviral studies in cell culture; S.B., B.C., B.C., J.-J.V., E.D. and F.D., manuscript writing and proofreading.

Notes

The authors declare no competing financial interest.

Acknowledgments

The research described here was part of the Virage project (M.H., J.-J.V., F.D., B.C., E.D.) supported by grant ANR-20-CE11-0024-02 from the French National Research Agency. M.H. acknowledges the ANR for the financial support of his PhD work (VIRAGE: ANR-20-CE11-0024-02). M.H., F.D. and J.-J.V. are grateful to Rostom Ahmed-Belkacem for fruitful discussions. This project has received funding from the European Union's Horizon 2020 Research and Innovation program under grants no. 101003627 (the SCORE project) and no. 101005077 (the CARE project) (E.D., B.C., A.D).

Appendix A. Supplementary data

Supplementary data to this article can be found online at :

References

- [1] Y. Wang, D. Zhang, G. Du, R. Du, J. Zhao, Y. Jin, S. Fu, L. Gao, Z. Cheng, Q. Lu, Y. Hu, G. Luo, K. Wang, Y. Lu, H. Li, S. Wang, S. Ruan, C. Yang, C. Mei, Y. Wang, D. Ding, F. Wu, X. Tang, X. Ye, Y. Ye, B. Liu, J. Yang, W. Yin, A. Wang, G. Fan, F. Zhou, Z. Liu, X. Gu, J. Xu, L. Shang, Y. Zhang, L. Cao, T. Guo, Y. Wan, H. Qin, Y. Jiang, T. Jaki, F.G. Hayden, P.W. Horby, B. Cao, C. Wang, Remdesivir in adults with severe COVID-19: a randomised, double-blind, placebo-controlled, multicentre trial, *Lancet*, 395 (2020) 1569-1578. [https://doi.org/10.1016/s0140-6736\(20\)31022-9](https://doi.org/10.1016/s0140-6736(20)31022-9).
- [2] S. Joshi, J. Parkar, A. Ansari, A. Vora, D. Talwar, M. Tiwaskar, S. Patil, H. Barkate, Role of favipiravir in the treatment of COVID-19, *Int. J. Infect. Dis.*, 102 (2021) 501-508. <https://doi.org/10.1016/j.ijid.2020.10.069>.
- [3] K. Akinosoglou, G. Schinas, C. Gogos, Oral Antiviral Treatment for COVID-19: A Comprehensive Review on Nirmatrelvir/Ritonavir, *Viruses*, 14 (2022). <https://doi.org/10.3390/v14112540>.
- [4] S.S. Spurr, E.D. Bayle, W. Yu, F. Li, W. Tempel, M. Vedadi, M. Schapira, P.V. Fish, New small molecule inhibitors of histone methyl transferase DOT1L with a nitrile as a non-traditional replacement for heavy halogen atoms, *Bioorg. Med. Chem. Lett.*, 26 (2016) 4518-4522. <https://doi.org/10.1016/j.bmcl.2016.07.041>.
- [5] T.U. Singh, S. Parida, M.C. Lingaraju, M. Kesavan, D. Kumar, R.K. Singh, Drug repurposing approach to fight COVID-19, *Pharmacol. Rep.*, 72 (2020) 1479-1508. <https://doi.org/10.1007/s43440-020-00155-6>.
- [6] L. Vangeel, W. Chiu, S. De Jonghe, P. Maes, B. Slechten, J. Raymenants, E. André, P. Leyssen, J. Neyts, D. Jochmans, Remdesivir, Molnupiravir and Nirmatrelvir remain active against SARS-CoV-2 Omicron and other variants of concern, *Antiviral Res.*, 198 (2022) 105252. <https://doi.org/10.1016/j.antiviral.2022.105252>.
- [7] A.K. Ghosh, J.L. Mishevich, A. Mesecar, H. Mitsuya, Recent drug development and medicinal chemistry approaches for the treatment of SARS-CoV-2 Infection and COVID-19, *ChemMedChem*, 17 (2022) e202200440. <https://doi.org/10.1002/cmdc.202200440>.
- [8] M. Romano, A. Ruggiero, F. Squeglia, G. Maga, R. Berisio, A structural view of SARS-CoV-2 RNA replication machinery: RNA synthesis, proofreading and final capping, *Cells*, 9 (2020) 1267. <https://doi.org/10.3390/cells9051267>.
- [9] D.R. Owen, C.M.N. Allerton, A.S. Anderson, L. Aschenbrenner, M. Avery, S. Berritt, B. Boras, R.D. Cardin, A. Carlo, K.J. Coffman, A. Dantonio, L. Di, H. Eng, R. Ferre, K.S. Gajiwala, S.A. Gibson, S.E. Greasley, B.L. Hurst, E.P. Kadar, A.S. Kalgutkar, J.C. Lee, J. Lee, W. Liu, S.W. Mason, S. Noell, J.J. Novak, R.S. Obach, K. Ogilvie, N.C. Patel, M. Pettersson, D.K. Rai, M.R. Reese, M.F. Sammons, J.G. Sathish, R.S.P. Singh, C.M. Steppan, A.E. Stewart, J.B. Tuttle, L. Updyke, P.R. Verhoest, L. Wei, Q. Yang, Y. Zhu, An oral SARS-CoV-2 M(pro) inhibitor clinical candidate for the treatment of COVID-19, *Science*, 374 (2021) 1586-1593. <https://doi.org/10.1126/science.aba4784>.

- [10] R. Nencka, J. Silhan, M. Klima, T. Otava, H. Kocek, P. Krafcikova, E. Boura, Coronaviral RNA-methyltransferases: function, structure and inhibition, *Nucleic Acids Res.*, 50 (2022) 635-650. <https://doi.org/10.1093/nar/gkab1279>.
- [11] N.S. Ogando, P. El Kazzi, J.C. Zevenhoven-Dobbe, B.W. Bontes, A. Decombe, C.C. Posthuma, V. Thiel, B. Canard, F. Ferron, E. Decroly, E.J. Snijder, Structure-function analysis of the nsp14 N7-guanine methyltransferase reveals an essential role in Betacoronavirus replication, *Proc. Natl. Acad. Sci. U S A*, 118 (2021). <https://doi.org/10.1073/pnas.2108709118>.
- [12] E. Decroly, B. Canard, Biochemical principles and inhibitors to interfere with viral capping pathways, *Curr. Opin. Virol.*, 24 (2017) 87-96. <https://doi.org/10.1016/j.coviro.2017.04.003>.
- [13] M. Bouvet, C. Debarnot, I. Imbert, B. Selisko, E.J. Snijder, B. Canard, E. Decroly, In vitro reconstitution of SARS-coronavirus mRNA cap methylation, *PLOS Pathog.*, 6 (2010) e1000863. <https://doi.org/10.1371/journal.ppat.1000863>.
- [14] W. Aouadi, C. Eydoux, B. Coutard, B. Martin, F. Debart, J.J. Vasseur, J.M. Contreras, C. Morice, G. Quérat, M.-L. Jung, B. Canard, J.-C. Guillemot, E. Decroly, Toward the identification of viral cap-methyltransferase inhibitors by fluorescence screening assay, *Antiviral Res.*, 144 (2017) 330-339. <https://doi.org/10.1016/j.antiviral.2017.06.021>.
- [15] R. Ahmed-Belkacem, P. Sutto-Ortiz, M. Guiraud, B. Canard, J.J. Vasseur, E. Decroly, F. Debart, Synthesis of adenine dinucleosides SAM analogs as specific inhibitors of SARS-CoV nsp14 RNA cap guanine-N7-methyltransferase, *Eur. J. Med. Chem.*, 201 (2020) 112557. <https://doi.org/10.1016/j.ejmech.2020.112557>.
- [16] S. Basu, T. Mak, R. Ulferts, M. Wu, T. Deegan, R. Fujisawa, K.W. Tan, C.T. Lim, C. Basier, B. Canal, J.F. Curran, L.S. Drury, A.W. McClure, E.L. Roberts, F. Weissmann, T.U. Zeisner, R. Beale, V.H. Cowling, M. Howell, K. Labib, J.F.X. Diffley, Identifying SARS-CoV-2 antiviral compounds by screening for small molecule inhibitors of nsp14 RNA cap methyltransferase, *Biochem. J.*, 478 (2021) 2481-2497. <https://doi.org/10.1042/BCJ20210219>.
- [17] R. Bobrovs, I. Kanepe, N. Narvaiss, L. Patetko, G. Kalnins, M. Sisovs, A.L. Bula, S. Grinberga, M. Boroduskis, A. Ramata-Stunda, N. Rostoks, A. Jirgensons, K. Tars, K. Jaudzems, Discovery of SARS-CoV-2 nsp14 and nsp16 methyltransferase inhibitors by high-throughput virtual screening, *Pharmaceuticals*, 14 (2021). <https://doi.org/10.3390/ph14121243>.
- [18] K. Devkota, M. Schapira, S. Perveen, A. Khalili Yazdi, F. Li, I. Chau, P. Ghiabi, T. Hajian, P. Loppnau, A. Bolotokova, K.J.F. Satchell, K. Wang, D. Li, J. Liu, D. Smil, M. Luo, J. Jin, P.V. Fish, P.J. Brown, M. Vedadi, Probing the SAM binding site of SARS-CoV-2 nsp14 in vitro using SAM competitive inhibitors guides developing selective bisubstrate inhibitors, *SLAS Discov.*, 26 (2021) 1200-1211. <https://doi.org/10.1177/24725552211026261>.
- [19] R. Kasprzyk, T.J. Spiewla, M. Smietanski, S. Golojuch, L. Vangeel, S. De Jonghe, D. Jochmans, J. Neyts, J. Kowalska, J. Jemielity, Identification and evaluation of potential SARS-CoV-2 antiviral agents targeting mRNA cap guanine N7-methyltransferase, *Antiviral Res.*, 193 (2021) 105142. <https://doi.org/10.1016/j.antiviral.2021.105142>.
- [20] L.A. Pearson, C.J. Green, D. Lin, A.P. Petit, D.W. Gray, V.H. Cowling, E.A.F. Fordyce, Development of a high-throughput screening assay to identify inhibitors of the SARS-CoV-2 guanine-N7-methyltransferase using RapidFire mass spectrometry, *SLAS Discov.*, 26 (2021) 749-756. <https://doi.org/10.1177/24725552211000652>.
- [21] O. Bobileva, R. Bobrovs, I. Kanepe, L. Patetko, G. Kalnins, M. Sisovs, A.L. Bula, S. Gri Nberga, M.R. Boroduskis, A. Ramata-Stunda, N. Rostoks, A. Jirgensons, K. Ta Rs, K. Jaudzems, Potent SARS-CoV-2 mRNA cap methyltransferase inhibitors by bioisosteric replacement of methionine in SAM cosubstrate, *ACS Med. Chem. Lett.*, 12 (2021) 1102-1107. <https://doi.org/10.1021/acsmchemlett.1c00140>.
- [22] T. Otava, M. Šála, F. Li, J. Fanfrlík, K. Devkota, S. Perveen, I. Chau, P. Pakarian, P. Hobza, M. Vedadi, E. Boura, R. Nencka, The structure-based design of SARS-CoV-2 nsp14 methyltransferase ligands yields nanomolar inhibitors, *ACS Infect. Dis.*, 7 (2021) 2214-2220. <https://doi.org/10.1021/acsinfectdis.1c00131>.
- [23] R. Ahmed-Belkacem, M. Hausdorff, A. Delpal, P. Sutto-Ortiz, A.M.G. Colmant, F. Touret, N.S. Ogando, E.J. Snijder, B. Canard, B. Coutard, J.J. Vasseur, E. Decroly, F. Debart, Potent inhibition of SARS-CoV-2 nsp14 N7-methyltransferase by sulfonamide-based bisubstrate analogues, *J. Med. Chem.*, 65 (2022) 6231-6249. <https://doi.org/10.1021/acs.jmedchem.2c00120>.

- [24] E. Jung, R. Soto-Acosta, J. Xie, D.J. Wilson, C.D. Dreis, R. Majima, T.C. Edwards, R.J. Geraghty, L. Chen, Bisubstrate inhibitors of severe acute respiratory syndrome coronavirus-2 nsp14 methyltransferase, *ACS Med. Chem. Lett.*, 13 (2022) 1477-1484. <https://doi.org/10.1021/acsmchemlett.2c00265>.
- [25] O. Bobileva, R. Bobrovs, E.E. Sirma, I. Kanepe, A.L. Bula, L. Patetko, A. Ramata-Stunda, S. Grinberga, A. Jirgensons, K. Jaudzems, 3-(Adenosylthio)benzoic Acid Derivatives as SARS-CoV-2 Nsp14 Methyltransferase Inhibitors, *Molecules*, 28 (2023). <https://doi.org/10.3390/molecules28020768>.
- [26] Y. Ma, L. Wu, N. Shaw, Y. Gao, J. Wang, Y. Sun, Z. Lou, L. Yan, R. Zhang, Z. Rao, Structural basis and functional analysis of the SARS coronavirus nsp14-nsp10 complex, *Proc. Natl. Acad. Sci. U S A*, 112 (2015) 9436-9441. <https://doi.org/https://doi.org/10.1073/pnas.1508686112>.
- [27] A. Czarna, J. Plewka, L. Kresik, A. Matsuda, A. Karim, C. Robinson, S. O'Byrne, F. Cunningham, I. Georgiou, P. Wilk, M. Pachota, G. Popowicz, P.G. Wyatt, G. Dubin, K. Pyrc, Refolding of lid subdomain of SARS-CoV-2 nsp14 upon nsp10 interaction releases exonuclease activity, *Structure*, 30 (2022) 1050-1054 e1052. <https://doi.org/10.1016/j.str.2022.04.014>.
- [28] N. Imprachim, Y. Yosaatmadja, J.A. Newman, Crystal structures and fragment screening of SARS-CoV-2 NSP14 reveal details of exoribonuclease activation and mRNA capping and provide starting points for antiviral drug development, *Nucleic Acids Res.*, (2022). <https://doi.org/10.1093/nar/gkac1207>.
- [29] J. Kottur, O. Rechkoblit, R. Quintana-Feliciano, D. Sciaky, A.K. Aggarwal, High-resolution structures of the SARS-CoV-2 N7-methyltransferase inform therapeutic development, *Nat. Struct. Mol. Biol.*, 29 (2022) 850-853. <https://doi.org/10.1038/s41594-022-00828-1>.
- [30] R. Amador, A. Delpal, B. Canard, J.J. Vasseur, E. Decroly, F. Debart, G. Clave, M. Smietana, Facile access to 4'-(N-acylsulfonamide) modified nucleosides and evaluation of their inhibitory activity against SARS-CoV-2 RNA cap N7-guanine-methyltransferase nsp14, *Org. Biomol. Chem.*, 20 (2022) 7582-7586. <https://doi.org/10.1039/d2ob01569b>.
- [31] L.P. Kotra, K.K. Manouilov, E. Cretton-Scott, J.-P. Sommadossi, F.D. Boudinot, R.F. Schinazi, C.K. Chu, Synthesis, biotransformation, and pharmacokinetic studies of 9-(β -D-arabinofuranosyl)-6-azidopurine: a prodrug for ara-A designed to utilize the azide reduction pathway, *J. Med. Chem.*, 39 (1996) 5202-5207. <https://doi.org/10.1021/jm960339p>.
- [32] Y. Yao, P. Chen, J. Diao, G. Cheng, L. Deng, J.L. Anglin, B.V.V. Prasad, Y. Song, Selective inhibitors of histone methyltransferase DOT1L: design, synthesis, and crystallographic studies, *J. Am. Chem. Soc.*, 133 (2011) 16746-16749. <https://doi.org/10.1021/ja206312b>.
- [33] S. Bhattarai, M. Freundlieb, J. Pippel, A. Meyer, A. Abdelrahman, A. Fiene, S.-Y. Lee, H. Zimmermann, G.G. Yegutkin, N. Sträter, A. El-Tayeb, C.E. Müller, α,β -methylene-ADP (AOPCP) derivatives and analogues: development of potent and selective ecto-5'-nucleotidase (CD73) inhibitors, *J. Med. Chem.*, 58 (2015) 6248-6263. <https://doi.org/10.1021/acs.jmedchem.5b00802>.
- [34] F. Seela, X. Ming, 7-Functionalized 7-deazapurine β -D and β -L-ribonucleosides related to tubercidin and 7-deazainosine: glycosylation of pyrrolo[2,3-d]pyrimidines with 1-O-acetyl-2,3,5-tri-O-benzoyl- β -D or β -L-ribofuranose, *Tetrahedron*, 63 (2007) 9850-9861. <https://doi.org/10.1016/j.tet.2007.06.107>.
- [35] F. Kunkel, R. Lurz, E. Weinhold, A 7-deazaadenosylaziridine cofactor for sequence-specific labeling of DNA by the DNA cytosine-C5 methyltransferase M.HhaI, *Molecules*, 20 (2015) 20805-20822. <https://doi.org/10.3390/molecules201119723>.
- [36] P. Nauš, O. Caletková, P. Perlíková, L. Poštová Slavětínská, E. Tloušťová, J. Hodek, J. Weber, P. Džubák, M. Hajdúch, M. Hocek, Synthesis and biological profiling of 6- or 7-(het)aryl-7-deazapurine 4'-C-methylribonucleosides, *Bioorg. Med. Chem.*, 23 (2015) 7422-7438. <https://doi.org/10.1016/j.bmc.2015.10.040>.
- [37] N. Milisavljevic, E. Konkolová, J. Kozák, J. Hodek, L. Veselovská, V. Sýkorová, K. Čížek, R. Pohl, L. Eyer, P. Svoboda, D. Růžek, J. Weber, R. Nencka, E. Bouřa, M. Hocek, Antiviral activity of 7-substituted 7-deazapurine ribonucleosides, monophosphate prodrugs, and triphosphates against emerging RNA viruses, *ACS Infect. Dis.*, 7 (2021) 471-478. <https://doi.org/10.1021/acsinfectdis.0c00829>.
- [38] J.G. Rodríguez, C. de los Rios, A. Lafuente, Synthesis of n-chloroquinolines and n-ethynylquinolines (n=2, 4, 8): homo and heterocoupling reactions, *Tetrahedron*, 61 (2005) 9042-9051. <https://doi.org/10.1016/j.tet.2005.07.043>.

- [39] A. Smeyanov, A. Schmidt, K_3PO_4 -KOH mixture as efficient reagent for the deprotection of 4-aryl-2-methyl-3-butyn-2-ols to terminal acetylenes, *Synth. Commun.*, 43 (2013) 2809-2816. <https://doi.org/10.1080/00397911.2012.744841>.
- [40] F. Peyrane, B. Selisko, E. Decroly, J.J. Vasseur, D. Benarroch, B. Canard, K. Alvarez, High-yield production of short GpppA- and 7MeGpppA-capped RNAs and HPLC-monitoring of methyltransfer reactions at the guanine-N7 and adenosine-2'O positions, *Nucleic Acids Res.*, 35 (2007) e26. <https://doi.org/https://doi.org/10.1093/nar/gkl1119>.
- [41] O. Trott, A.J. Olson, AutoDock Vina: improving the speed and accuracy of docking with a new scoring function, efficient optimization, and multithreading, *J. Comput. Chem.*, 31 (2010) 455-461. <https://doi.org/10.1002/jcc.21334>.
- [42] F. Touret, C. Baronti, O. Goethals, M. Van Loock, X. de Lamballerie, G. Querat, Phylogenetically based establishment of a dengue virus panel, representing all available genotypes, as a tool in dengue drug discovery, *Antiviral Res.*, 168 (2019) 109-113. <https://doi.org/https://doi.org/10.1016/j.antiviral.2019.05.005>.
- [43] F. Touret, M. Gilles, K. Barral, A. Nougairède, J. van Helden, E. Decroly, X. de Lamballerie, B. Coutard, In vitro screening of a FDA approved chemical library reveals potential inhibitors of SARS-CoV-2 replication, *Sci. Rep.*, 10 (2020) 13093. <https://doi.org/10.1038/s41598-020-70143-6>.
- [44] S.J.F. Kaptein, O. Goethals, D. Kiemel, A. Marchand, B. Kesteleyn, J.-F. Bonfanti, D. Bardiot, B. Stoops, T.H.M. Jonckers, K. Dallmeier, P. Geluykens, K. Thys, M. Crabbe, L. Chatel-Chaix, M. Münster, G. Querat, F. Touret, X. de Lamballerie, P. Raboisson, K. Simmen, P. Chaltin, R. Bartenschlager, M. Van Loock, J. Neyts, A pan-serotype dengue virus inhibitor targeting the NS3-NS4B interaction, *Nature*, 598 (2021) 504-509. <https://doi.org/10.1038/s41586-021-03990-6>.
- [45] F. Touret, J.S. Driouich, M. Cochin, P.R. Petit, M. Gilles, K. Barthélémy, G. Moureau, F.X. Mahon, D. Malvy, C. Solas, X. de Lamballerie, A. Nougairède, Preclinical evaluation of Imatinib does not support its use as an antiviral drug against SARS-CoV-2, *Antiviral Res.*, 193 (2021) 105137. <https://doi.org/10.1016/j.antiviral.2021.105137>.
- [46] M.P. Egloff, D. Benarroch, B. Selisko, J.L. Romette, B. Canard, An RNA cap (nucleoside-2'-O)-methyltransferase in the flavivirus RNA polymerase NS5: crystal structure and functional characterization, *The EMBO journal*, 21 (2002) 2757-2768. <https://doi.org/10.1093/emboj/21.11.2757>.
- [47] W. Aouadi, A. Blanjoie, J.J. Vasseur, F. Debart, B. Canard, E. Decroly, Binding of the Methyl Donor S-Adenosyl-l-Methionine to Middle East Respiratory Syndrome Coronavirus 2'-O-Methyltransferase nsp16 Promotes Recruitment of the Allosteric Activator nsp10, *J. Virol.*, 91 (2017). <https://doi.org/10.1128/jvi.02217-16>.
- [48] E.F. Pettersen, T.D. Goddard, C.C. Huang, G.S. Couch, D.M. Greenblatt, E.C. Meng, T.E. Ferrin, UCSF Chimera--a visualization system for exploratory research and analysis, *J. Comput. Chem.*, 25 (2004) 1605-1612. <https://doi.org/10.1002/jcc.20084>.
- [49] G.M. Morris, R. Huey, W. Lindstrom, M.F. Sanner, R.K. Belew, D.S. Goodsell, A.J. Olson, AutoDock4 and AutoDockTools4: Automated docking with selective receptor flexibility, *J. Comput. Chem.*, 30 (2009) 2785-2791. <https://doi.org/10.1002/jcc.21256>.
- [50] R.A. Laskowski, M.B. Swindells, LigPlot+: multiple ligand-protein interaction diagrams for drug discovery, *J. Chem. Inf. Model.*, 51 (2011) 2778-2786. <https://doi.org/10.1021/ci200227u>.
- [51] A. Weiss, F. Touret, C. Baronti, M. Gilles, B. Hoen, A. Nougairède, X. de Lamballerie, M.O.A. Sommer, Niclosamide shows strong antiviral activity in a human airway model of SARS-CoV-2 infection and a conserved potency against the Alpha (B.1.1.7), Beta (B.1.351) and Delta variant (B.1.617.2), *PloS one*, 16 (2021) e0260958. <https://doi.org/10.1371/journal.pone.0260958>.